SOFIA PEREIRA SERRANO

Bachelor in Conservation and Restoration

Dissertation for the obtention of the Master's Degree in Conservation and Restoration, specialization area Conservation Sciences - Metals

STUDY OF GOLD ALLOY PRODUCTIONS FROM LATE BRONZE AGE AND IRON AGE

TECHNOLOGIES AND GOLDWORK

MASTER IN CONSERVATION AND RESTORATION - CONSERVATION SCIENCES

NOVA University Lisbon
December, 2022

STUDY OF GOLD ALLOY PRODUCTIONS FROM LATE BRONZE AGE AND IRON AGE

TECHNOLOGIES AND GOLDWORK

SOFIA PEREIRA SERRANO

Bachelor in Conservation and Restoration

Dissertation for the obtention of the Master's Degree in Conservation and Restoration, specialization area Conservation Sciences - Metals

Adviser: Elin Figueiredo
Assistant Researcher, FCT-NOVA Lisbon

Co-adviser: Rui Silva
Associate Professor, FCT-NOVA Lisbon

MASTER IN CONSERVATION AND RESTORATION - CONSERVATION SCIENCES

NOVA University Lisbon
December, 2022

Study of gold alloy productions from Late Bronze Age and Iron Age

Acknowledgements

Primeiramente, agradeço aos meus orientadores. À professora Elin Figueiredo, por todo o seu apoio, por me ter desafiado a ser sempre melhor e por todas as oportunidades que me proporcionou até hoje. Ao professor Rui Silva, por me ter introduzido ao estudo dos materiais metálicos e por todos os ensinamentos. Agradeço também à FCT NOVA, ao Museu Nacional de Arqueologia, em particular à conservadora-restauradora Margarida Santos, e ao Laboratório José de Figueiredo, em particular à técnica superior Ana Machado, sem os quais a elaboração desta dissertação não teria sido possível.

Aos meus pais e irmão, Pedro, Celina e Luís, pelo carinho ao longo dos anos e por sempre me terem dado toda força e oportunidades para alcançar os meus sonhos. Agradeço ainda a toda a minha família, por todo apoio que esteve sempre presente.

Ao João, por toda a paciência e amor, por lá ter estado sempre que dizia "não vou conseguir" e nos piores momentos arranjar sempre uma maneira de me fazer sorrir.

À Elisa e Bento, por desde o primeiro dia de jornada na FCT me terem proporcionado as melhores histórias, gargalhadas e por toda a amizade. À Bicas e Prada, por terem passado por tudo comigo até ao fim, pelas noites passadas na faculdade sem dormir e desabafos. Obrigada queridas amigas, sem vocês isto não seria possível. À Mariana, Ana e Francisco, por serem o grupo mais desajeitado e feliz, pela preocupação constante, e por serem uma segunda família que levo da universidade. Ao Juan e ao Miguel, por toda a ajuda e bons momentos passados que acompanharam os momentos da escrita deste trabalho. A todos aqueles que não menciono aqui mas que marcaram este percurso de alguma forma, os meus sinceros agradecimentos.

"All that is gold does not glitter,
Not all those who wander are lost;
The old that is strong does not wither,
Deep roots are not reached by the frost." (J.R.R. Tolkien)

ABSTRACT

This master's dissertation focuses on the archaeometallurgical study and conservation of thirteen gold alloy earrings attributed to the Late Bronze Age and Iron Age from the Western Iberia. Most of the artefacts studied are from the collection "*Treasures of Portuguese Archaeology*" of the National Museum of Archaeology (Lisboa, Portugal). Based on typological and decoration features, they were divided into two groups: eight plain gold rings, attributed to the LBA, which are bulk objects with a smooth surface, and five IA earrings with complex goldwork, like gold wires, sheets, granules and gilding.

The aim of the study includes: *i)* the study of the alloy compositions; *ii)* the study of the detailed fine goldwork of the objects; *iii)* contribute to the understanding of technological evolutions from LBA to IA; *iv)* determination of heterogeneities in gold alloys at the surface level, due to corrosion, technological features or previous treatments, with an influence on their conservation. To achieve these goals complementary analytical and examination techniques were used, such as general photography, multifocus microscopy, elemental analysis by portable and micro X Ray Fluorescence Spectrometry (XRF) and microscopy and elemental analysis by Scanning Electron Microscopy with Energy Dispersive Spectroscopy (SEM-EDS).

Results showed variations on the artefacts composition, being mostly composed by an Au-Ag alloy (8-20 wt.% Ag), with small amounts of Cu. The only exception are two IA earrings, with absence of Cu, unusual for alloys from this period. It also allowed to carry out compositional characterizations at different depths, concluding that heterogeneities exist within surface areas but can be more significant at different depths. Overall, a superficial loss in Ag was found, possibly due to corrosion phenomena, being that any conservation and restoration treatment could interfere with the final surface composition. It was found that the goldwork performed in some earrings is very fine, showing that ancient goldsmiths were able to produce wires and granules with less than 1 mm in diameter, as well as gilding. The results obtained are significant for the study of ancient technologies as well as for future conservation approaches to Proto-historic goldworks.

Keywords: Gold, Silver, Iron Age, Iberian Peninsula, XRF, OM, Goldwork.

Resumo

A presente dissertação de mestrado foca-se no estudo arqueometalúrgico e conservação de treze brincos em ligas de ouro, atribuídos à Idade do Bronze Final e Idade do Ferro, provenientes da Península Ibérica Ocidental. A maioria dos artefactos é da coleção "*Tesouros da Arqueologia Portuguesa*", do Museu Nacional de Arqueologia (Lisboa, Portugal). Com base na sua tipologia e elementos decorativos, foram divididos em dois grupos: oito anéis de ouro lisos, atribuídos à IBF, objetos maciços de superfície lisa, e cinco brincos da IF com trabalho fino em ouro, como fios, chapas, grânulos e douramento.

O estudo tem como objetivos: *i)* estudar a composição das ligas e *ii)* o trabalho fino realizado em ouro nos objetos; *iii)* contribuir para o estudo da evolução tecnológica entre a IBF e IF; *iv)* determinar heterogeneidades nas ligas ao nível da superfície, devido a corrosão, características técnicas ou intervenções anteriores, com influência na sua conservação. Para tal, recorreu-se a técnicas analíticas e de examinação complementares, como fotografia geral, microscopia ótica, análise elementar por Espectroscopia de Fluorescência de Raios X (XRF) portátil e micro, e análise microscópica e elementar por Microscopia Eletrónica de Varrimento com Espectroscopia de Energia Dispersiva (SEM-EDS).

Os resultados mostraram variações composicionais nos vários objetos, maioritariamente compostos por Au-Ag (8-20 wt.% Ag), com baixos teores de Cu. A única exceção foram dois brincos da IF, com ausência de Cu, pouco comum para ligas deste período. Também permitiu a realização de caracterizações composicionais em diferentes profundidades, concluindo-se que existem heterogeneidades ao nível da superfície, embora sejam mais notórias em maiores profundidades. No geral, uma perda superficial de Ag foi observada, possivelmente devido a fenómenos de corrosão, em que intervenções de conservação e restauro podem influenciar a composição final da superfície dos objetos. O trabalho de ourivesaria realizado nos brincos revelou-se muito detalhado, mostrando que na antiguidade os ourives conseguiam produzir fios e grânulos com diâmetro inferior a 1 mm, assim como douramento. Os resultados foram significativos para o estudo de tecnologias da antiguidade, assim como para abordagens de conservação em ourivesaria Proto-histórica.

Palavras-chave: Ouro, Prata, Idade do Ferro, Península Ibérica, XRF, MO, Ourivesaria.

CONTENTS

LIST OF FIGURES

List of Tables

Glossary

alloy   Two or more mixed and united metals, usually over fusion and dissolving as they melt. Depending on the quantities of each metal used, the melting temperature and cooling time, different properties (both colour and thermo-mechanical) can be obtained.[1] 2

burnishing   Polishing metals by rubbing the surface with a hard and smooth object to obtain a shiny surface.[1] 4

casting-on   Method of joining two or more metallic elements by pouring a new metal onto the parts to be joined. The metal could be in a clay mould and the metal that is poured fuses onto the original object.[1] 2

chisel   Cutting instrument made of iron or steel with a sharping edge at one end, used for sculpting and engraving, producing marks or reliefs on the surface of objects. Very used technique for the continuous reproduction of a similar motifs.[2, 3] 2

filigree   Ornament and decorative technique, in which very fine wires with a circular or near-circular cross-section are twisted in a braid-like form and welded simultaneously, to produce decorative motives used in earrings, necklaces, and diadems, for example. Exclusive of gold and silver work.[2, 4, 5] 2

forging   Technique of shapping a metal by hammering while it is still hot. Technique consists of heating the metal, to soften it and then hammering it.[1] 19

gilding Process of applying a gold coating onto base metal or other material, with a very low thickness. This process could be achieved by using: a mercury amalgam (also known as fire-gilding); gold leafs (by means of an adhesive called mordant); gold paint; a bath in a gold alloy; electroplating; by applying gold powder on the object's surface; through depletion gilding.[1, 6] 2

granulation Ornament and decorative technique, in which small spheres of gold or silver are welded through semi-fusion to a surface. It creates patterns or textures that decorate earrings, necklaces, and diadems, for example. The granules are obtained through the smelt in a flame of the tip of a gold or silver wire, being that the drops that would fall would be collected to be later soldered to the object. They can have a uniform size, but their surface can be imperfect. The spheres can reach a diameter of 0,02mm. To place them on the surface of the object, they would be heated up to their fusion point, and then placed on the desired surface.[2, 7] 2

hammering Technique of deforming metals by beating up their surface in order to obtain the desired dimensions or shapes. Used for the production of metal sheets.[1] 4

ingot The remains of broken or unusable metal objects that were remelted and reused in the form of bars or circular shapes. They were also a way of accumulating raw material to be reused later.[8, 9] 19

lost wax casting A method of producing metal objects or sculptures by pouring molten metal into a plaster mould of an object built on a wax model. The wax was eliminated by the melted metal, producing massive objects built in one piece.[1] 2

melting The process of heating metal until it reaches the liquid state.[1] 19

native gold Gold found in its natural state, usually in alluvial areas, with the aid of panning. It has a characteristic yellowish colour and low copper (less than 1%) and variable silver contents. Many of the Protohistoric objects were made in this material since it was not required to produce metallic alloys for its use.[10, 11] 2

plaiting Decorative technique that consists of braiding two metal wires in the same direction, clockwise or counterclockwise. The two wires used can be twisted individually.[1] 7

polishing Process used to make metallic surfaces smooth and glossy. To do this, it must be rubbed with various abrasive materials and tools.[1, 3] 28

punch This is a tool used for engraving metals on steel, used by the goldsmith to draw or cut out what he wants to mark or relief. Very used technique for the continuous reproduction of a similar motifs.[1, 3] 2

repousse Decorative technique used on metallic sheets to produce reliefs, with instruments such as punches, that were beaten on the reverse of the piece with the help of hammering.[1, 2] 8

rolling Surface smoothing process of twisted wires by rolling them between two wooden plates.[1] 30

soldering Process used to join two parts of an object. For this, a metal alloy or molten metal powder, usually with a lower melting temperature than the body of the object (in the case of gold alloys, the solder usually has higher Ag or Cu contents). It is placed in the area to be joined and heated in order to make the union.[1, 3, 12] 2

welding Process of joining two or more metal parts by heating the metals to near their melting temperature without applying pressure.[1] 8

Acronyms

OM   Optical Microscopy 10, 20, 26, 30, 35, 36, 45

pXRF   Portable X-Ray Fluoroscence Spectrometry 10, 11, 13, 14, 15, 18, 22, 23, 25, 26, 27, 43, 46

SE   Secondary Electrons 11
SEM   Scanning Electron Microscopy 11, 13, 14, 21, 29, 43
SM   Snap Mode 10

XRF   X-Ray Fluoroscence Spectrometry 10, 11, 13

Symbols

A   Ampere 11
Ag   Silver 2
Au   Gold 2

°C   Degree Celsius 3
cm³   Cubic centimetre 46
Cu   Copper 2

eV   Electronvolt 11

g   Gram 14

kV   Kilovolt 10

mm   Millimetre 10
mm²   Square millimetre 11

μA Milliampere 10
μm Micrometre 11

wt.%   Weight Percentage 2

<div align="right">

1

</div>

<div align="right">

Introduction

</div>

1.1   The beginning of gold exploitation

Gold firstly caught the attention of men, shining in alluvial zones in the form of small golden granules [13]. The noble gold element attracted mankind inevitably, perhaps due to the way that it kept and mirrored all the luminosity, splendor and similarity to the sun [13, 14]. It has since been used as the raw material of adornment objects and could certainly provide some power to who would wear such objects since it was a desired, attractive and rare good that could be beyond the reach of the majority of the population [13, 15]. Over the centuries, gold revolutionized and dominated the world economy, and even nowadays, it still is an important economic good, having a huge impact in technological, economic, and social aspects [13, 16, 17].

With the manipulation of gold a new type of work with some symbolic functionality was born, and with this the goldsmith [15]. The first form of obtaining gold was in its primary form, in fluvial placers, by panning. Due to the gold malleability, it was easily worked through mechanical deformation to obtain the first gold artefacts [13, 18].

The Iberian Peninsula (IP) has one of the greatest gold deposits in Europe, making the access to gold relatively easy. In western IP, the use of gold has been documented, at least, since the third millennium before Christ (B.C.) [19]. During the Iron Age (IA) (c. 800 B.C. – 0), it got aesthetic and technical influences from Cultures from the Mediterranean, such as from the Phoenicians, Etruscans, Greeks, and Romans [13]. A large number of objects recovered at the IP reveal a high technical quality and beauty, observed in the variety of techniques and typologies of the objects [18].

1.2   Bronze Age transition to the Iron Age in the Iberian Peninsula

Through times, with the evolution of technologies and contact with other cultures, the goldsmith techniques evolved as well [20].

In the Bronze Age (BA) (c. 2000 – 800 B.C.), the production of gold objects was mostly

made of native gold obtained from panning from alluvial deposits [21]. In the Early Bronze Age (EBA), the artefacts that present more connections with artefacts from other Atlantic territories are from the Atlantic facade of the IP (Galicia and Portugal), being that the artefacts were placed in tombs, and mainly produced by mechanical deformation and with the use of fire [15, 21]. However, in the Late Bronze Age (LBA), objects were placed in recoverable deposits, inside recipients, near the villages [15]. During this later period, more advanced modelling and joining techniques start to be used, like the lost wax casting and casting-on, although the mechanical deformation and the use of fire were still the most used techniques for simple shaped objects [13, 14, 21]. Overall, the BA was characterized by the production of artefacts such as necklaces, bracelets, diadems, earrings and torcs that were bulky and decorated with geometric motives on the surface made with a chisel and/or a punch [13, 21, 22].

It is during the IA that the contact with cultures from the Mediterranean and the East intensifies, leading to the improvement of the techniques of extraction and refining, and to the appearance of the first intentional alloy [17, 18]. In the Early Iron Age (EIA) specific compositions were manufactured of Au, Ag and Cu [17, 18]. These alloys were frequently more "economic", with higher Ag and Cu contents than native gold, and also give the objects specific colour and hardness properties, with possible repercussions in an increase in the jewellery industry [17, 18, 23]. Also in the EIA, the use of solid structural elements is commonly made on a different materials, as well as techniques of the lost-wax cast, the casting-on to join two structural elements and plastic shaping techniques, whose use becomes more common [18]. In the Late Iron Age (LIA), the recurrent use of more advanced techniques is notorious, with the recurrent use of filigree, granulation, soldering, and gilding techniques [18, 24].

1.3   The composition of gold alloys

With the evolution in the manufacturing of gold alloys in IP, it was possible to achieve different compositions.

In the BA, the composition of the alloys would be different depending on the native gold that was used (the composition of native gold would vary according to the gold source and its localization) [24, 25]. In the IP, the gold alloys in the BA had Ag contents between 5 to 25wt.%, but the Cu contents would be very low and much more regular, in most cases lower than 1 wt.% [9, 21]. This means that, on one hand, the Cu presence could be associated with residues and impurities in the production of the artefacts, or, in the other hand, that it would be present in very small amounts in native gold (mostly composed by Au and Ag) [9, 21].

During IA, it is possible to track some changes in the composition of the gold alloys. One of the main differences is a general increase in Cu contents, with repercussions in the *liquidus* temperature of that alloy, which tends to decrease [12]. This allowed the use of techniques such as soldering, using an alloy of lower *liquidus* temperature to join two or

2

more elements of an alloy of higher *liquidus* temperature [12]. These alloys, with a very variable composition, had, in its majority, Ag contents above 20 wt.%, and Cu contents between 2 to 10 wt.% (Figure 1.1) [26–31].

Considering previous analyses made of gold alloys from the BA and IA from the IP (Figure 1.1), it is possible to see the increase in the contents of Ag and Cu from BA to IA, with repercussions in the fusion temperatures (as from 1050 to 900ºC) and metal colours (from yellow to pale greenish yellow) (Figure 1.2).
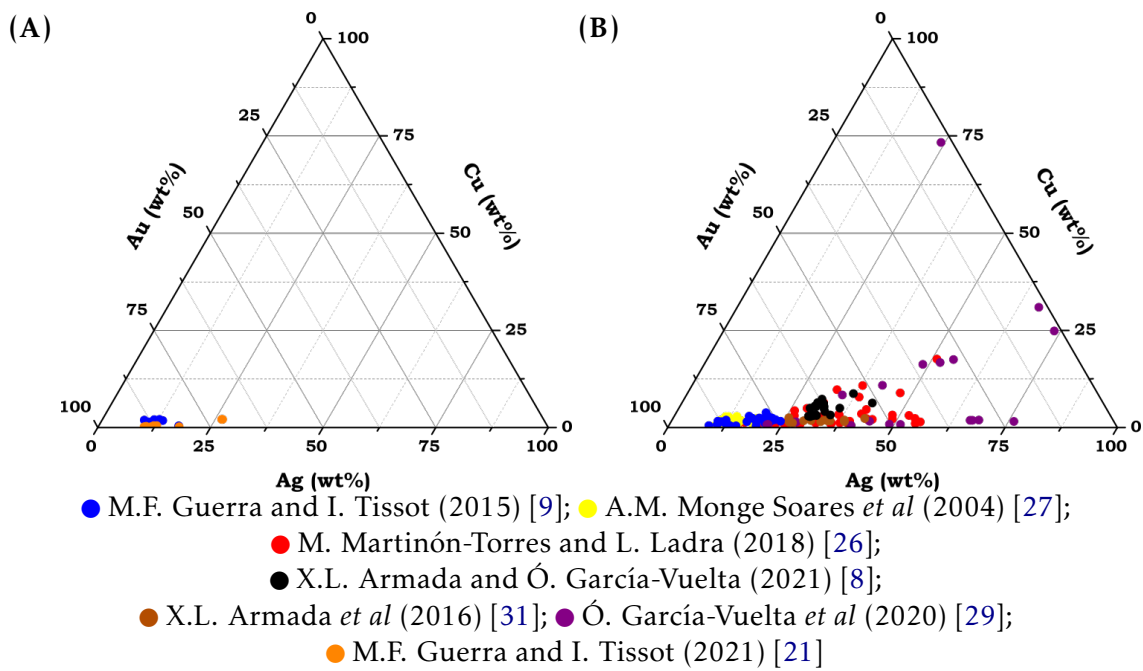
Figure 1.1: Ternary Diagrams with XRF analyses of BA and IA, from the IP: **(A)** Objects from the BA (19 analyses); **(B)** Objects from the IA (174 analyses).
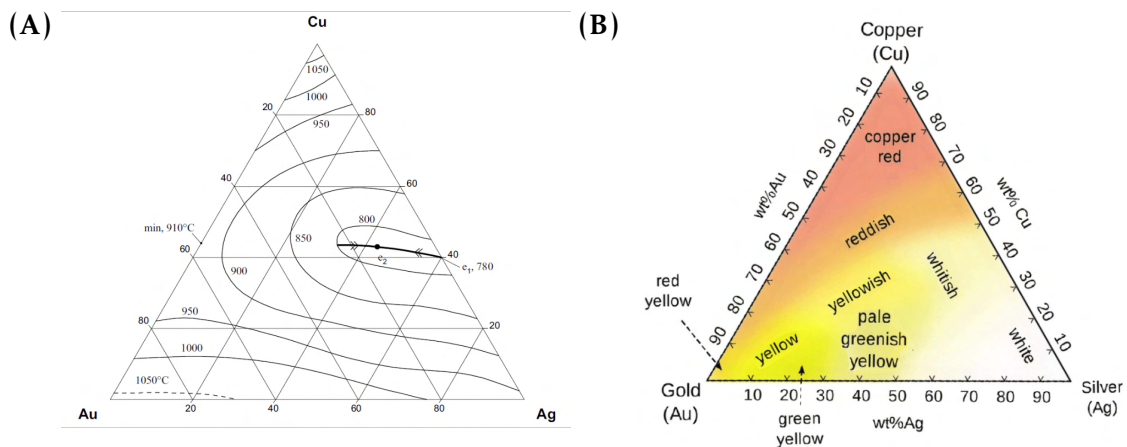
Figure 1.2: Ternary diagrams of the alloys composed by Au-Ag-Cu: **(A)** Phase diagram [32]; **(B)** Different colors obtained with different alloy compositions [33].

3

1.4   The degradation and conservation of gold alloys

Gold, in its pure state, is assumed not to undergo any type of corrosion, but gold in its native state isn't pure, and usually contains appreciable amounts of silver (from 5 to 45 wt.%) and some copper (from 0.1 to 5 wt.%) [6]. This means that being a natural or intentional alloy will not prevent some corrosion due to the presence of other elements besides gold in the alloy. Also, due to the malleability and ductility of gold alloys, the artefacts can be easily subjected to abrasion and physical deformation [6, 25]. Based on [6, 25], there are five main types of degradation that ancient gold artefacts may suffer:

   i **Tarnishing:** ternary Au-Ag-Cu alloys usually exhibit a thin film on the surface, with a grey-brown shade, usually due to deposition of metallic ions from solution or reactions with sulphur-containing contaminants, like H_2S. Usually, in ternary alloys, it forms Ag_2S or Cu_2S on the surface of the metals. The tarnishing rate will increase with higher contents of Ag, and when exposed to high relative humidity. Only alloys with Au contents higher than 95 wt.% can prevent the appearance of tarnishing. [6]

   ii **Dissolution of anodic constituents:** in noble metal alloys, it is common that the less noble metals suffer a selective dissolution during anodic corrosion, which leads to the preferential dissolution of those elements (in ternary gold alloys, the Ag and Cu) at the surface of the objects and at an appreciable depth. This leads to an enrichment of the surface in the noblest element, in this case, gold. This is due to the electrochemical potential between Au, Ag, and Cu being so different. [6, 34]

  iii **Stress corrosion cracking and embrittlement:** burnishing operations and inter-crystalline corrosion can lead to internal embrittlement, making the artefacts subject to stress-corrosion cracking. It depends on the burial conditions, usage of the object, and the conservation treatments that the object was subject to. This type of degradation can be visible without any corrosion products and on the surface or body of the object. [6]

  iv **Changes due to order-disorder transformations:** The changes in (crystal) structure can occur due to: **(1)** Ordering – due to quenching in water, which will suppress the ordering process and change it in the hammering process, which will be easier, once the alloy is more ductile (note that when phases are formed over a longer period of time, the alloy tends to be less ductile and to be more prone to fracture); **(2)** Age-hardening – structural change can occur over long periods of time, leading to the hardening of the objects and consequent embrittlement; **(3)** Spinodal decomposition – modulated structures show higher hardness values, which can lead to a subsequent deterioration, as well as differences in composition, that can make the object more easily penetrated by corrosive agents. [6]

v **Abrasion and physical deformation:** the original topography of the gold alloys are usually altered since it was produced. It may not be easy to determine all reasons, but it can be due to wear by friction (a result of continuous use); conditions of the burial environment; or alterations suffered after the artefact was excavated. [25]

For the study of technological evidence and the preservation of gold Proto-historic artefacts, the conservation of alloys that present these types of corrosion is very important, to understand the impact that the artefacts had in terms of technology, symbolic, political, economic, and ideological significance, and finally to promote better stability of the objects itself [6, 25]. Depending on the owner or curatorial staff, the decision of what type of intervention will be made on the artefact can vary, being that, from an archaeological point of view, the aim should always be to preserve as much as possible of the information given by the object, usually meaning to maintain corrosion layers in the surface of the object [6].

1.5 National Museum of Archaeology: Treasures of Portuguese Archaeology

The National Museum of Archaeology (MNA - *Museu Nacional de Arqueologia*), located in the Jerónimos Monastery, in Lisbon, is the largest archaeological museum in Portugal. It was founded in 1893, under the name "National Museum of Archaeology and Ethnology" [2, 35]. In the year 1980 the permanent exhibition "*Treasures of Portuguese Archaeology*" was inaugurated [35]. It possesses objects of ancient jewellery, originating from excavation sites or bought by goldsmiths or finders [2]. It is an extremely rich collection, with objects from all over the Portuguese territory, allowing the comprehension of the evolution of metalwork from the Chalcolithic to the Middle Ages [2]. It has over 400 gold and silver artefacts, from several typologies, such as necklaces, earrings, vases, torcs and bracelets, some with exceptional goldwork like filigree, granulation, gilding, and soldering.

Some of these artefacts have been studied previously within archaeological, historical or analytical studies, but more recently detailed studies haven't been carried out. With the present work, it was aimed to study a small number of artefacts from BA and IA. The importance of the study of this collection is to understand better the goldwork techniques but the timing is also pertinent because the Museum will be submitted to restructuring works for the next 4 to 5 years. It is fundamental to keep records of the current state of the objects so that their conservation state can be monitored during these years.

In the present dissertation, it will be presented some detailed studies on a selection of artefacts from this collection, mainly earrings. The aim is to study their composition and process of manufacture, to provide further details on western Iberian fine goldwork.

<div align="right">

| 2

</div>

<div align="right">

Studied Artefacts

</div>

A selection was made based on the typology and individual features of the objects. The selection of these artefacts also considered their attributed geographical origin and previous studies that have been performed. In this way, objects from the central and southern areas of Portugal were selected, since they are among the objects with a smaller number of previous analyses.

Ten artefacts were selected from the MNA's collection, attributed to both BA/EIA and LIA[1]. Additionally, three artefacts from particular collections and from recent excavations were added to the study.

The artefacts were divided into two groups, according to their type of goldwork: ***i.*** Plain gold rings (4.1); ***ii.*** Earrings with complex goldwork (4.2).

2.1   Plain gold rings

This group is composed of eight plain gold rings (*"sanguessuga"* – leech-type, according to the MNA terminology), probably destined to be earrings. Two of them from a recent excavation (2017.5135 and 2017.5136), and the remaining from the MNA's collection (Au 11, Au 12, Au 195, Au 196, Au 571 and Au 592).

According to the MNA references and studies previously carried out on the objects, they are attributed to the EIA [2, 9, 36]. Although they come from different provenances, they are quite similar in appearance, characteristics, and dimensions. They present a solid body of circular section, with a crescent shape with short and thin terminals, slimming from the center to slightly apart ends (Figure 2.1).

The artefacts from MNA with the same provenance were given as pairs (Au 11 and Au 12; Au 195 and Au 196; Au 571 and Au 592), as were the two from a recent excavation, of the same provenance and found within the same excavation (2017.5135 and 2017.5136).

---

[1]All the objects in the MNA's collection were subjected to a conservation and restoration intervention at least in 2001, in which deionized water, ethanol, neutral detergent and acetone solvents were used, as well as cleaning with extra-fine calcium carbonate and the use of an ultrasonic bath.
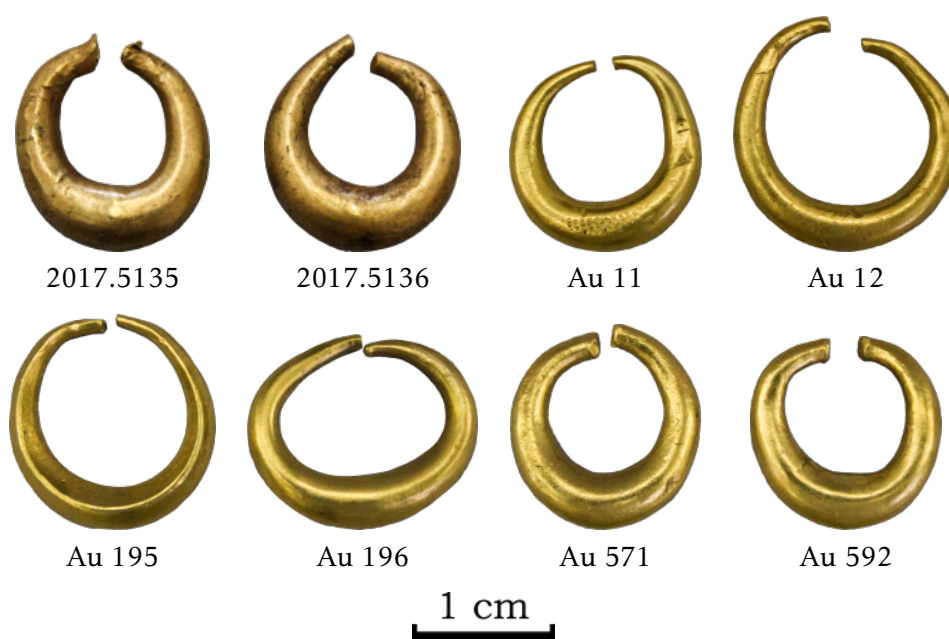
Figure 2.1: Selected artefacts assigned to the BA/EIA (**Dimensions**, width × lenght × thickness (cm): **2017.5135,** 1.41×1.61×0.14-0.48; **2017.5136,** 1.43×1.58×0.16-0.50; **Au 11,** 1.61×1.60×0.10-0.44; **Au 12,** 1.90×1.97×0.12-0.40; **Au 195,** 1.63×1.67×0.10-0.34; **Au 196,** 1.84×1.56×0.10-0.44; **Au 571,** 1.48×1.60×0.17-0.45; **Au 592,** 1.50×1.51×0.17-0.45.).

2.2 Earrings with complex goldwork

This group consists of five artefacts, probably destined to be earrings, which show greater work in terms of detail and techniques used for the decoration of the objects.

Given the technologies used in the production of each artefact, these were subdivided into two groups, one concerning the objects in the MNA's collection (Au 16, Au 180, Au 494 and Au 561), and the other an artefact from a private collection, which appears to present a gilding technique (PART01). According to the MNA references and studies previously carried out on the objects, they are attributed to the LIA, with the exception of Au 180, which is attributed to the EIA [2, 9, 36].

2.2.1 Earrings with filigree, granulation and gold sheets

The four earrings from MNA have distinct typologies and elements between them (Figure 2.2):

Au 16: The artefact is composed of an open hoop with a triangular drop ending. The hoop is a solid body of circular section, that is contoured internally by two gold wires plaiting together. On its exterior, it has two symmetrically positioned rings, of rectangular section. The lower appendice is formed by gold sheets, decorated with filigree and granulation on its surface. It is also decorated with gold wires

7

placed as spirals and forming semi-circles and pear-shaped ornaments. The reverse and the obverse are identical.

Au 180: The artefact is composed by two hollow c-shaped gold sheets, welding together, with repousse decoration. The bottom is outlined by two gold wires plaited together, as well as granules. The top, only presents a wire with a row of granules. The tapering ends present a wire placed in an ondulated shape. On one of the ends, two rings of rectangular section are placed on top of a wire spiral. The reverse and the obverse are identical, with the exception of two gold wires plaited together, on the lower outline, which is only present on one side.

Au 494: The object is composed of a central circular body, with a diamond shape drop ending. The circular body is hollow, composed of two gold sheets, with repousse decoration. It also presents filigree decoration placed in concentric circles (5 circles). In the center, there is a circle surrounded by a spiral wire ring. At the top, on one of the sides, there is a curved gold pin element, affixed at one end. The object is outlined by spheric hollow gold sheets (5 on each side), with granules on their center. The drop ending is overlapping the central body, made of gold sheets and with filigree decoration on the top. The reverse is plain, being the inverse of the obverse.

Au 561: The object consists of a convex and hollow body pear-shaped, composed of two gold sheets, with repousse decoration, outlined by a gold wire. The bottom is also outlined by two plaited gold wires. In the center, there are four wire spirals, with a granule on the center of each one. One of the ends presents two gold rings placed together. The reverse and the obverse are identical.

Au 16   Au 180   Au 494   Au 561

1 cm

Figure 2.2: Selected artefacts from the EIA (Au 180) and LIA (Au 16, Au 494 and Au 561) from the MNA's collection (**Dimensions**, width × lenght × thickness (cm): **Au 16,** 1.89×2.47×0.11-0.36; **Au 180,** 2.24×2.02×0.29-0.39; **Au 494,** 2.63×4.02×0.13-0.45; **Au 561,** 1.68×2.36×0.25-0.65.).

2.2.2 Gilded earring

The artefact PART01 (Figure 2.3), is composed of a c-shape body, composed of six gold wires. One of the ends presents a hole. The bottom is outlined by seven granules, of which two are missing. The reverse and the obverse are identical, having one side more cleaned than the other. The object appears to be gilded (details in this work).

PART01

Figure 2.3: Artefact from the IA presenting gilding (**Dimensions**, width × lenght × thickness (cm): 2.56×2.26×0.04-0.18.).

2.3 Objectives

Four main aims were outlined for the present work:

   i Study the goldsmith work of antiquity, both in terms of alloys used and their composition, and in terms of the evolution of the decorative work carried out in the IP, studied with artefacts from the MNA and also from recent excavations, currently at the Institute for Nanostructures, Nanomodelling and Nanofabrication (CENI-MAT|i3N), at NOVA School of Science and Technology (FCT NOVA);

   ii Study the details of fine gold work carried out in antiquity, with technologies much more rudimentary than those of today;

  iii To analyse the evolution of alloys in IP from the EIA to the LIA, and how they have changed, both in composition and in technologies;

  iv To access heterogeneities in the gold alloys composition at a surface level due to corrosion, technological features, or previous interventions, with consequences in the study of alloys compositions and conservation state of the artefacts.

Part of the present study was performed in the framework of two larger projects: IberianTin (PTDC/HAR-ARQ/32290/2017) and Gold.PT (2022.02608.PTDC), that will study a larger number of artefacts dating to the IA. The *in-situ* MNA analyses of the artefacts presented in this study were performed by a team of three people from FCT NOVA and José de Figueiredo Laboratory (JFL) - Directorate-General for Cultural Heritage (DGPC).

<div align="right">

3

</div>

<div align="right">

Analytical Methods

</div>

3.1 Macro Photography

All artefacts were photographed with a Canon EOS 2000D camera, with 24.1 megapixels, to keep an updated and uniform record of their surfaces. Photographs were performed using natural light, on all sides (reverse, obverse, and profile photographs).

3.2 Digital Optical Microscopy

Digital Optical Microscopy (OM) was performed on all the studied artefacts, using a Dino-Lite AM7915MZTL – EDGE, with 5 megapixels. With this equipment, it was possible to use the Snap Mode (SM) and Extended Depth of Field (EDOF), essential for the record of non-flat surfaces due to its multi-focus ability, as well as a magnification of 10-140×. For greater stability in capturing images, the Dino-Lite Rack (RK-10A) was used. This was an extremely important analysis, once it allowed the observation and measurement of very detailed work carried out by the goldsmiths, namely details that cannot be easily seen with the naked eye. It allowed a better interpretation of the manufacturing techniques, of possible corrosion products and also the record of altered surfaces due to physical or chemical damages.

3.3 X-Ray Fluorescence Spectrometry

X-Ray Fluoroscence Spectrometry (XRF) analyses were performed with two different equipments:

- Portable X-Ray Fluoroscence Spectrometry (pXRF) was performed with a Tracer 5*i* Bruker, with a Be window, Rh source, a voltage of 40kV, a current of 30μA, and an acquisition time of 100 seconds. At least two analyses were made in different areas, being that all the thirteen artefacts studied were analysed with this equipment. The analysed area is approximately 3 mm in diameter. In the case of the earrings with

complex gold work, due to the small size of the decoration elements, each analysis
may include more than one structural/decorative element.

- Micro X-Ray Fluoroscence Spectrometry (micro-XRF) was performed with an ArtTax
  (Intax GmbH; Bruker) spectrometer, with a Be window, Mo source, a voltage of 40
  kV, current of 600 μA, and acquisition time of 100 seconds. Only the artefact
  PART01 was analysed by this technique in different spots. The area of analysis is
  approximately 100 μm in diameter.

Qualitative analyses were carried out with the ARTAX software, and quantitative analyses were made with the software bAxil, which uses a fundamental parameter method
and experimental calibration factors that were calculated with certified reference materials: *Gold ERM-EB506*, *Gold ERM-EB507* and *Gold ERM-EB508* for the pXRF analysis;
Au-Ag-Cu standard *IAEA I, II, III* and *IV* for the micro-XRF analysis.

The experimental relative error for the pXRF analysis was calculated as lower than 7
wt.% for major elements, and quantification limits as: 0.06 wt.% Au; 0.09 wt.% Ag (Kα
lines); 0.11 wt.% Ag (Lα lines); 0.03 wt.% Cu. The experimental relative error for the
micro-XRF analysis was calculated as lower than 4 wt.%, while quantification limits are:
0.03 wt.% Au; 1.30 wt.% Ag (Kα lines); 1.34 wt.% Ag (Lα lines); 0.15 wt.% Cu.

Quantitative analyses were performed taking into account the Lα and Kα lines of
silver, to consider for different depths of analysis (L lines emerge from a smaller depth
than the K lines) [37].

The XRF is one of the main techniques used in the analysis of ancient metals [38, 39]
since it is non-destructive. In the present work it was used with the advantage of being
able to perform analyses *in-situ* in the MNA and for the investigation of small areas in
the gilded artefact.

3.4 Scanning Electron Microscopy with Energy Dispersive Spectroscopy

The Scanning Electron Microscopy (SEM) analysis was carried out in a Zeiss DSM 962
equipment, with Secondary Electrons (SE), Backscattered Electrons (BSE) and an Energy
Dispersive Spectroscopy (EDS) detector (Oxford INCAx-act LN2-free Analytical 10 mm^2,
resolution of 125 eV) [39]. The working distance was of 25 mm, an acceleration voltage
of 20 kV, a filament current of ~3 A, and an emission current of 70 μm [39]. The analyses
were performed without any superficial conductive coating [39].

The SEM-EDS analyses are extremely useful, once they provide images with high-
quality of the morphological details on the surface of the objects, often related to the
manufacturing processes or to marks of use [38]. Also, it provides a non-destructive
micro-analysis that gives information about the chemical composition of the alloys at

selected areas [38]. It allows a greater magnification than OM. In the present study it was applied to the 2017.5135, 2017.5136 and PART01 artefacts.

Results and Discussion

4.1 Plain gold rings

4.1.1 Superficial compositional variations

Firstly, the analysis of artefacts 2017.5135 and 2017.5136 is discussed, since they were analysed by both pXRF and SEM-EDS (Table 4.1). These results allowed an evaluation of the surface composition of the objects at different depths since the SEM-EDS analyses are more superficial than the pXRF ones [11, 40].

The results showed that towards the surface, the Au content is higher, while at greater depth, the Ag content tends to increase, from 5-7.5 wt.% to 12.5-15 wt.% (Figure 4.1). These results may be related to the dissolution of the anodic constituents at the surface of the gold alloys. From the present analysis it is not possible to detect very significant changes in the Cu contents. The values at greater depth, that is, those obtained when using the Kα lines of Ag in XRF analyses, are thus probably more representative of what would be the original composition of the artefacts.

With the SEM-EDS analysis, it is also possible to analyse different areas of variable dimensions. These areas reveal some composition heterogeneities that can be related to some superficial dirt, but also some heterogeneities in the contents of Ag that can be related to superficial corrosion, visible in the elemental mapping by SEM-EDS of the earring 2017.5136 (Figure 4.2).

Table 4.1: Elemental composition of the plain gold rings by pXRF and SEM-EDS, normalised to 100 wt.% (regarding Ag, using Kα lines addresses for a more deep analysis than using Lα lines). Average and standard deviation of at least three analyses are presented.

Inv. No.	Weight (g)	Provenance	Element	Normalised Values (100 wt.%)		
				pXRF (wt.%) using		SEM-EDS (wt.%)
				Ag Kα lines	Ag Lα lines	
2017.5135	5.45	São Julião, Aveiro	**Au**	84.55 ± 0.75	91.65 ± 0.35	92.26 ± 1.26
			Ag	14.00 ± 0.70	6.76 ± 0.23	6.86 ± 1.82
			Cu	1.47 ± 0.05	1.57 ± 0.08	0.89 ± 0.23
2017.5136	5.70	São Julião, Aveiro	**Au**	86.20 ± 0.40	95.05 ± 0.78	93.51 ± 3.68
			Ag	13.05 ± 0.35	4.19 ± 1.41	5.73 ± 3.14
			Cu	0.60 ± 0.03	0.77 ± 0.05	0.76 ± 0.58
Au 11	5.18	Boiça do Louro, Lisboa	**Au**	86.85 ± 0.67	91.98 ± 0.78	
			Ag	12.58 ± 0.48	7.37 ± 0.71	
			Cu	0.60 ± 0.31	0.63 ± 0.35	
Au 12	4.76	Boiça do Louro, Lisboa	**Au**	87.88 ± 0.38	92.62 ± 0.32	
			Ag	10.77 ± 0.29	5.98 ± 0.43	
			Cu	1.36 ± 0.15	1.42 ± 0.18	
Au 195	4.87	Outeiro da Cabeça, Lisboa	**Au**	89.57 ± 0.17	92.17 ± 1.72	
			Ag	10.20 ± 0.08	7.59 ± 1.82	
			Cu	0.25 ± 0.10	0.25 ± 0.13	
Au 196	5.17	Outeiro da Cabeça, Lisboa	**Au**	85.10 ± 0.45	89.30 ± 0.92	
			Ag	12.70 ± 0.16	8.41 ± 0.39	
			Cu	2.20 ± 0.47	2.28 ± 0.58	
Au 571	5.18	Boiça, Leiria	**Au**	86.60 ± 0.08	89.00 ± 0.52	
			Ag	11.93 ± 0.09	9.49 ± 0.59	
			Cu	1.50 ± 0.13	1.54 ± 0.17	
Au 592	4.76	Boiça, Leiria	**Au**	82.50 ± 0.22	91.23 ± 0.55	
			Ag	17.03 ± 0.25	8.28 ± 0.68	
			Cu	0.47 ± 0.12	0.51 ± 0.17	
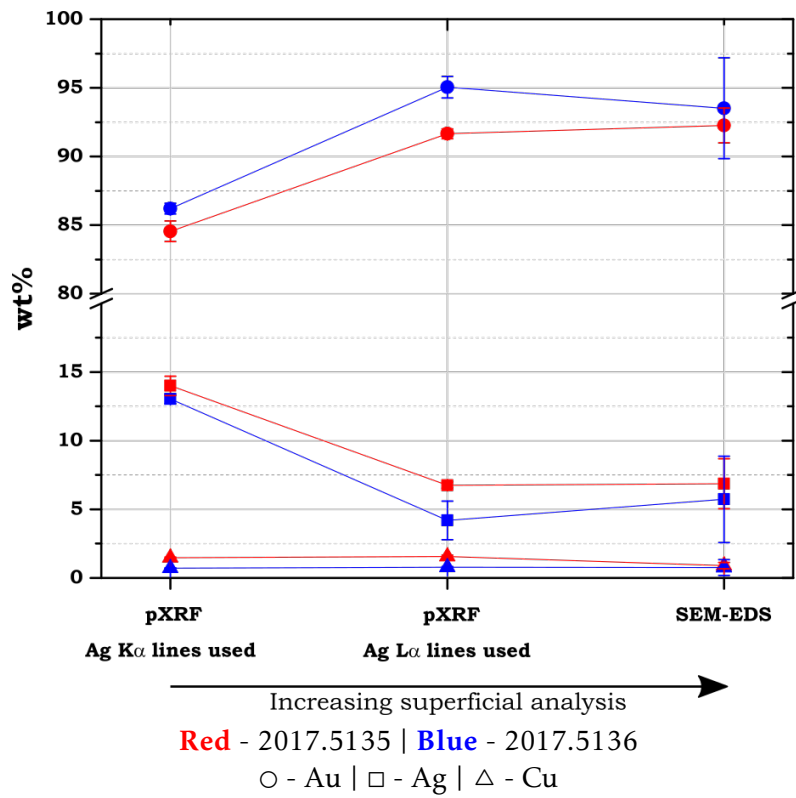
Figure 4.1: Elemental analysis (Au, Ag and Cu contents) of the artefacts 2017.5135 and 2017.5136 by pXRF and SEM-EDS. The type of analysis is ordered following an increase in the type of superficial analysis (average and standard deviation results are presented).
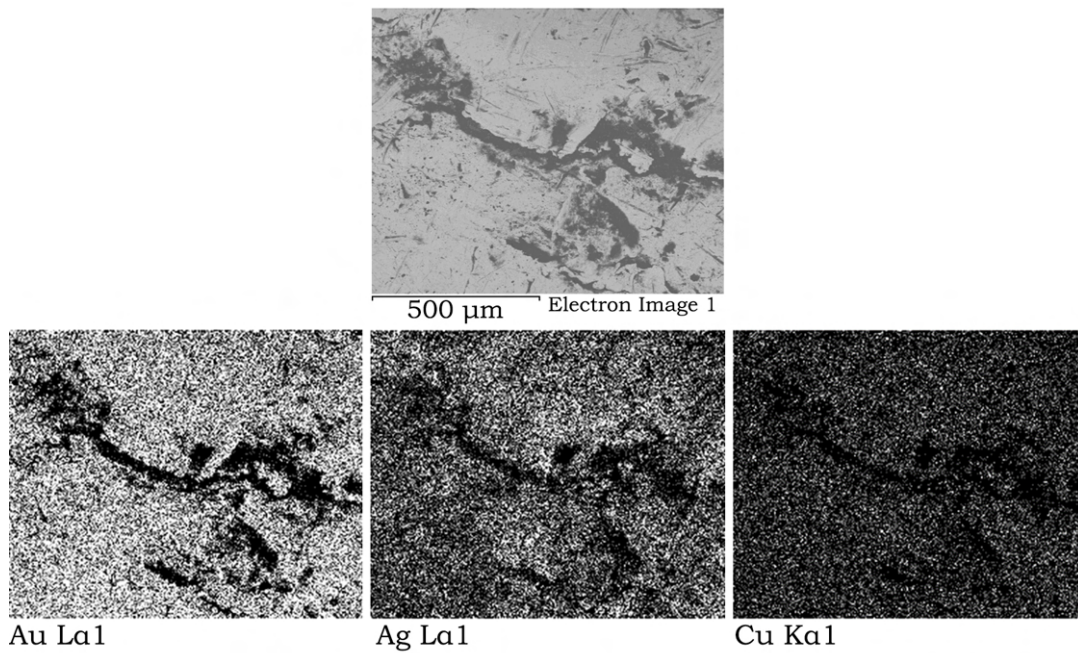
Figure 4.2: SEM-EDS (BSE image) elemental mapping of the artefact 2017.5136, showing heterogeneity of the Ag distribution at the surface.

The pXRF results of these two objects were then compared with the results from the

15

six artefacts of similar typology from MNA (Table 4.1), using both Ag Kα and Lα lines for quantification, so that it is possible to perceive possible composition heterogeneities on the surface of the earrings (Figure 4.3). It was found that the Au and Ag contents are inversely related, that is, the higher the Au content, the lower the Ag content, and vice-versa, being that higher Ag values were obtained when using Kα lines (related to deeper analyses). Again, the Ag content seems to be lower towards the surface. A relation between Au or Ag values and Cu content is not obvious.

In the case of artefacts 2017.5136 and Au 592, there is a greater difference between the Ag content towards surface (Lα lines) than towards internal zones (Kα lines), namely near 10 wt.% difference, when the other artefacts present a difference smaller than 7 wt.%. Again, this may be a result from Ag lixiviation at surface. In the case of the artefacts Au 195 and Au 571 the difference obtained for the respective Kα and Lα lines of Ag is smaller when compared with the other artefacts, thus revealing a more homogeneous composition at different depths. Since the artefacts in the MNA have already been subject to conservation and restoration treatments, a slightly more abrasive cleaning that may have been carried out may have removed the outer layer of alteration.
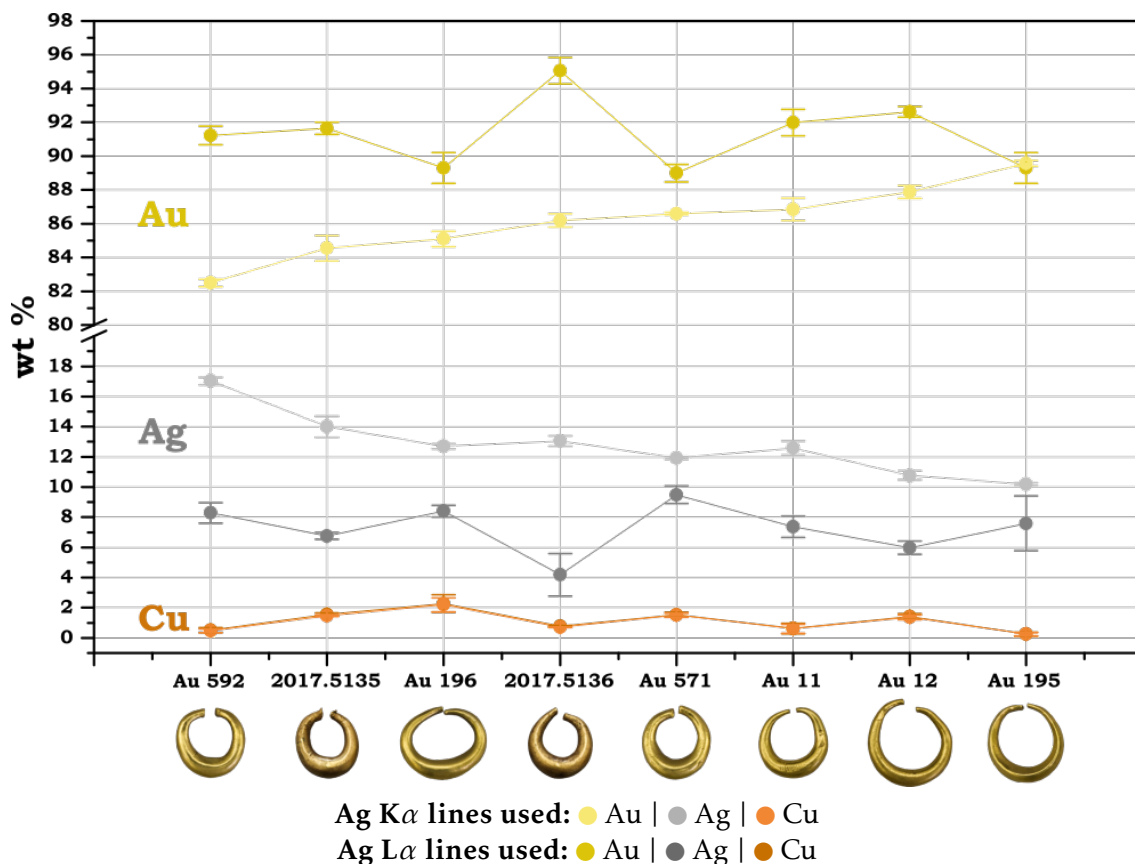
Figure 4.3: Elemental composition of the plain gold rings by pXRF (average with standard deviation values used), comparing the results obtained when using the Ag Kα and Lα lines, showing that there are composition heterogeneities towards the surface.

These results also showed that the value of the standard deviation obtained for the analysis of each object is lower than the difference between the values obtained with the Ag Kα and Lα lines, with the exception of the Au 195 artefact. It thus shows that there is a greater difference between the innermost and outermost composition of the artefact than throughout the surface of whole object. It reveals that the depth of analyses bond by the equipment or methodology used is more significant in explaining variations of the composition results than analyses on different areas of the artefacts.

By directly comparing the results obtained for the Ag Kα and Lα lines of all artefacts it becomes clear that a silver depletion at the surface of the object has occurred (Figure 4.4). As previously mentioned, the Au 195 and Au 571 artefacts, which present a more homogeneous composition or a loss of the most superficial/altered layer, present the closest Ag contents for both Kα and Lα lines.

■ 2017.5135 | □ 2017.5136 | ● Au 11 | ○ Au 12
▲ Au 195 | △ Au 196 | ◆ Au 571 | ◇ Au 592
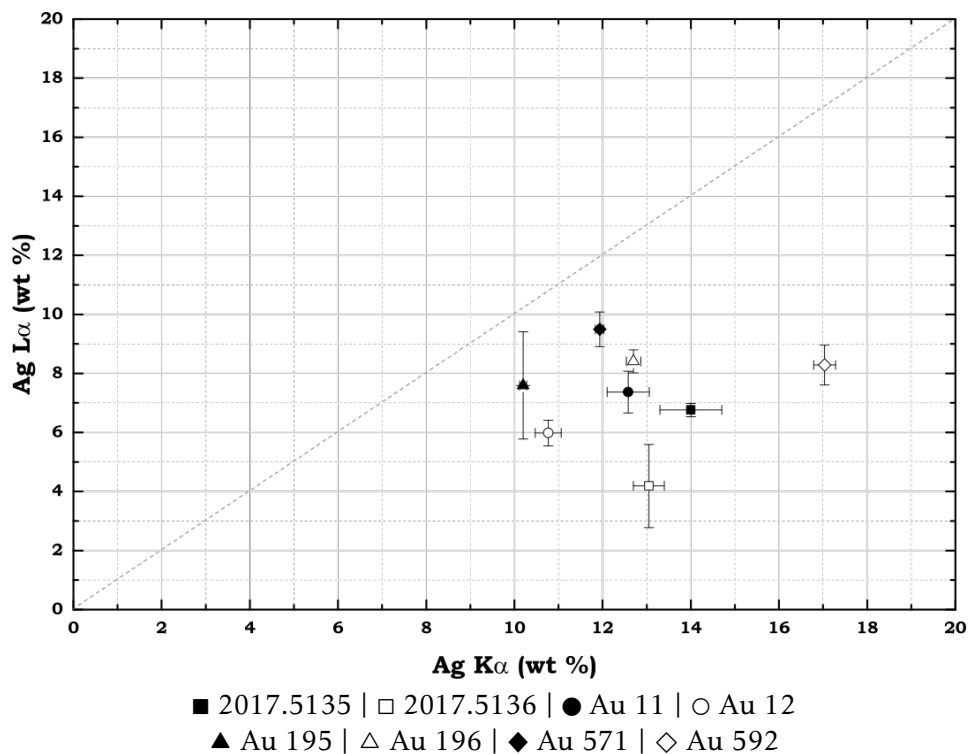
Figure 4.4: Comparison of the Ag contents obtained with the Ag Kα and Lα lines of the plain gold rings, by pXRF (average with standard deviation values used).

No relationship between artefacts of the same provenance and their composition was found, being that the composition of the eight objects is quite similar to each other. The most distinct of all is artefact 2017.5136, whose composition may be related to a greater surface leaching, showing a higher Au and lower Ag content, compared to the other objects. All artefacts show an average composition in a range of 82 to 89 wt.% Au, 11 to 17 wt.% Ag (using the Ag Kα lines) and 0.2 to 1.5 wt.% Cu.

Previous published analyses of the six artefacts from MNA by Energy Dispersive X-Ray Fluorescence (EDXRF) [9] and by Optical Emission Spectroscopy (OES) of four of

them (Au 11, Au 12, Au 195 and Au 196) [41] are presented in Figure 4.5. Since OES analyses require a sample from the interior of the objects, these analyses represent the most deep analysis. It should be noted that the results presented by Hartmann must be converted [8, 41, 42]. Ag values are presented in relation to the specific volume of the object, which according to R. B. Warner and M. Cahill [42] may present a relative uncertainty (1 s.d.) of 25%. The Cu and Sn values are presented as a percentage of the Au value (Au = 100%), and these values should be properly converted for a correct interpretation [41, 42].

By comparison with the previous EDXRF analyses and those performed in the present study, the same trend of higher Ag composition towards the interior of the artefacts is observed. It was possible to observe that the Ag content inside the objects is much higher in the results of the OES analysis, referring again to the dissolution of the anodic constituents on the surface of the objects. Thus, in a more superficial analysis (Lα lines of Ag in the pXRF) the Ag contents are among 4 to 10 wt.%, while in the OES analysis the Ag increase to values among 9 to 19 wt.%. Generally, an increase to the double is therefore observed, but regarding single objects higher differences can be present, as in Au 11 where an increase from ~5 wt.% (pXRF Lα lines) to ~20 wt.% (OES) was observed. It was also found that the results obtained previously by EDXRF fall within the results obtained by the most recent analyses (pXRF), as would be predicted given that both use the same technique.

Red - pXRF (Ag Kα lines used) | Black - pXRF (Ag Lα lines used)
Yellow - EDXRF [9] | Blue - OES [41]
● Au 11 | ○ Au 12 | ▲ Au 195 | △ Au 196 | ◆ Au 571 | ◇ Au 592
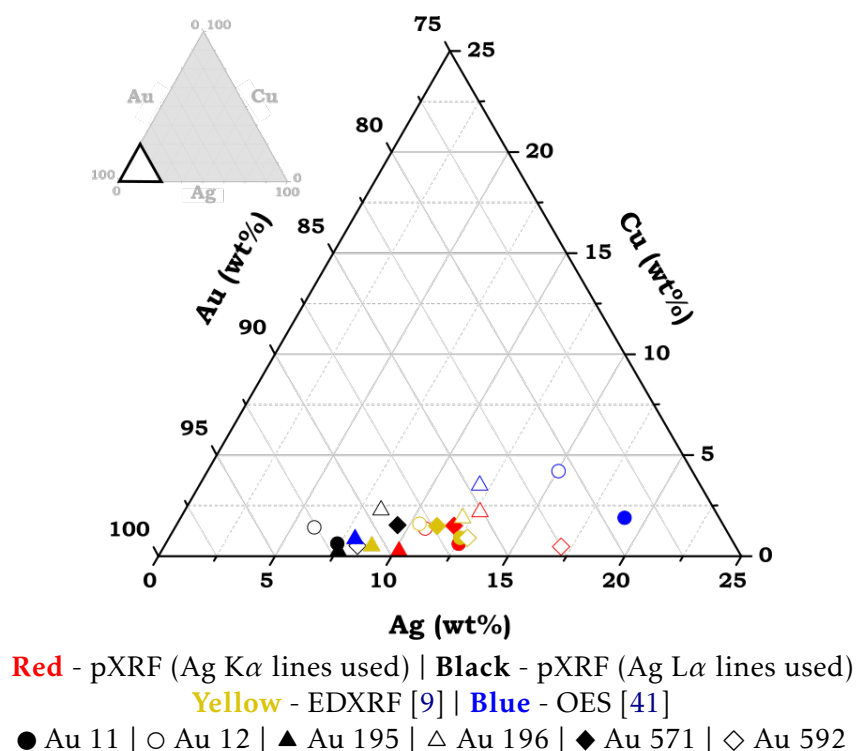
Figure 4.5: Results obtained by pXRF, using Ag Kα and Lα lines (average values) for the plain gold rings from MNA, with the results of previous analyses carried out by EDXRF [9] and OES [41].

4.1.2 Manufacturing techniques - superficial decorations and heterogeneities

The production of the plain gold rings (Figure 4.6) could be made initiating from melting metal cast to the shape of an bar-type ingot, using native gold, which would after undergo deformation to obtain a rounder and longer shape, that was the base shape of the ring [7, 40, 43]. It would then be further heated and deformed (forging) to lengthen the ends while maintaining the size of the central area of the shape, resulting in the final object that this central area presents a small edge (Figure 4.7). It was afterwards placed around a cylindrical shape in order to obtain the final ring shape.
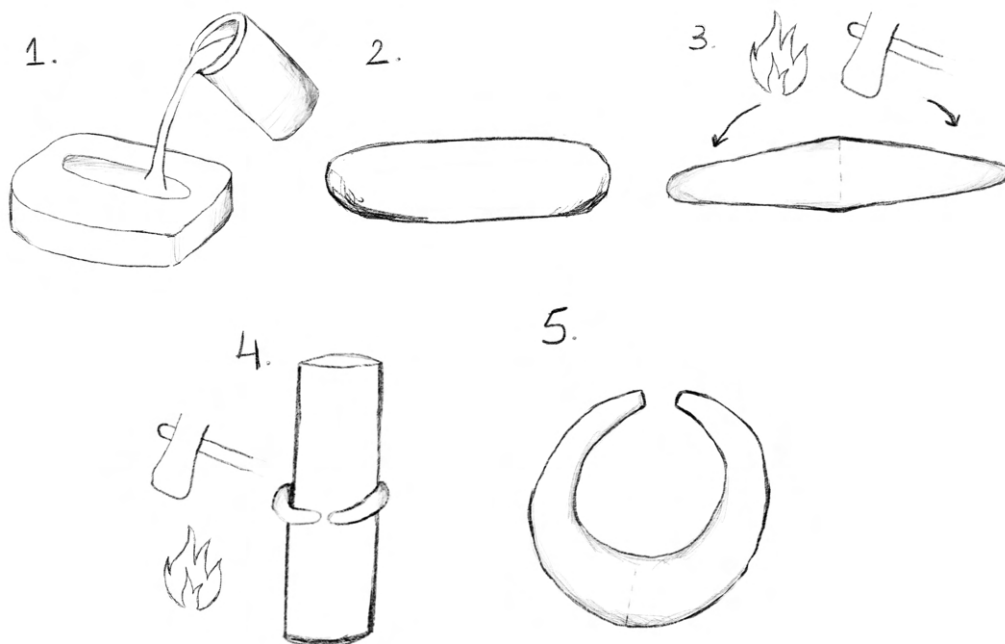
Figure 4.6: Proposal for the production phases of the plain gold rings.
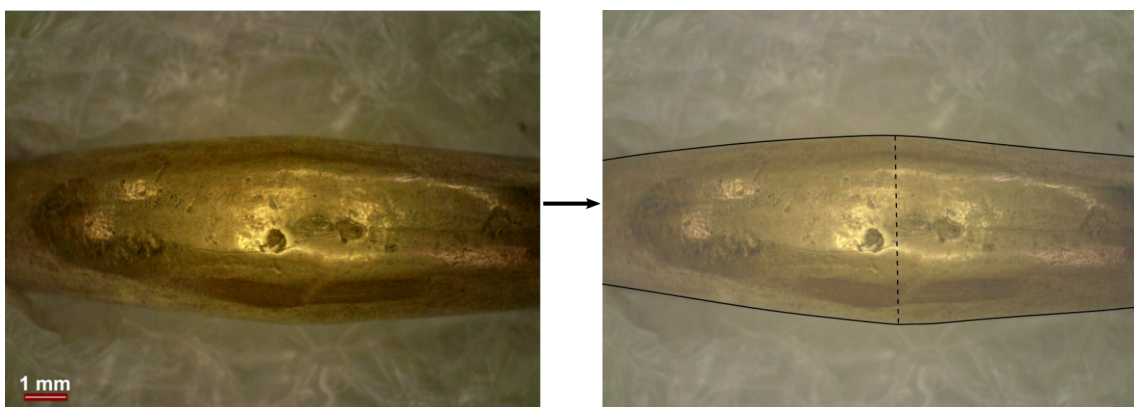
Figure 4.7: Au 196 (OM image), example of the shape at the central area that shows a ridge that could have been a result of step 3 of Figure 4.6.

19

Although the eight plain gold rings present a similar typology, it was possible to observe that three of them present decorative motifs that distinguish them from the others. That is the case of the following objects (Figure 4.8): 2017.5136, which shows, on one side, small incisions, possibly made with a chisel and punch, which form a shape of a triangle; Au 11, which, on both sides, in the centre, shows small incisions, made with a chisel or punch; Au 195, which shows a crescent-shaped angular form on one of the sides, which might have resulted from the thermo-mechanical shaping process.
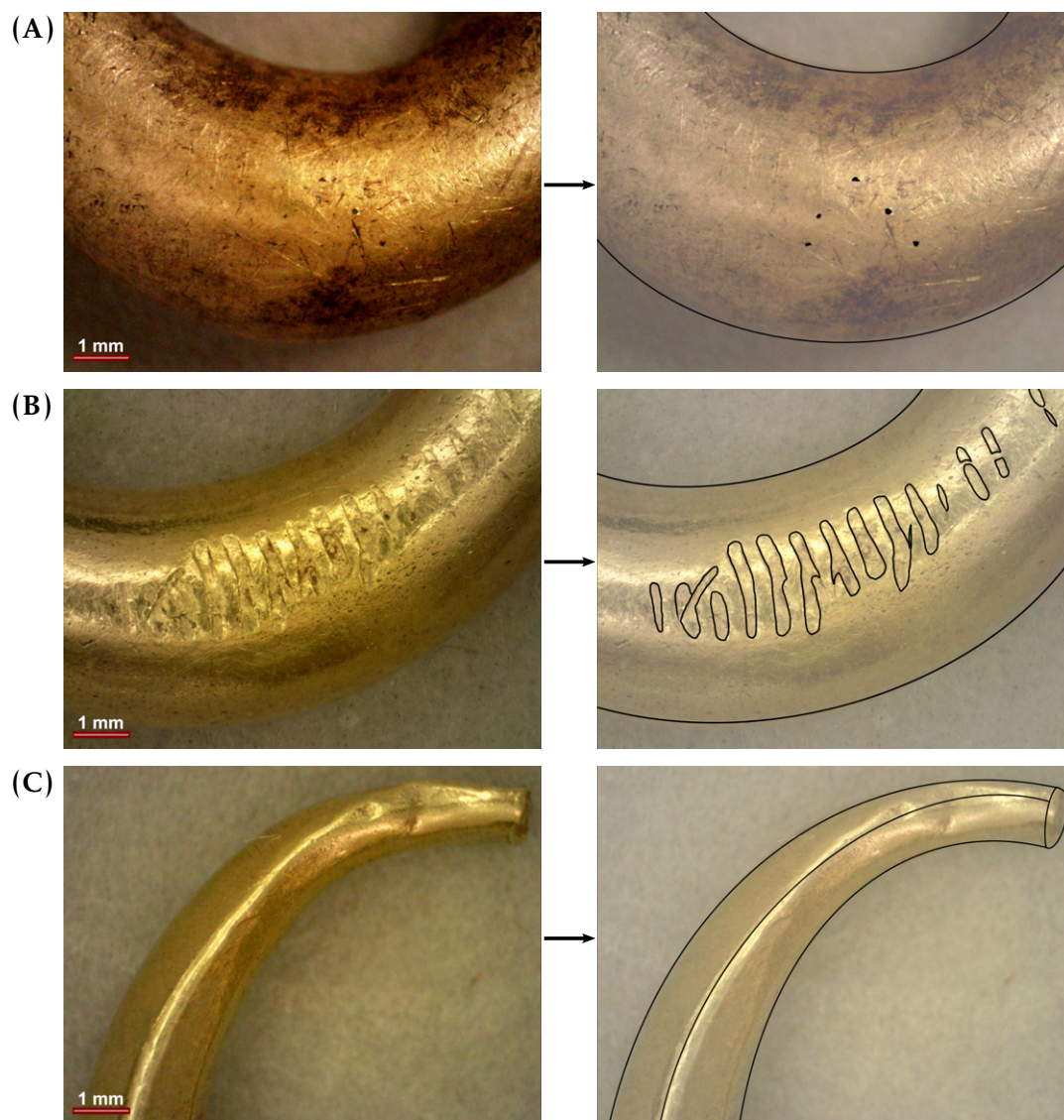
Figure 4.8: OM images of the details of the decoration in the earrings: **(A)** 2017.5136, small incisions which form the shape of a triangle; **(B)** Au 11, small incisions that exist on both sides of the artefact; **(C)** Au 195, crescent-shaped angular form on one of the sides.

All the artefacts, at first sight, appear to have a smooth surface. However, the observation by OM reveals that their surfaces present some irregularities, from small detachments to areas that, due to their handling, use and/or the position in which they were buried, have lost their original shape (Figure 4.9). Surface texture heterogeneities

are more noticeable in artefacts 2017.5135 and 2017.5136, since they have not been subject to conservation and restoration treatments. In these artefacts, by SEM-EDS, it was also possible to observe some micro-detachments, deformations and scratches, probably caused by the conditions in which they were buried (Figure 4.10).
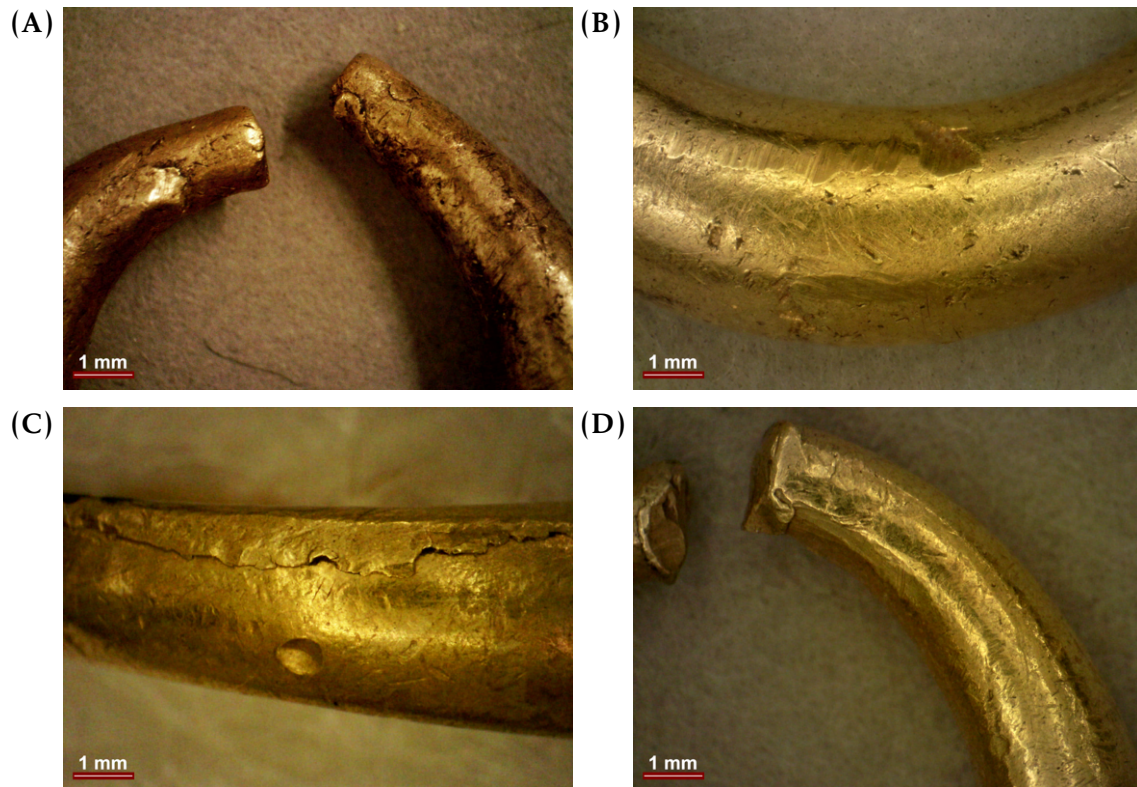
Figure 4.9: OM detailed images of the irregularities on the plain gold rings surfaces: **(A)** 2017.5136, deformations and cracks in the terminal area; **(B)** Au 12, deformations and possible wear marks in the central body area of the object; **(C)** Au 195, marks due to the production process near a terminal; **(D)** Au 571, deformations and scratches on the object's terminals.
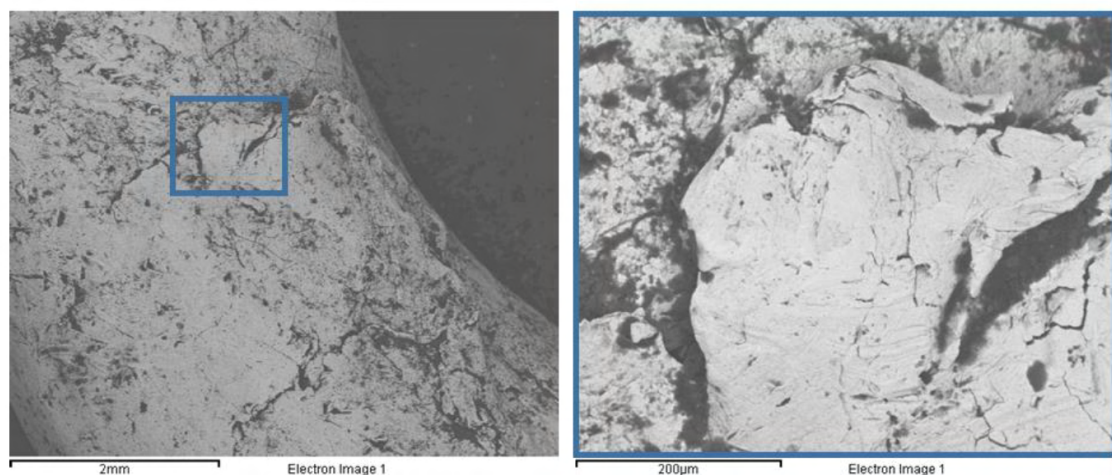
Figure 4.10: BSE image detail (SEM-EDS) of a detachment on the surface of the artefact 2017.5135.

4.2 Earrings with complex goldwork

4.2.1 Gold alloy compositions

The analyses by pXRF of the four artefacts from MNA which present similar typological elements led to different conclusions. It was observed that the Au 16 artefact has the highest Cu content (about 4.5 wt.%), while in the others have lower Cu content (1.7 wt.% in Au 180) or absence of Cu (Cu was not detected in Au 494 and Au 561). In artefact Au 494, Cu was only found in the analysis made over the curved gold pin element, providing a content of about 2.2 wt.% of Cu. Regarding Au and Ag contents, when the Ag Kα lines are considered, the Au content is higher in the Au 16 and Au 494 objects (about 87 wt.%) and lower in the Au 561 artefact (about 83.7 wt.%), and the opposite is true for Ag contents, which are higher in the Au 561 artefact (about 16.3 wt.%) and lower in the Au 16 artefact (about 8.1 wt.%) (Table 4.2).

Table 4.2: Elemental composition of the artefacts from MNA by pXRF, normalised to 100 wt.%.

Inv. No.	Weight (g)	Provenance	Element	Normalised Values (100 wt.%) pXRF (wt.%) using	
				Ag Kα lines	Ag Lα lines
Au 16	2.92	Monte Molião, Faro	Au	87.37 ± 1.43	87.70 ± 1.59
			Ag	8.10 ± 0.37	7.71 ± 1.85
			Cu	4.55 ± 1.15	4.57 ± 1.21
Au 180	3.03	Santana das Cambas, Beja	Au	86.38 ± 1.16	89.45 ± 0.88
			Ag	11.93 ± 0.67	8.79 ± 0.96
			Cu	1.73 ± 0.45	1.78 ± 0.48
Au 494	6.67	Castro de Cabeça de Vaiamonte, Portalegre	Au	87.48 ± 0.28	87.30 ± 0.71
			Ag	12.52 ± 0.28	12.70 ± 0.71
			Cu	*n.d.*	*n.d.*
			Au	83.00	84.50
			Ag	14.80	14.80
			Cu	2.19	2.22
			(analysis to the curved gold pin element)		
Au 561	2.82	Castro de Cabeça de Vaiamonte, Portalegre	Au	83.70 ± 0.00	86.43 ± 0.31
			Ag	16.30 ± 0.00	13.57 ± 0.31
			Cu	*n.d.*	*n.d.*

Compared to the plain gold rings, the analyses using Kα or Lα lines for Ag in these IA objects does not show such great differences. Nevertheless, the Ag content decreases in the more superficial analyses (using Ag Lα lines) for all artefacts except Au 180 (that maintains the content), referring to the dissolution of the anodic constituents at the surface of the object (Figure 4.11). Generally, and taking into consideration that these artefacts possess various elements which were not possible to analyze independently (except for the curved gold pin element in Au 494), the results represent a mixture of various elements (filigree, granules, sheets). Also, the composition results show no clear differences among the artefacts, except for the fact that two of them (Au 494 and Au 561) have their main body made with very low or absence of Cu. Interestingly, these two

artefacts have the same provenance, which can indicate that both have been made in the same workshop.

Red - Ag Kα lines used | **Black** - Ag Lα lines used
★ Au 16 | ▼ Au 180
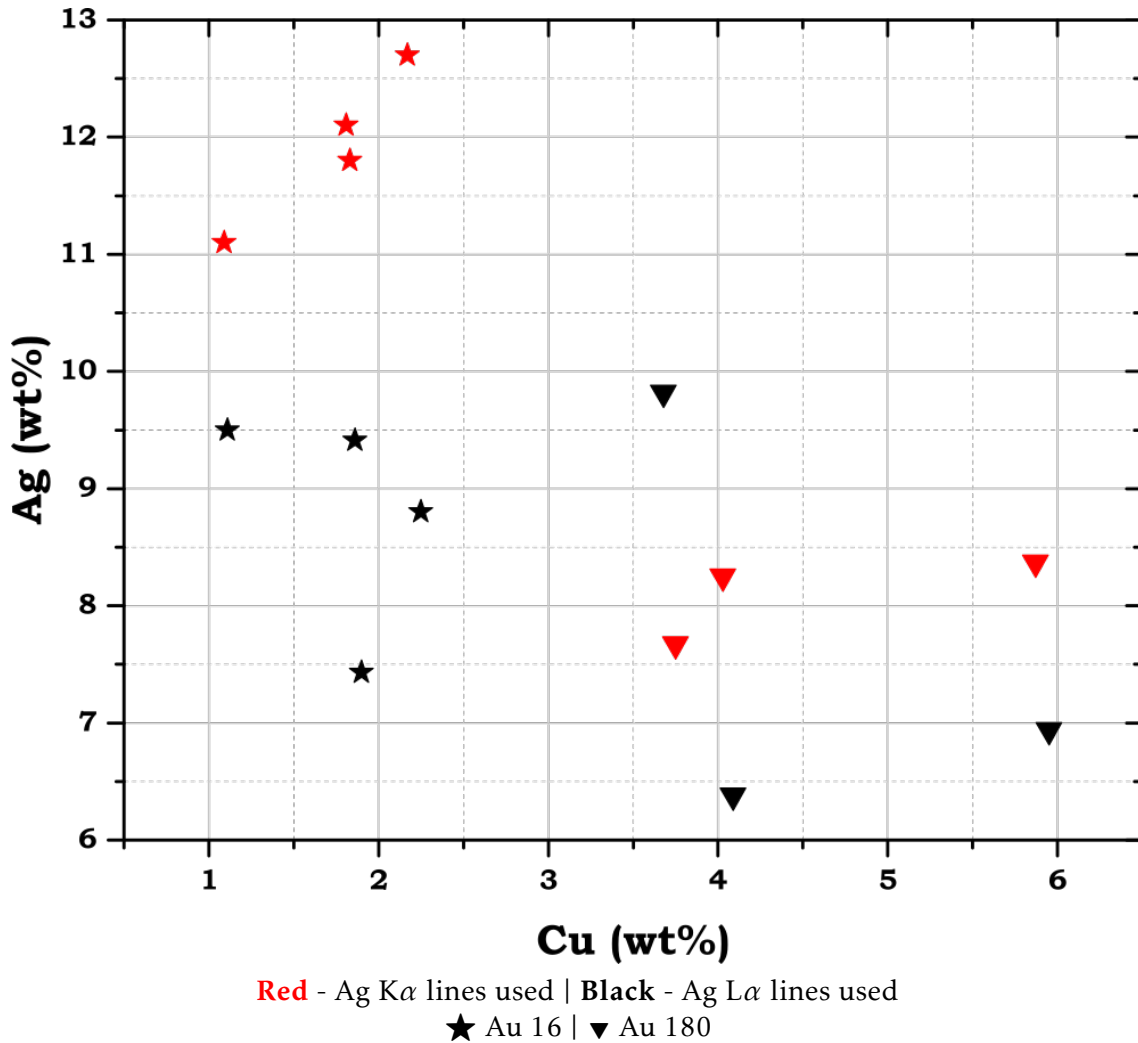
Figure 4.11: Elemental composition of Au 16 and Au 180 by pXRF (the two artefacts in which Cu was detected), comparison of the results obtained for Cu content with those of Ag, showing that there is no linear relationship between the compositions of both artefacts.

The artefacts Au 494 and Au 561 are exceptional cases of objects attributed to the LIA in the IP. In the case of Au 494, it can be assumed that it is made of at least two distinct alloys, since the main body of the object did not show Cu in the pXRF analysis, but the curved gold pin element already showed a Cu content. This element may have been added later or was purposely made in a different alloy.

Three of the artefacts show a standard deviation of the Ag content smaller than the difference between the results obtained for the Ag Kα and Lα lines, with the exception of Au 16, which can be due to the alteration of the surface due to a more abrasive cleaning (Figure 4.12).

Ag Kα lines used: ● Au | ● Ag | ● Cu
Ag Lα lines used: ● Au | ● Ag | ● Cu
○ **Au 494**, curved gold pin element
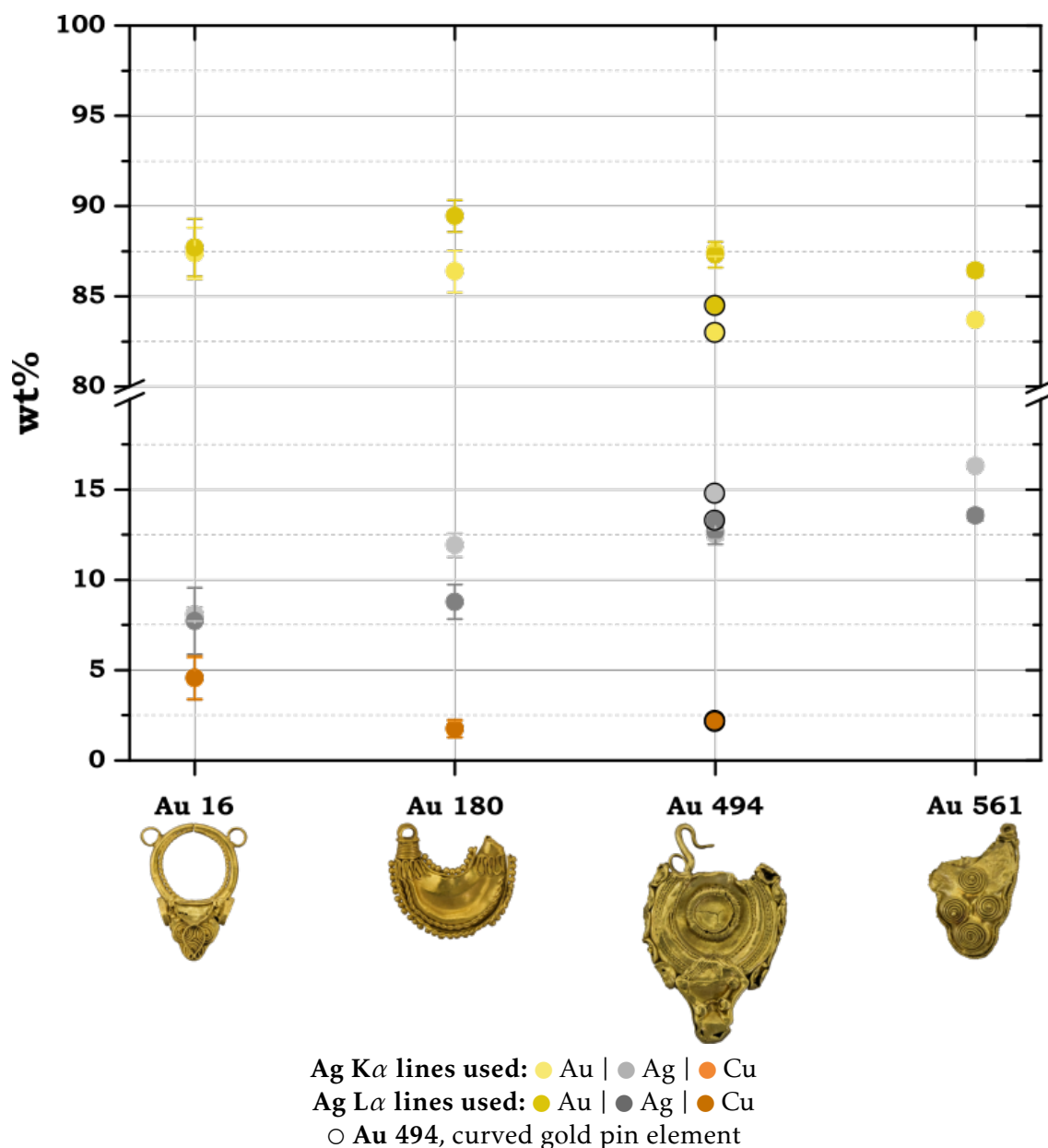
Figure 4.12: Elemental composition of Au 16, Au 180, Au 494 and Au 561 by pXRF (average with standard deviation values showed), comparing the results obtained when using the Ag Kα and Lα lines (relative to depth compositional differences).

In the case of Au 561, in which no evidence of Cu was detected, both the Au and Ag contents were lower, according to the Ag Kα lines, when compared to those obtained for the body of the Au 494 object. In the case of Au 561 and Au 180, the difference between the values obtained for the Ag Kα and Lα lines show a higher interval between them (of ~3 wt.% Ag), revealing a thicker surface layer with less Ag content. It should also be noted that, with three different analysis areas, the results obtained for the Ag Kα lines were identical, revealing a fairly homogeneous composition throughout the object.

These four artefacts have also been previously analysed by OES [41]. Those analyses show that in the Au 494 and Au 561 a low amount of Cu exists at greater depths (0.9 and

0.19 wt.%, respectively) and that for the Au 16 and Au 180 artefacts the Cu content is also higher than determined by pXRF (3-5 wt.% increase). This means that Cu has probably also been selectively lost at the surface, as Ag. Again, the Ag values are higher in the OES analysis than those by pXRF. However, given the small amount of Cu detected, only with deep sample analyses, it could mean that the alloy used to create these objects had no Cu intentionally added, a rare case for artefacts attributed to the IA.
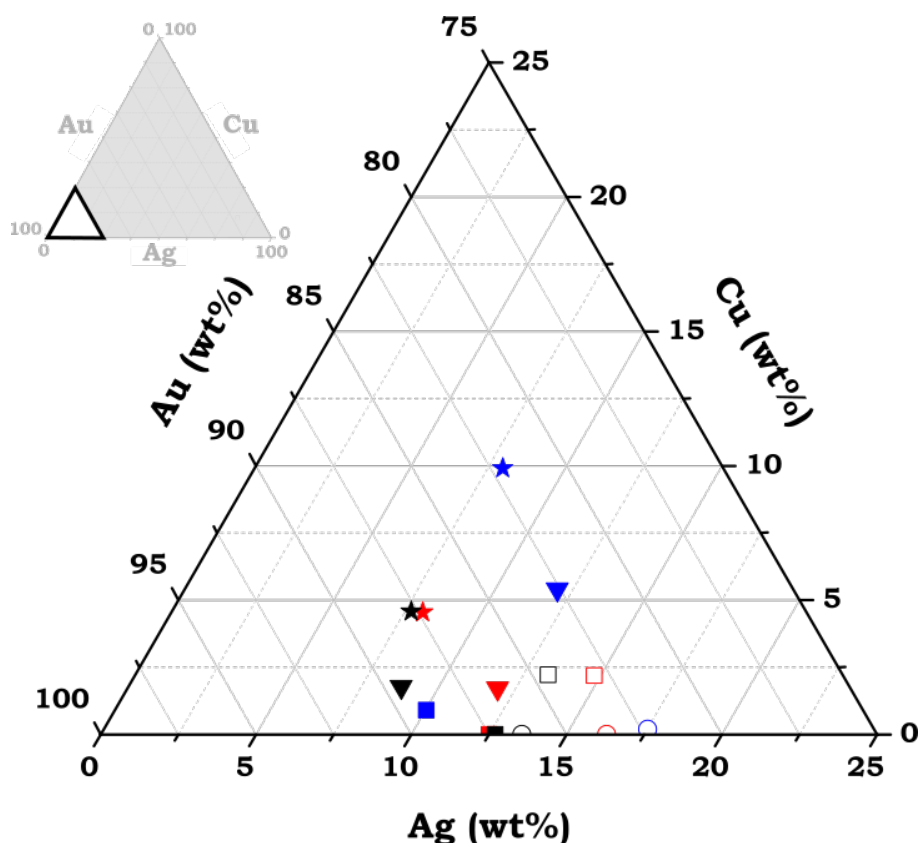
Red - pXRF (Ag Kα lines used) | **Black** - pXRF (Ag Lα lines used) | **Blue** - OES [41]
★ Au 16 | ▼ Au 180 | ■ Au 494 | □ Au 494 (*curved gold pin*) | ○ Au 561

Figure 4.13: Results obtained by pXRF, using Ag Kα and Lα lines (average values), with the results of previous analyses carried out by OES for the MNA artefacts [41].

4.2.2 Gilding

For the analysis of artefact PART01, the results obtained by pXRF analysis will be first discussed, since the analysis area is about 3 mm, and provides an idea of the overall composition of the artefact. The results showed a fairly homogeneous composition (with a low standard deviation), and the difference obtained between the Ag Kα and Lα lines was also similar to the results obtained previously for earrings with a complex goldwork. In comparison to the previous earrings, it presents significantly higher Ag contents, of ~25-30 wt.% (comparing to 7-16 wt.% Ag in the MNA earrings) and a higher Cu content, of about 8 wt.% (Table 4.3).

Table 4.3: Elemental composition of PART01 by pXRF, normalised to 100 wt.%.

Inv. No.	Weight (g)	Provenance	Element	Normalised Values (100 wt.%) pXRF (wt.%) using	
				Ag Kα lines	Ag Lα lines
PART01	1.13	Western IP	**Au**	61.47 ± 1.22	66.67 ± 0.45
			Ag	30.57 ± 1.86	24.80 ± 1.18
			Cu	7.98 ± 0.72	8.51 ± 0.72

Observation by OM was performed both to the body of the piece and to the beads, which to the naked eye appeared to have an interior in a different material than the outside. It was found that, indeed, there is an interior dark material (*core*) and an exterior that suggests a gold-like covering (*coating*). In other areas, such as the sides, and small gaps, it was also possible to see these differences in materiality, besides the presence of some superficial deposits, which presented many similarities to the inner part of the granules (Figure 4.14).
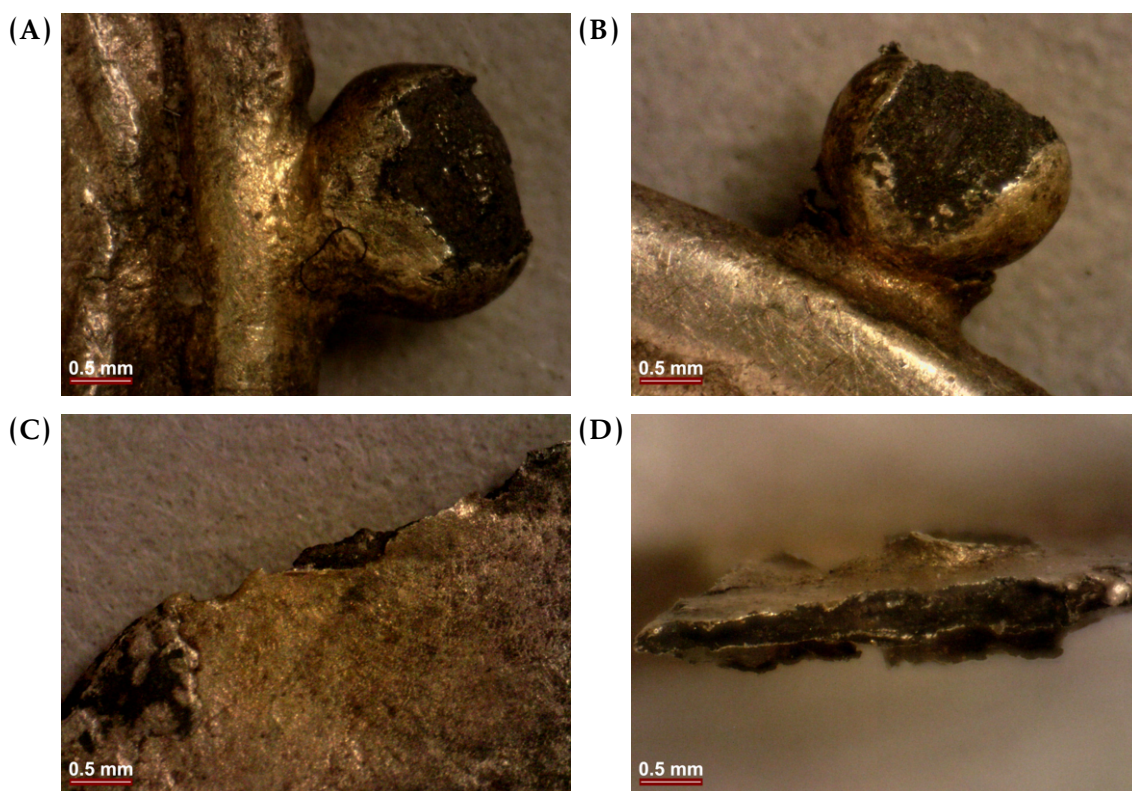
Figure 4.14: OM images of details of the earring PART01: **(A)** and **(B)** detail of interior dark material on the granules; **(C)** detail of a gap on the earrings' surface; **(D)** detail of the earring's top, from profile.

Micro-XRF analyses were performed in order to evaluate heterogeneities in different areas of the object. The analysis of the granules was made in the interior dark material and the gold-like exterior. This revealed that the granule interiors are mostly made of silver, with only 8 to 12 wt.% of Au on them, in opposition to the granule exteriors, which

have between 40 and 60 wt.% of Au. Thus, it was concluded that the granules are in a silver-rich alloy, now corroded, and they have a gold-rich coating, now partially missing (Figure 4.15).

Granule interior (6 spot analyses, wt.%)			Granule exterior (7 spot analyses, wt.%)		
Au	Ag	Cu	Au	Ag	Cu
8-12	87-91	0.4-0.9	40-60	27-53	4-8
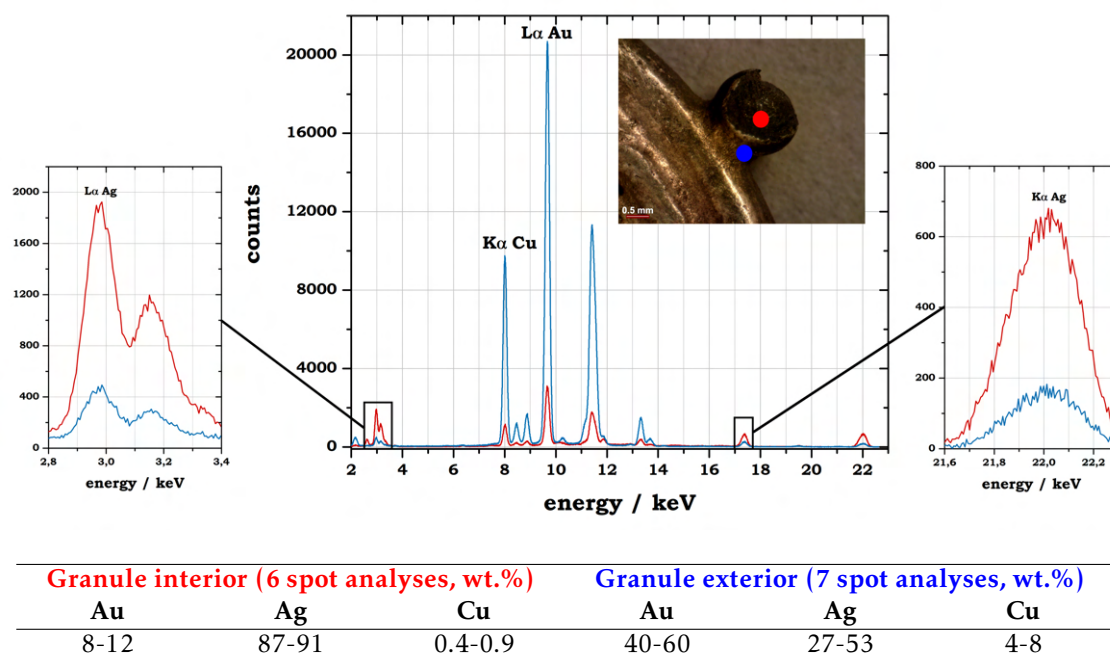
Figure 4.15: micro-XRF spectrum of the interior and exterior of a granule in PART01 artefact, with the results of the analyses at the bottom (using Ag Kα lines).

To understand if this difference of materials was only present in the granules, the wires and the area between them was also analysed, taking into account different depths of analysis when considering the Lα and Kα lines of the silver (Figure 4.16). The results show that in the analyses made over the wires, there is an increase in the Ag values and a decrease in the Cu values and that in the analyses made over the areas between the wires, there is a decrease in Ag and an increase in Cu values. This shows that the Cu contents are most likely associated with the Au contents, then Ag. It was also possible to observe that, for the same spot analysis, when using the Kα lines, the content of Ag is higher in comparison with the Lα lines, in agreement with the results obtained by pXRF.
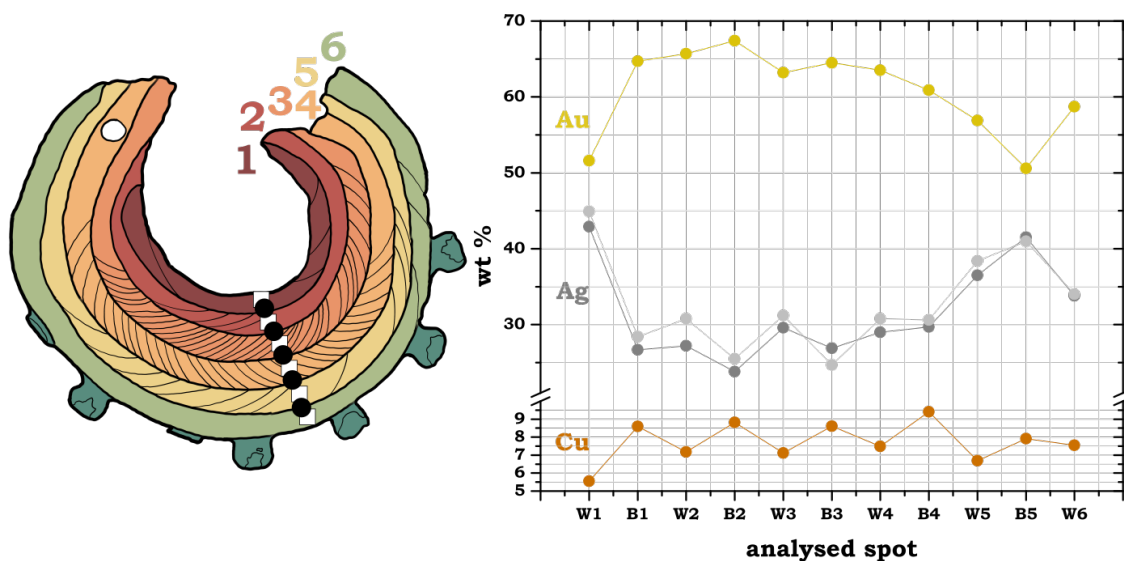
□ Wires (**W**) | ● Between Wires (**B**) | ● Au | ● Ag (Lα lines) | ● Ag (Kα lines) | ● Cu

Figure 4.16: Micro-XRF analysis of wires (1 to 6) and the area between the wires of artefact PART01, showing that there is a higher concentration of Au and Cu between the wires.

In order to study in greater detail and to have the clearest information on the gilding technique, a small surface polishing[1] was made in a lateral area. After, the area was analysed by micro-XRF. The results showed that the polished area (corresponding to more internal region) is silver-rich, in opposition to adjacent areas less polished or not polished at all, which are Au and Cu-richer (Figure 4.17). The area corresponding to the most internal region reaches ~75 wt.% Ag.

● Au | ● Ag | ● Cu
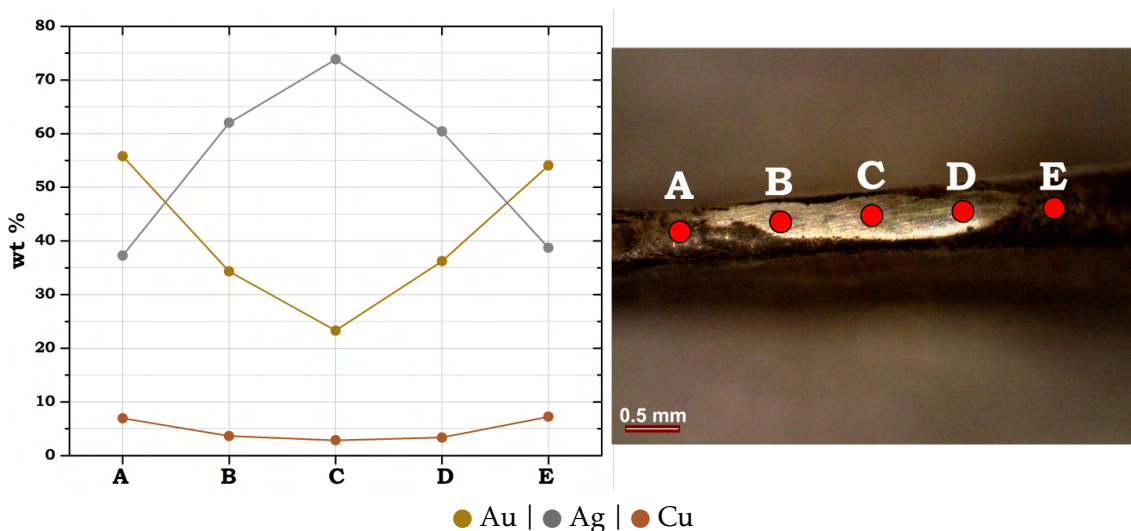
Figure 4.17: PART01 micro-XRF analyses of the polished area, showing the compositional difference between the unpolished and polished area.

---

[1]The polishment was made using, in the first place, two kinds of sandpaper, with different granulometry. The first sandpaper was a P2500, and the second one was a P4000 of granulometry. After that, a diamond paste was applied to the area, with a cotton swab, with a granulometry of 1μm, in the same direction as the sandpaper. Before the analysis, alcohol was also applied, to remove impurities that may be on the surface.

The same polished area was also analysed by SEM-EDS. An elemental line scan revealed a gradual Ag enrichment towards the center of the polished area, as well as an Au and Cu decrease (Figure 4.18).

For the present artefact, an explanation of the difference in surface composition to the interior of the object based on a dissolution of the anodic constituents at the earring surface was excluded. This would not explain the higher Cu content at the surface. For the present object, the results lead to the conclusion that the earring is a gilded object, i.e. a silver-rich core alloy coated by a gold-copper-rich alloy. Thus, it reveals that a gilding technique was applied to this object, possibly in a way to confer a greater value (economic and/or aesthetic) to the object. To note that Hg was not detected in any of the analyses, thus excluding a amalgam gilding technique [1]. Further studies may focus on the determination of the gilding of this object.
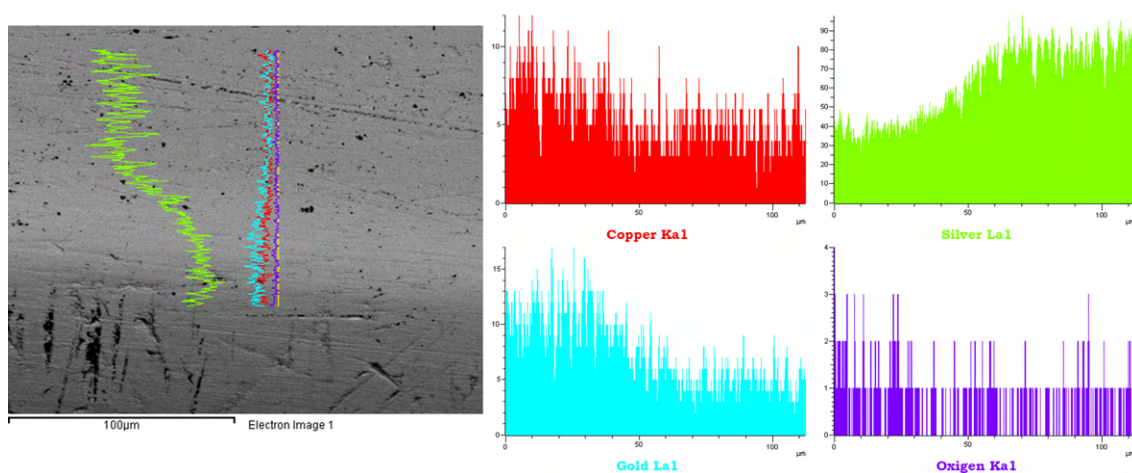
Figure 4.18: SEM-EDS analysis (BSE image) of PART01 object, showing the position of the line scan on the polished area, showing that in the center of the polishing the Ag content is higher and in the unpolished area there is an increase in Au and Cu contents.

The analysis of this earring proved of extreme importance since it is the first identification of a gilded earring from IA Western IP. Also, the analysis can provide guidelines for future non-destructive approaches to the detection of other gilded objects. Additionally, since Au-rich and Ag-rich alloys have different susceptibilities to corrosion, the results are very important for future conservation approaches.

4.2.3 Decoration techniques

The decoration carried out on the earrings with complex goldwork is extremely rich and detailed. One of the detailed works was the use of metal wires, with different shaped cross-sections. Generally, there were two main techniques for twisting metal wires (Figure 4.19 and 4.20):

Block-twist made from an ingot that was hammered in order to obtain a thin rod, or from a metal strip. It was then rolled, usually between two smooth surfaces, in

order to twist the metal. When finished, it could have two strokes or, if it was of a more square section, four seams [1, 5].

Strip-twist metal wires were made from a metal strip, which was then wrapped (around an existing wire, later removed, or with nothing in the centre), so as to obtain an all-round, more or less open shape. It was obtained by hammering, burnishing or rolling processes. It presents a scam spiralling along its lenght [1, 5, 7].
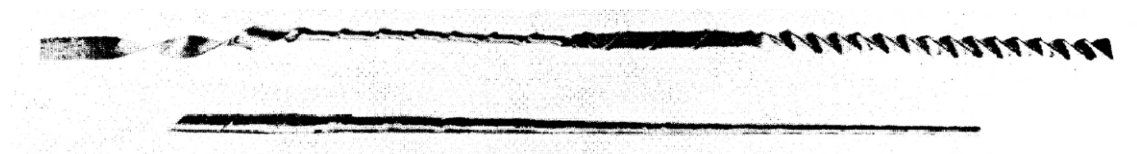
Figure 4.19: Example of the techniques block-twist (top) and strip-twist (bottom) adapted from [5].

(A)

(B)
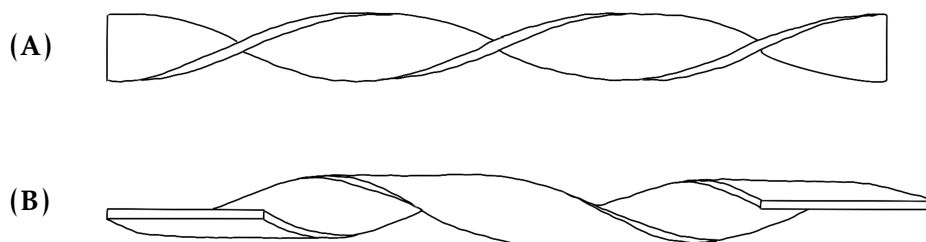
Figure 4.20: Schematic examples of **(A)** block-twist and **(B)** strip-twist techniques adapted from [5].

The observation of these techniques is often only possible through large magnifications since very small dimensions were achieved in their production. With the detailed observation by OM of the five artefacts, it was possible to detect which of these techniques were used, as well as the direction in which the wires were twisted ("*S*"(clockwise direction) or "*Z*"(counterclockwise direction)) and which dimensions (diameter) were possible to achieve.

The artefact Au 16 features three wires in the triangular drop ending, identical on both sides of the object (six wires in total), twisted with the strip-twist technique and *z*-twisted, having been subsequently placed in the shape of spirals. These wires present a circular cross-section. The hoop is contoured internally by two wires plaited together, split in the centre area, forming a total of four wires. These were individually twisted with the strip-twist technique and *z*-twisted, and only afterwards plaited together, that were *s*-twisted. These two wires present a rectangular cross-section. The object also features a hoop, solid, of circular cross-section, which must have had a production process similar to that of the plain gold rings presented earlier. Overall, the artefact presents a total of ten gold wires with a diameter of 0.3-0.8 mm (Figure 4.21).
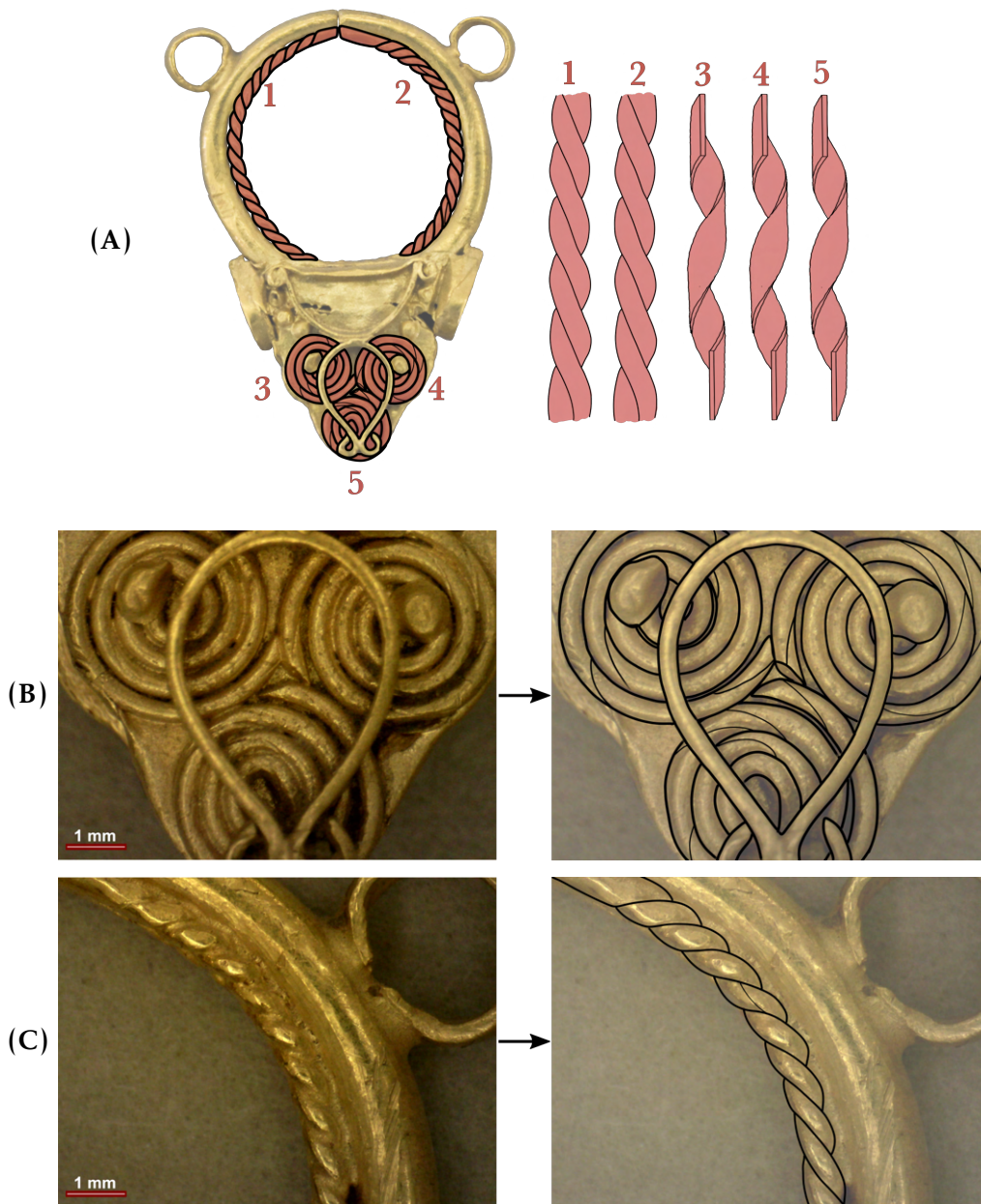
Figure 4.21: Au 16 wires and respective twisting techniques used: **(A)** mapping of the wires identified in the object, where wires 1 and 2 were plaited and twisted with the strip-twist technique individually. Wires 3, 4 and 5 were twisted with the strip-twist technique; **(B)** wires twisted with the strip-twist technique, in the area of the lower appendix of the piece (OM image); **(C)** wires twisted in the inner area of the hoop, with the strip-twist technique, subsequently plaited (OM image).

The Au 180 artefact presents, in the two tapering ends, a wire on both sides of the object (prefacing a total of four wires). These were twisted with the strip-twist technique, in the *s*-twist. In the lower outline, it presents four gold wires, plaited each two. Individually, they were also s-twisted with the strip-twist technique. When plaited, one pair was *z*-twisted and the other *s*-twisted. The lower and upper outlines have one wire each,

z-twisted with the strip-twist technique. At one end, it presents a spiral-shaped wire, first made with the *s*-twist strip-twist technique. The artefact presents a total of eleven gold wires, all with a circular cross-section of 0.3-0.6 mm in diameter (Figure 4.22)
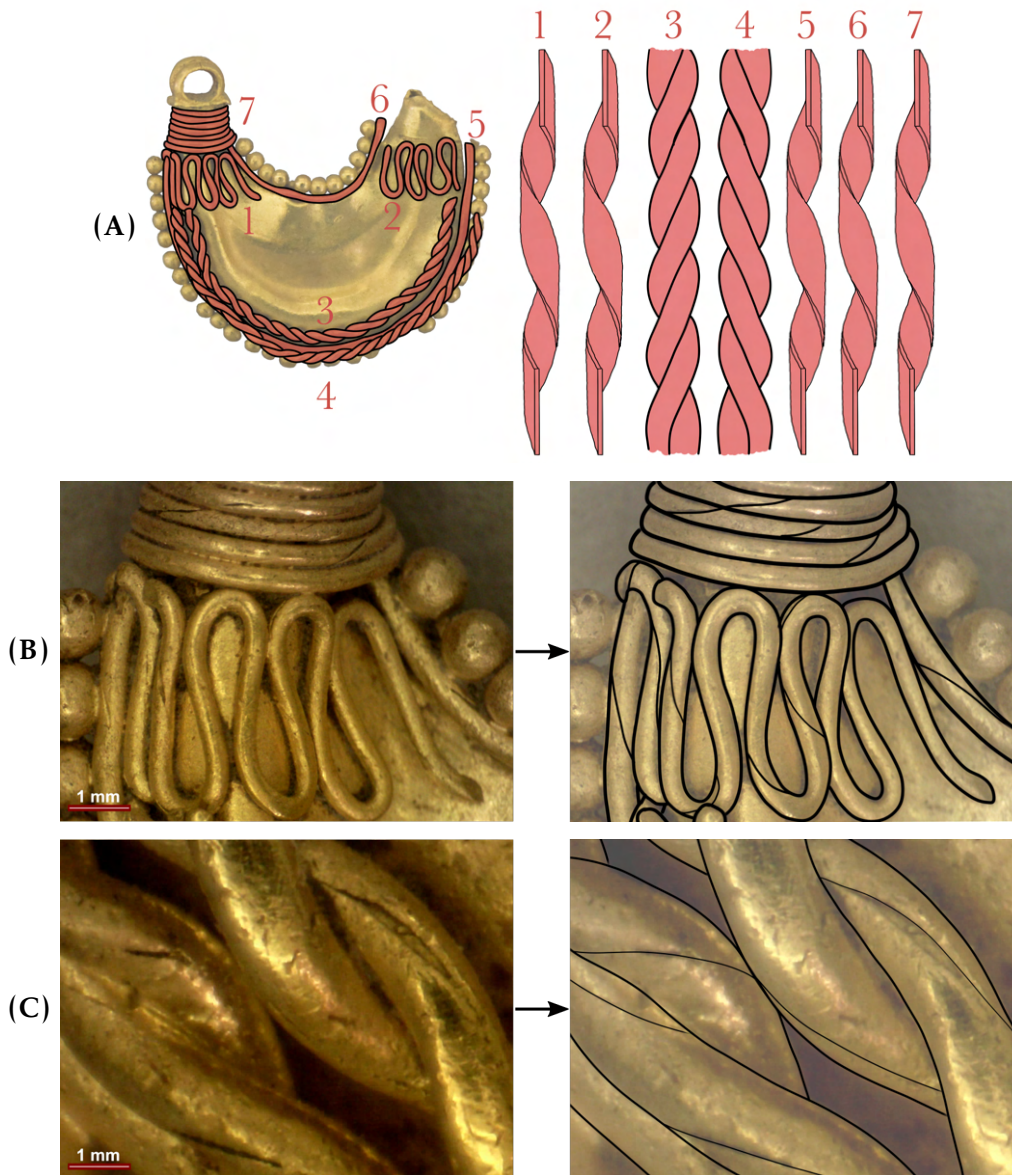
Figure 4.22: Au 180 wires and respective twisting techniques used: **(A)** mapping of the wires identified in the piece, where wires 1, 2, 5, 6 and 7 were twisted with the strip-twist technique, and wires 3 and 4 were plaited, having been first twisted with the strip-twist technique; **(B)** wires twisted with the strip-twist technique, at one of the ends (OM image); **(C)** wires plaited in the outline area of the object, with the strip-twist technique (OM image).

The central body of the Au 494 artefact shows two concentric circles of plaited wires: the outermost circle shows four plaited wires on each side, for a total of sixteen wires; the innermost circle has two plaited wires, making a total of eight wires. All these wires, before being plaited, were *z*-twisted with the strip-twist technique. The plait was made in the same *z*-direction. In the centre, the earing features a spiral of wires wrapped around

a circle, *z*-twisted with the strip-twist. At the beginning of the appendix at the bottom of the object, there are still seven plaited wires, in a total of fourteen wires, twisted in the same way as the wires that form the concentric circle, differing only in the direction in which they were twisted at the end, *s*-twisted. Some of these wires are quite deformed, due to use, manufacturing process, or post-depositional factors, so that it is not possible to clearly define which technique was used in their production. The artefact presents a total of thirty-nine gold wires, all with a circular cross-section with a diameter ranging from 0.1-0.4 mm (Figure 4.23).
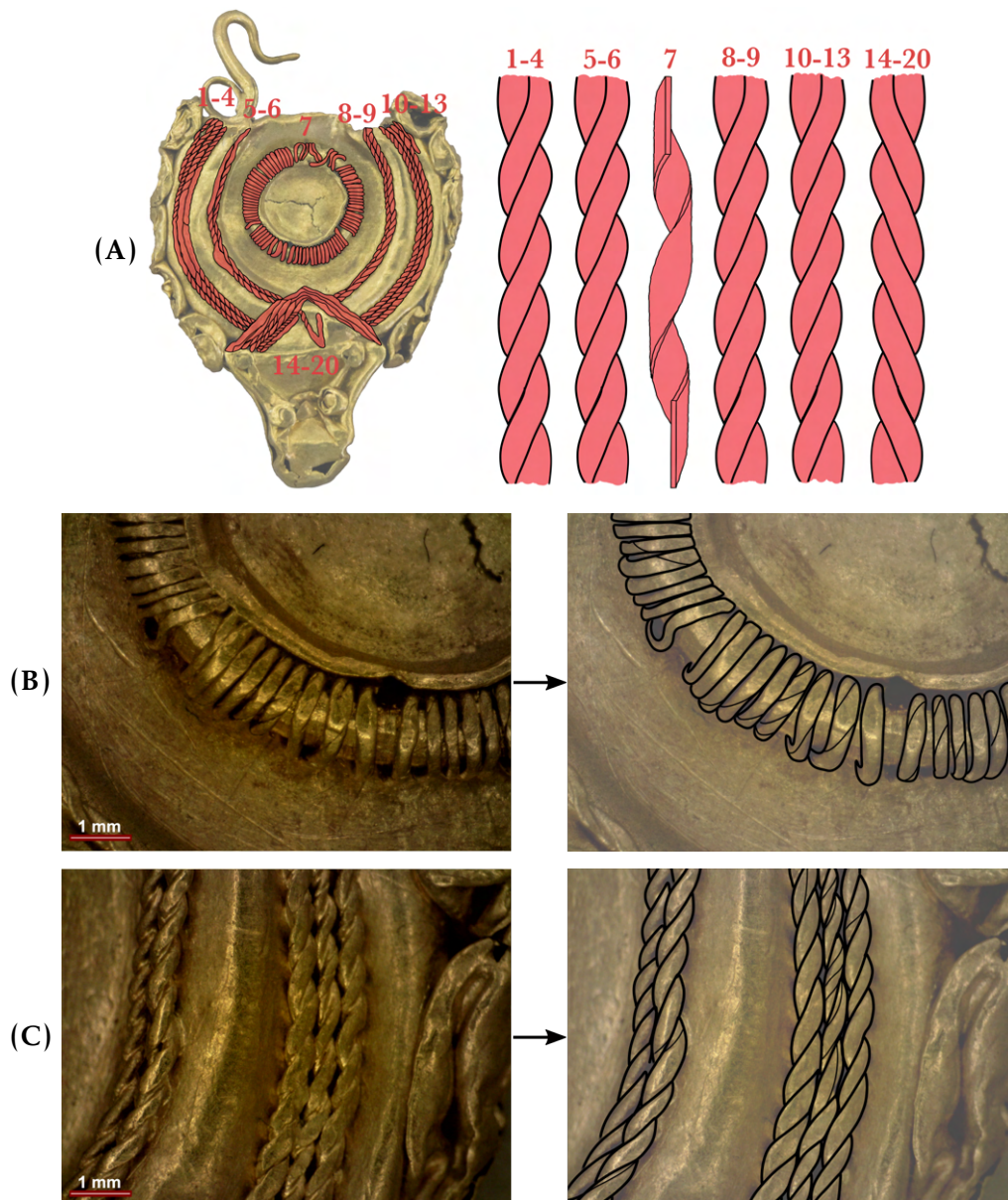
Figure 4.23: Au 494 wires and respective twisting techniques used: **(A)** mapping of the wires identified in the object, where all the wires were twisted with the strip-twist technique and subsequently plaited, with the exception of wire 7, which remained individual; **(B)** wires twisted with the strip-twist technique, around a circle (OM image); **(C)** wires plaited in the area of the concentric circles of the object, with the strip-twist technique (OM image).

33

The Au 561 artefact features two spiral wires on both sides, for a total of four wires. These were *s*-twisted with the strip-twist technique and present a circular cross-section of 0.3-0.6 mm diameter. The artefact is outlined by two wires, individually twisted with the block-twist technique, each one in a different direction, "*Z*"and "*S*", respectively, with a rectangular cross-section of 0.2-0.4 mm diameter. The artefact features a total of six gold wires (Figure 4.24).
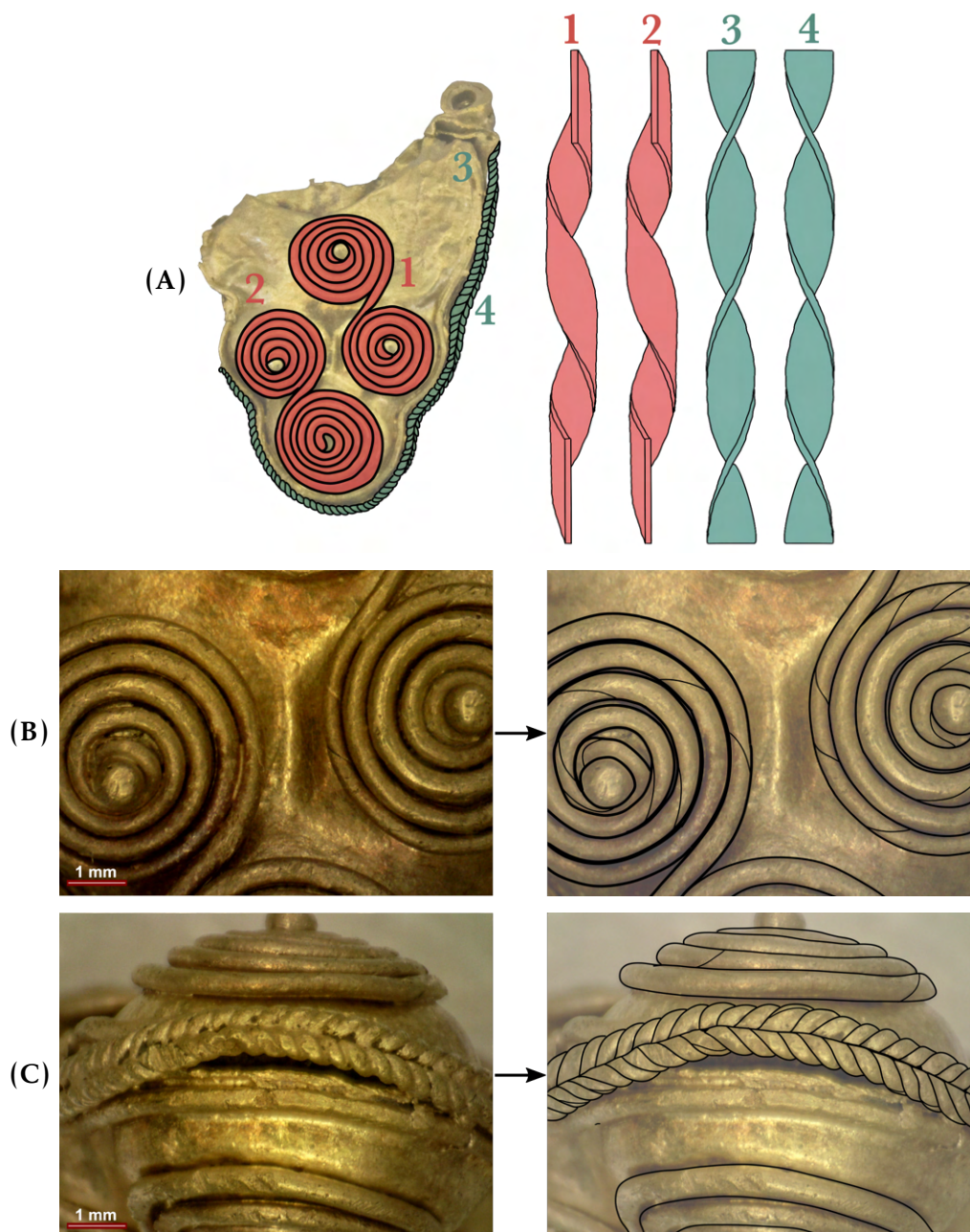
Figure 4.24: Au 494 wires and respective twisting techniques used: **(A)** mapping of the wires identified in the object, where wires 1 and 2 have been twisted with the strip-twist technique, and wires 3 and 4 with the block-twist technique; **(B)** wires twisted with the strip-twist technique, in the centre of the object, placed in a spiral (OM image); **(C)** wires twisted with the block-twist technique, in the outline of the object (OM image).

Finally, the artefact PART01 is composed of six wires, which compose the central body of the object, numbered from 1 to 6. Two of the wires were twisted with the block-twist technique (wires 3 and 4) and the remaining four with the strip-twist technique. Wires 1 and 4 were *z*-twisted and wires 2, 3, 5 and 6 were *s*-twisted. It should also be noted that the two outer wires show more torsion in comparison to the two wires adjacent to them (Figure 4.25).
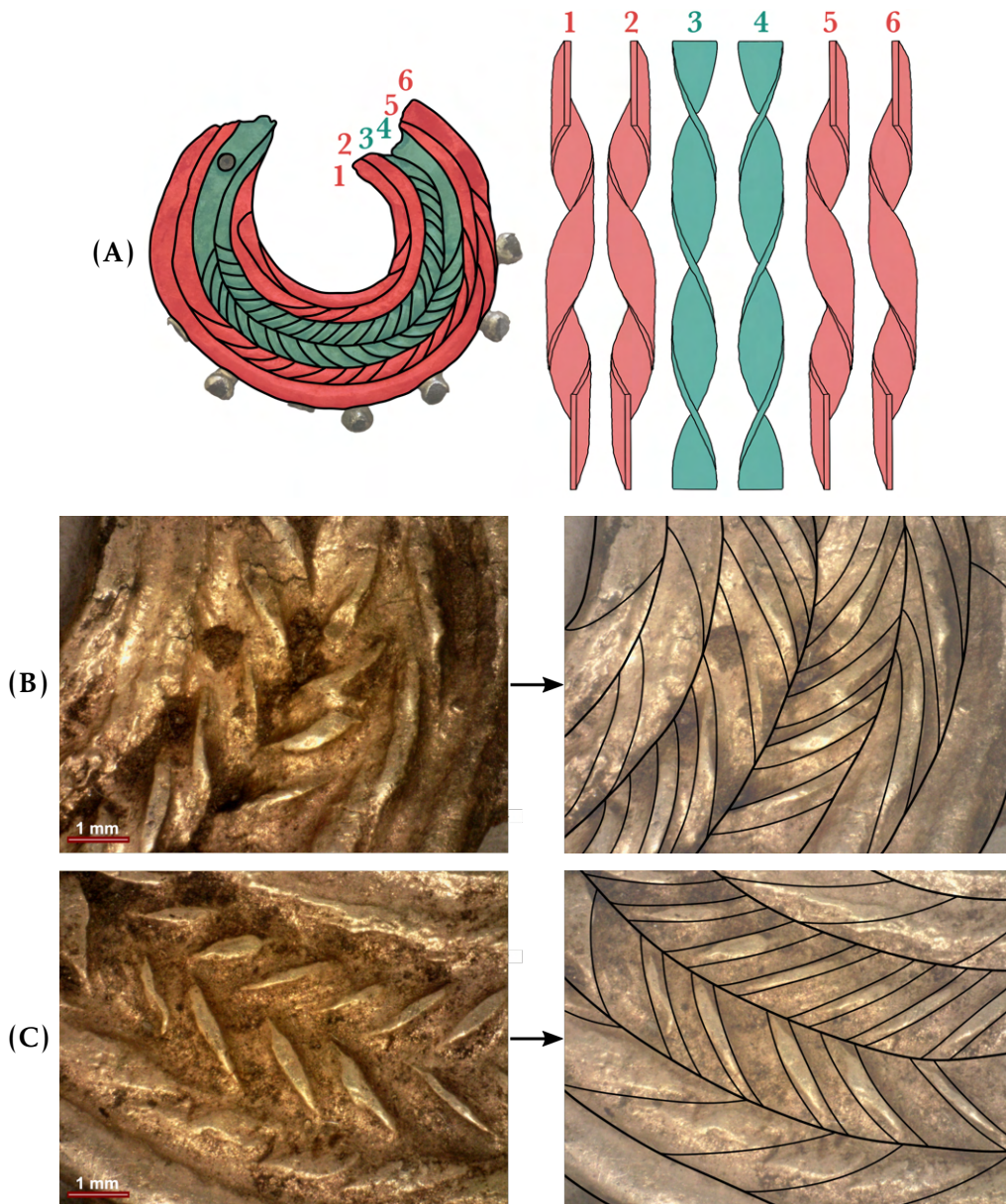
Figure 4.25: PART01 wires and respective twisting techniques used: **(A)** mapping of the wires identified in the object, where the strip-twist technique was used in wires 1, 2, 5 and 6 and the block-twist technique in wires 3 and 4; **(B)** and **(C)** wires in the central area of the object, showing both the use of strip-twist and block-twist techniques (OM images).

By observing the artefact with the naked eye or using an OM, it was found that the six wires probably have a rectangular cross-section. A proposal was made of how the

object should look if a cross-section was made, as exemplified in Figure 4.26. This helps to visualize the proposed manufacturing technique, where the wires and granules have been made in an Ag-rich alloy and were later covered by a Au-Cu-rich alloy.
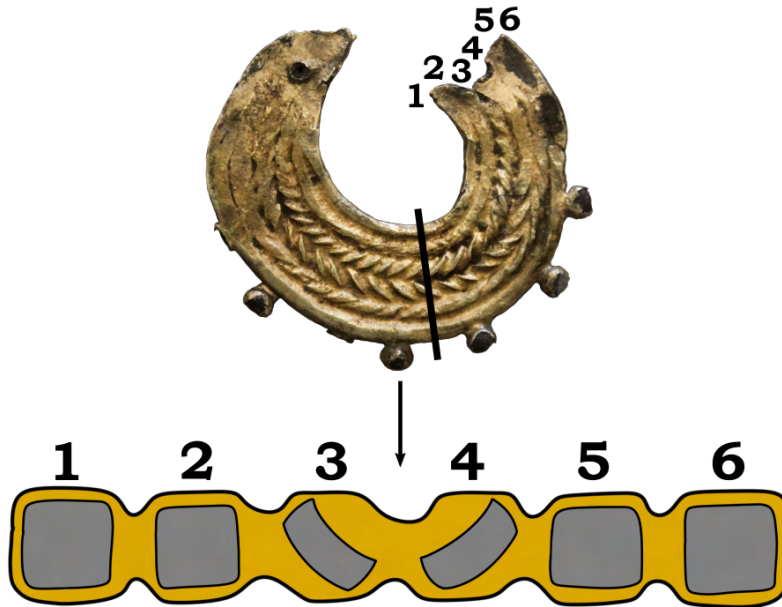
Figure 4.26: Proposal of a cross-section along the object PART01, representing the wires inside the object that have a rectangular cross-section, and were made in an Ag-rich alloy, were later gilded, in an Au-Cu-rich alloy.

The maximum and minimum dimensions for the wire diameters of each object were measured and it was found that in all the artefacts it was possible to attain wires with much less than 1 mm in diameter, with only the artefact PART01 having the wires with a larger diameter, greater than 1 mm (Table 4.4).

Table 4.4: Wires torsion techniques used and their minimum and maximum diameter.

Inv. No.	Torsion Technique	Torsion Direction	Min-Max Diameter (mm)
Au 16	strip-twist	Z	0.299-0.761
Au 180	strip-twist	S	0.285-0.584
Au 494	strip-twist	Z	0.100-0.376
Au 561	strip-twist	S	0.295-0.560
	block-twist	S and Z	0.202-0.409
PART01	strip-twist	S and Z	0.629-1.296
	block-twist	S and Z	0.564-1.217

It was found that, with regard to the torsion of the wires of each artefact, the direction used is always "S" or "Z" on the same object, except in cases where a mirror effect of the torsion of the wires is intended, as in the case of the artefacts Au 561 and PART01.

The analysis by OM also showed that in the IA manufacturing techniques did evolve to use less raw material. The artefacts Au 180, Au 494 (central body) and Au 561 all

present a central structure made from gold sheets to create volume to the objects, using small amounts of material (their interiors is hollow) (Figures 4.27, 4.28 and 4.29). These gold sheets are very thin, varying between 0.05 and 0.19 mm in thickness (Table 4.5).
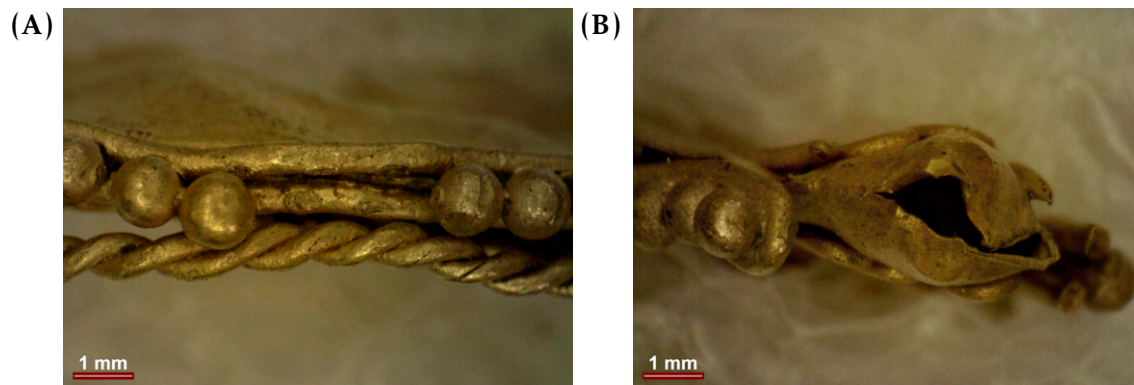
Figure 4.27: OM images of Au 180, regarding the use of gold sheets: **(A)** detail on the outline of a gap between the two gold sheets; **(B)** detail on one of the ends of hollow between the two gold sheets.
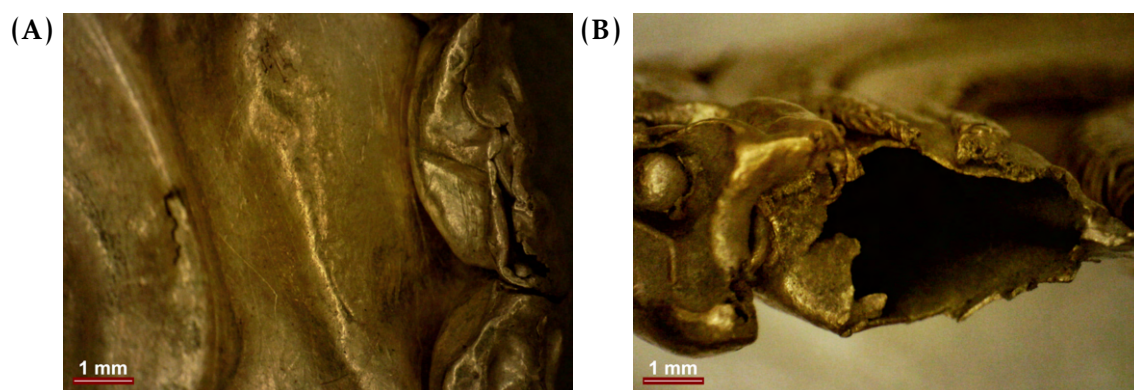
Figure 4.28: OM images of Au 494, regarding the use of gold sheets: **(A)** detail of the central body of the object, with gold sheets used for the circle area and the details on the sides; **(B)** detail of the top end, showing that the object is hollow between the two gold sheets.
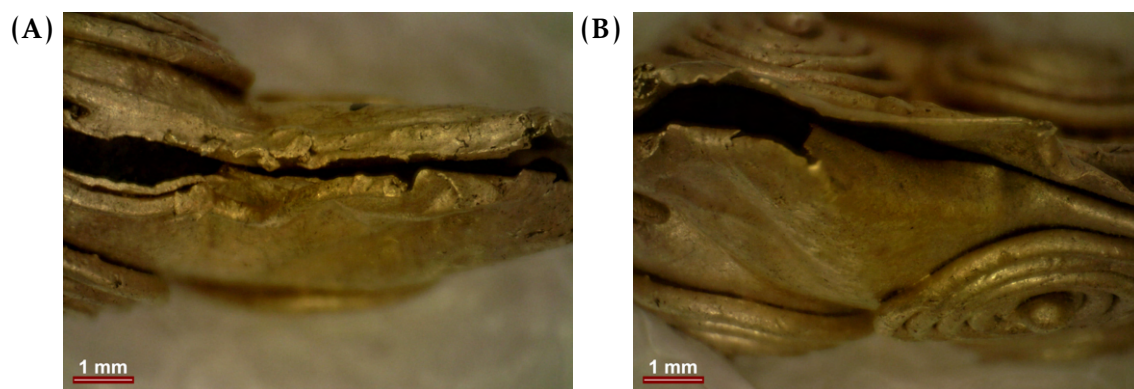
Figure 4.29: OM images of Au 561, regarding the use of gold sheets: **(A)** and **(B)** details of the outlines, showing the use of gold sheets and the hollow between them.

Table 4.5: Gold sheets minimum and maximum measured thickness.

Inv. No.	Min-Max gold sheets thickness (mm)
Au 180	0.055-0.133
Au 494	0.077-0.190
Au 561	0.041-0.181

In the case of the drop endings of the artefacts Au 16 and Au 494, these are also made with gold sheets, both on their exterior and interior, aimed to give volume to the object without using a solid body (Figure 4.30).
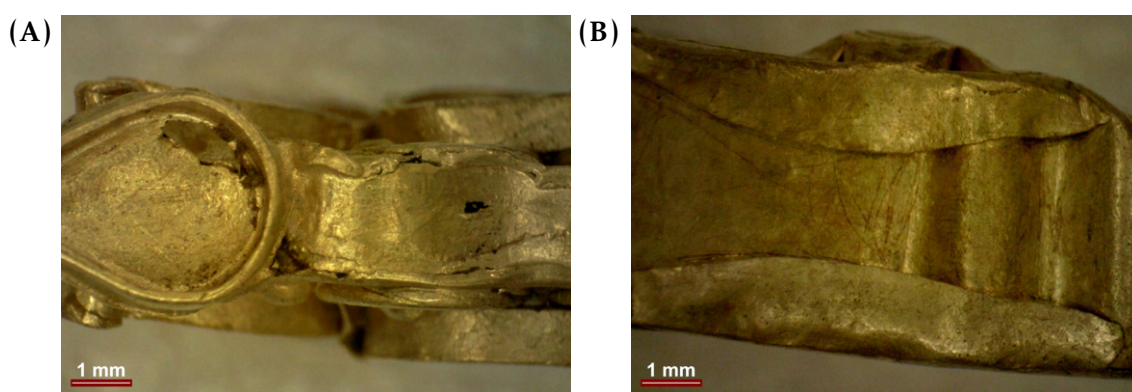
Figure 4.30: OM images regarding the use of gold sheets to create volume to the objects: **(A)** Au 16, detail of the drop end's side, showing the use of gold sheets to give volume; **(B)** Au 484, detail of the drop end's side, showing the use of gold sheets to give volume.

The use of granules was observed in all five objects. In the case of objects Au 180 and PART01, the granules were placed in the outline of the shape (Figure 4.31), while in objects Au 16, Au 494 and Au 561 they were used sporadically in the front and reverse faces of the earrings: in Au 16 and Au 561 they were placed in the center of the spiral wires, while in Au 494 they were placed in the center of the gold sheets, along the object's contour (Figure 4.32).
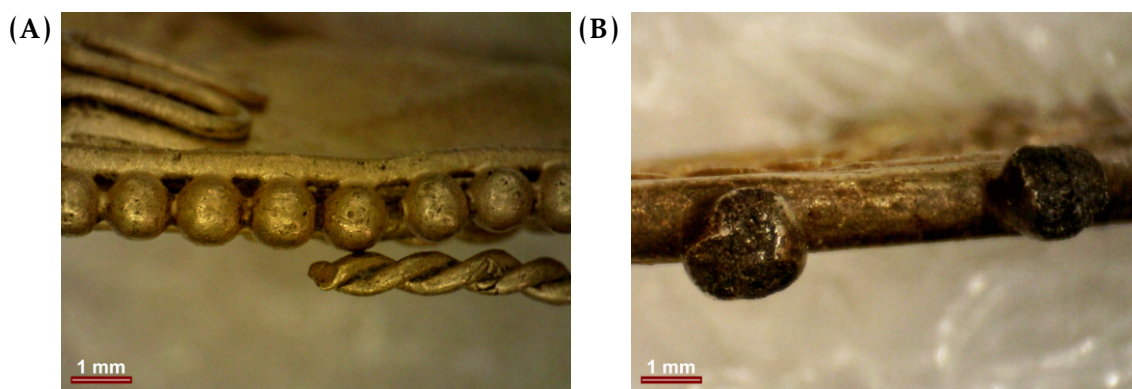
Figure 4.31: OM images of the granules: **(A)** granules on the bottom outline of the object Au 180; **(B)** granules on the bottom outline of object PART01.
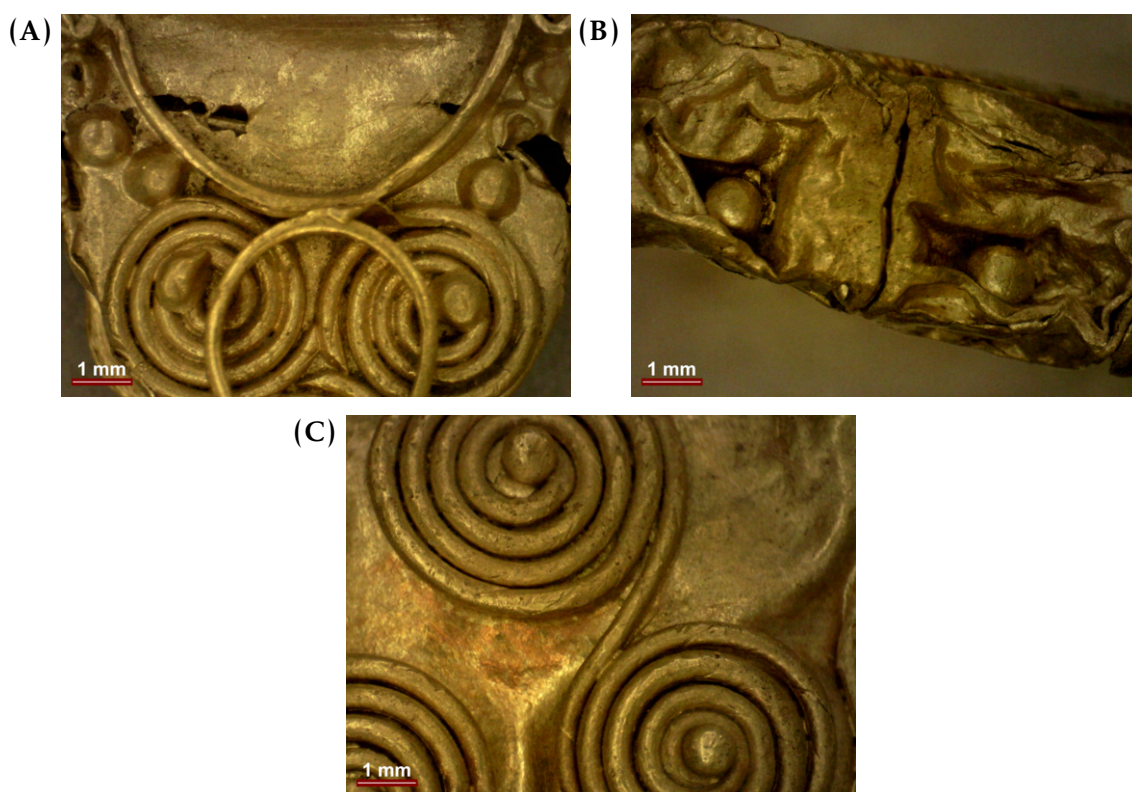
Figure 4.32: OM images of the granules: **(A)** granules in the center of the spiral wires, and on the artefact surface of the object Au 16; **(B)** granules on the outline of the object, in the gold sheets of the object Au 494; **(C)** granules in the center of the spiral wires of the object Au 561.

The minimum and maximum diameter for the granules of each object was determined as close to 1 mm in all objects, with the exception of artefact PART01 in which the granules are larger, reaching more than 2 mm in diameter. It was found that these dimensions, within each object, had very small variations. It thus reveals that the granules could have to be made at the same time for each earring, as by using one wire cut into pieces of the same dimension. In the case of object PART01, the relatively larger variations can be explained as partial loss of the superficial coating in some of the granules, which influence its measured dimensions (Table 4.6).

Table 4.6: Number of granules in each artefact and their minimum and maximum diameter.

Inv. No.	No. Granules	Min-Max granule diameter (mm)
Au 16	20	0.836-1.160
Au 180	40	0.962-1.156
Au 494	9	0.828-1.159
Au 561	5	0.859-0.995
PART01	5	1.582-2.266

With this study, it was possible to observe that, in IA, with was possible to achieve wires with a diameter smaller than 0.2 mm, gold sheets smaller than 0.1 mm and granule spheres as small as 0.8 mm. The only object that differs in size is the PART01, being that

the wires are not only decorative, but also structural, making the main body of the object (Figure 4.33).
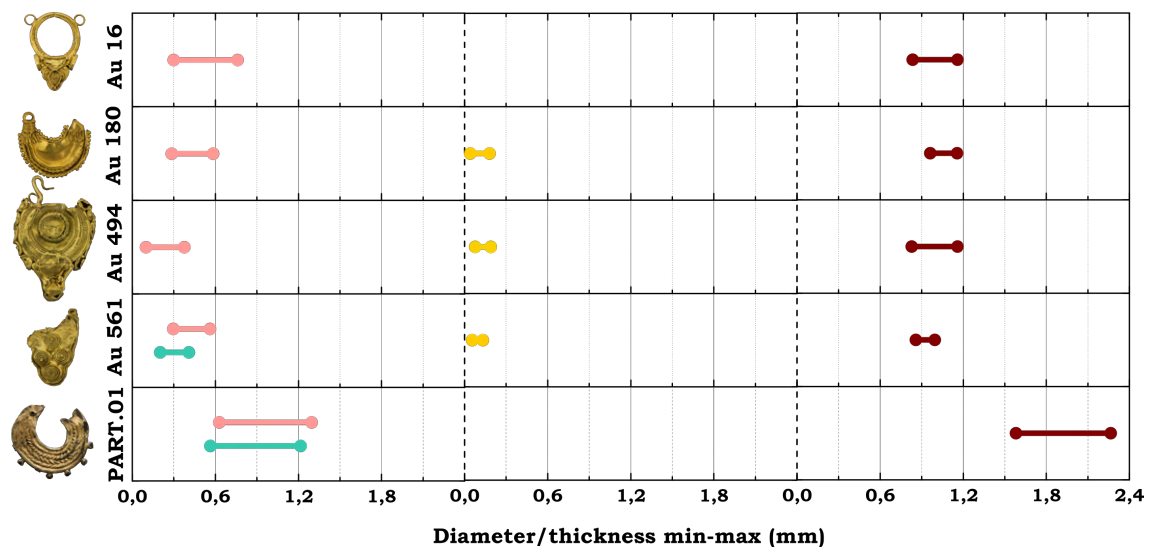
Figure 4.33: Wires, gold sheets and granules and their minimum and maximum diameter/thickness.

5

Final Discussion

After the individual analysis of the two groups of artefacts presented, the results obtained are here compared, taking into account the distinct typologies of the objects.

The plain gold rings, attributed to the LBA/EIA and from different provenances, showed no clear compositional relationship within each pair element, even when compared to the other pairs. The group showed 10-17 wt.% Ag and <3 wt.% Cu. Thus, although each pair being visually quite similar variations in Ag content of 5 wt.% between each individual pair and of 2 wt.% in the Cu content are found. The objects from IA (MNA) show more dispersed compositions, but again with a range of values quite similar to those previously described to the plain gold rings. i.e. 8-16 wt.% Ag and <5 wt.% Cu. (Figure 5.1).

The Au 16 artefact was the one with the highest Cu content (about 4.5 wt.%), a value that corresponds to results available in references regarding artefacts from the same period, IA, from the IP. This characteristic makes it distinct from the Au 494 and Au 561 objects, also attributed to IA, which presents very low amounts of Cu in their composition (only detected in the OES analysis). Very low amounts of Cu in IA artefacts is an exception, since gold alloys in IP dating to IA are normally described as having Cu in their composition in higher amounts than those of LBA. The present analysis shows that that may not be true for all artefacts, ant that exceptions do exist. This is even more interesting given the high amount of fine goldwork that these two objects contain, where it could be supposed that different alloys were used, being that some did have Cu in significant contents (Figure 5.1).

In the case of the artefact PART01, it was not possible to make direct comparisons with the previous earrings, since it is an artefact mostly made of an Ag-rich alloy covered by an Au and Cu layer whose original composition was not possible to determine. However, the analysis of this artefact contributes to the widening of the knowledge of the metallurgical technologies that the IA communities were able to perform. It was possible to determine that the gilding of Ag with an alloy of Au with some Cu was performed due to the correlation of Cu to Au instead of Ag (Figure 5.2). Possible, future analyses of other gilded artefacts can add more information about these ancient gilding techniques.
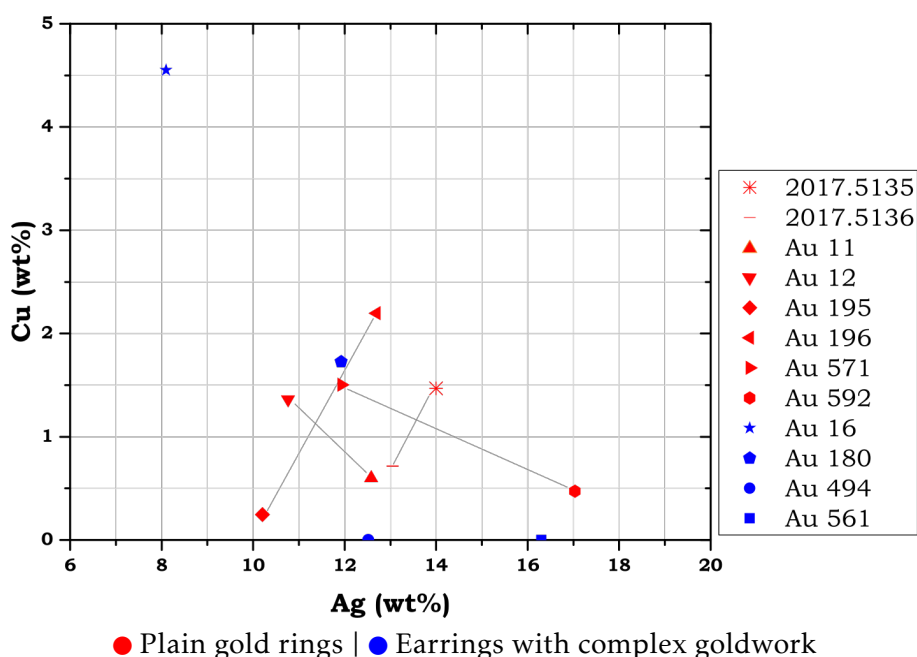
Figure 5.1: Elemental composition of the plain gold rings and decorated earrings from MNA 2017.5135, 2017.5136, Au 11, Au 12, Au 195, Au 196, Au 571, Au 592, Au 16, Au 180, Au 494 and Au 561 by pXRF (average values used), results obtained when using the Ag Kα lines (most representative values from the interior of the objects), showing the compositional differences between them, by comparing the Ag and Cu contents (Au remaining). Lines connect the pairs of the LBA plain gold rings.
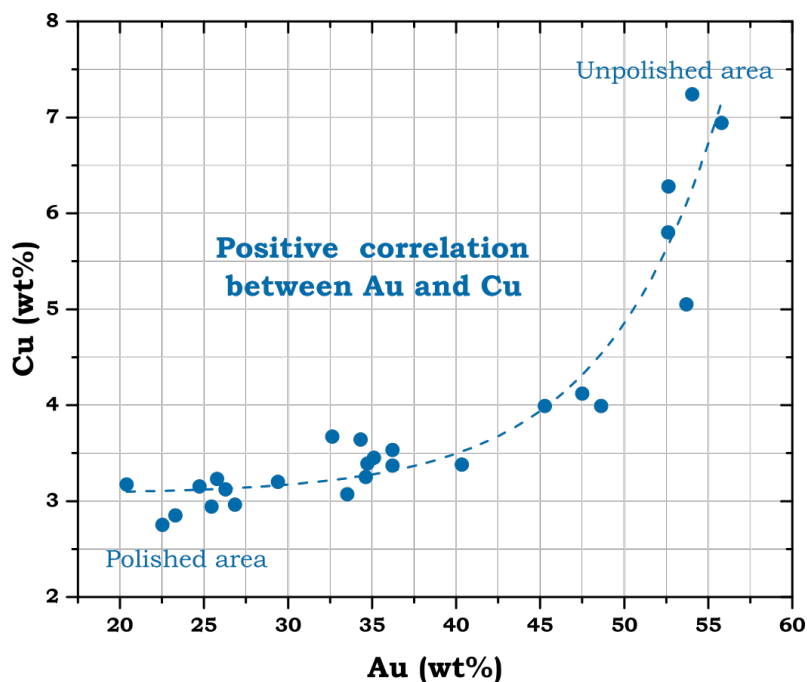
Figure 5.2: Elemental composition of the artefact PART01 by micro-XRF (Ag Kα lines values used), analyses between the polished and unpolished area, showing that there is a positive correlation between the Au and Cu contents, demonstrating that the Cu content is associated with the alloy used.

42

With this study it was possible to carry out analyses that represent different depths, thus allowing a characterisation in stratigraphic terms of the composition of the artefacts. We took into account the values obtained for SEM-EDS, pXRF when using the Ag Lα lines, pXRF when using the Ag Kα lines, and the results obtained by OES in 1982 (from the first to the last they represent analyses from the most superficial to the most interior of the objects) (Figure 5.3).

It can be seen that the smaller the difference in the values obtained when comparing the pXRF results using the Ag Kα and Lα lines, the greater the probability that a more abrasive conservation and restoration process was carried out on the artefacts, having removed a greater layer of corrosion, visible in the analyses of the objects Au 195, Au 571, Au 16 and Au 494. In these cases, it can be seen that in the OES analysis the values are not very different from those obtained by pXRF, showing a more homogeneous composition overall, resulting from the intervention mentioned above.

It was also found that, by tendency, Ag corrodes more easily than Au, being more easily lixiviated at the surface. It is observed that, in the OES analysis, the Ag content has higher values than those obtained by the pXRF analysis, with the exception of the Au 195 and Au 494 artefacts. In the case of the Au 949, this can be due to the fact that different elements, with different compositions, have been analysed. Cu also tends to have a higher content at greater depths, which can also be explained by its preferential loss at the surface due to corrosion and lixiviation (Figure 5.3).
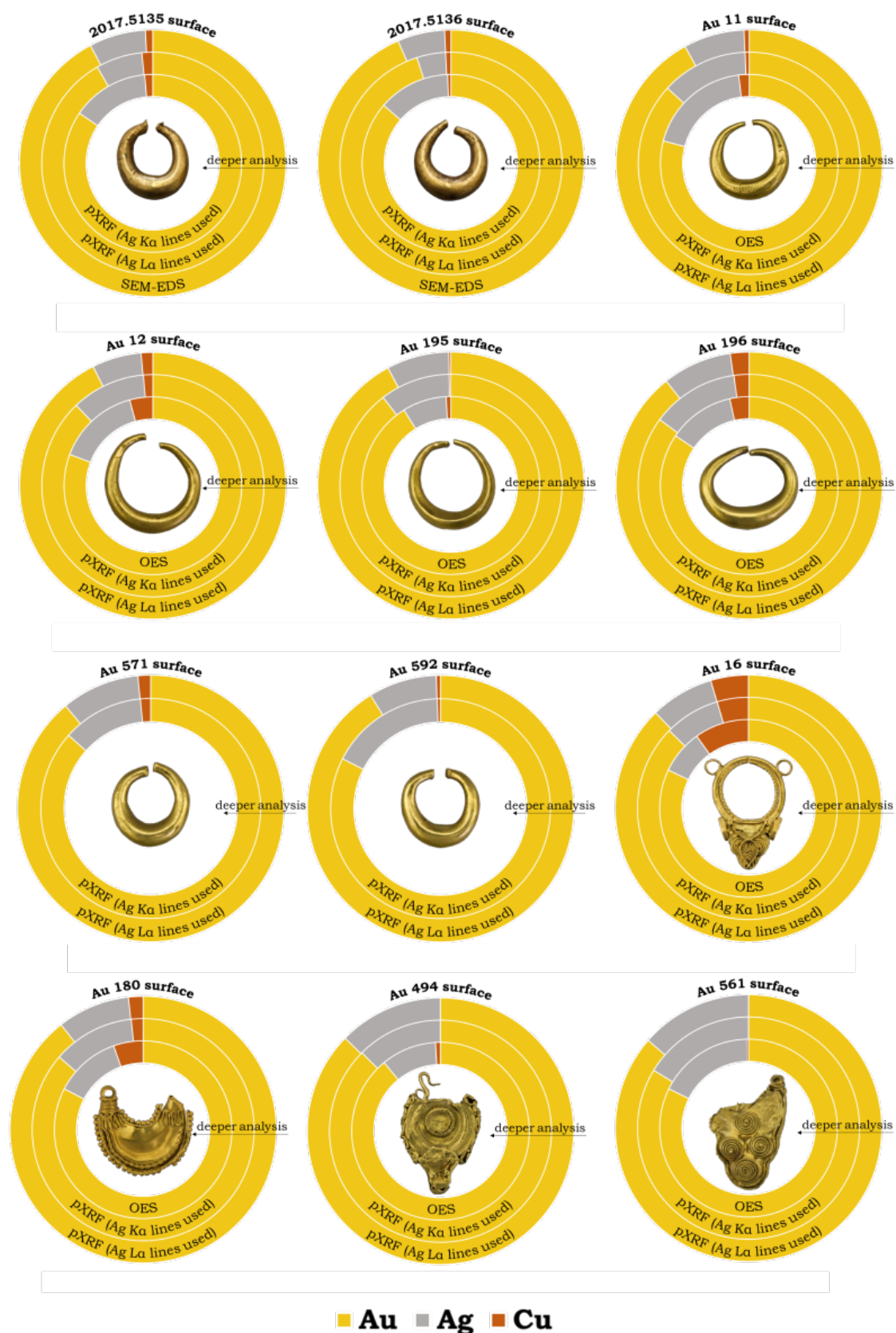
Figure 5.3: Compositions obtained (normalised values to 100 wt.%) for the artefacts in study, showing the differences in composition when analysed with techniques with a range at different depths.

44

With the OM observations, in which it was possible to study the fine goldwork done on each object, the question of the objects' dimensions, their weight and how this changed between different typologies/chronologies was raised. In a first approach, when placed side by side, the objects show quite similar dimensions (Figure 5.4). The estimated volume of the objects was then calculated and compared with their weight.

Figure 5.4: Artefacts under study: eight plain gold rings and five earrings with complex goldwork, all represented to the same scale.

It was found that the object that is both heavier and more voluminous is the Au 494. The remaining objects have similar volumes, but great differences in their weights: plain gold rings weight 4.7-5.7g.; the earrings with a complex goldwork weight <3.0g (Table 5.1). In order to understand the relationship between the volume and weight of

45

the objects, the density was calculated. Results show that all plain gold rings have much higher densities (9-13g/cm^3), than the IA artefacts (3-6g/cm^3) (Figure 5.5). It reveals then that in IA an economy in the use of raw material was a common practice, compensated by very fine works.

Table 5.1: Weights, volumes (calculated by approximation) and density (ratio between weight and volume) obtained for the artefacts in study.

Inv. No.	Weight (g)	Volume (cm^3) (approximation)	Density (Weight (g)/Volume (cm^3))
2017.5135	5.45	0.60	9.08
2017.5136	5.70	0.63	9.11
Au 11	5.18	0.45	11.49
Au 12	4.76	0.54	8.81
Au 195	4.87	0.37	13.25
Au 196	5.17	0.53	9.76
Au 571	5.18	0.52	9.94
Au 592	4.76	0.46	10.32
Au 16	2.92	0.69	4.22
Au 180	3.03	0.44	6.82
Au 494	6.67	2.28	2.92
Au 561	2.82	0.91	3.11
PART01	1.13	0.36	3.14

● Plain gold rings | ● Earrings with complex goldwork
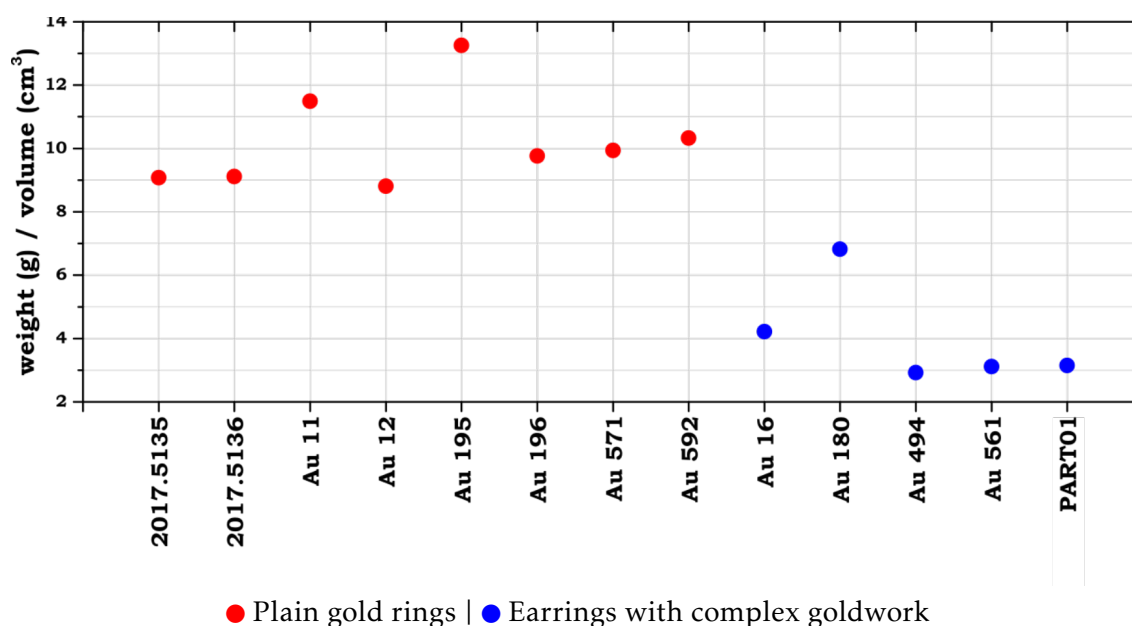
Figure 5.5: Density calculated as the ratio between weight and volume (estimated) for the artefacts under study, showing that the plain gold rings present a higher density than the earrings with complex goldwork.

Finally, the composition of the alloys was taken into account and whether this would have any influence on their colour, especially in the case of the Au 494 and Au 561 artefacts, in which Cu was not detected. However, when superimposed the analyses performed by pXRF, using the Ag Kα lines, with the ternary Au-Ag-Cu diagram with

corresponding colours of the alloys with distinct compositions, all the objects were super-imposed in the same region, corresponding to the colour of the yellow alloy. This result shows that the (relatively small) differences in the Ag and Cu contents determined for the objects would not have resulted from any intentional addition of Ag or Cu with the aim of producing different colour hues (Figure 5.6).
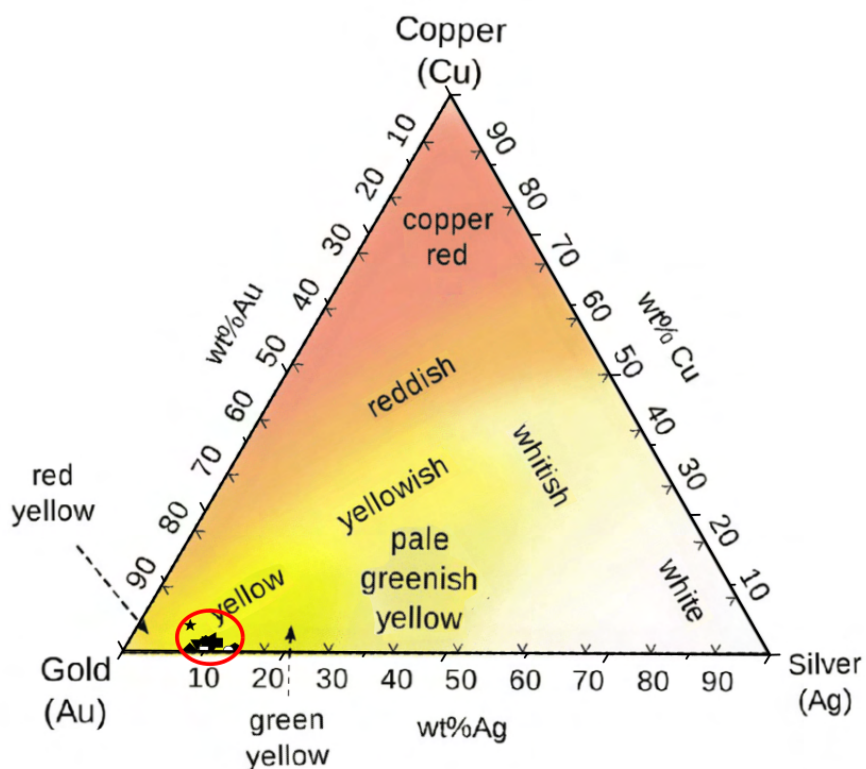
Figure 5.6: Ternary phase diagram Au-Ag-Cu, with the representation of the colours obtained when alloys with distinct compositions were used following [33]. The composition of the objects under study (obtained by pXRF, using the Ag Kα lines) are depicted on the diagram.

Conclusions

The present work had as its main focus the compositional and technological study of gold alloys attributed to LBA and IA from the western IP, to provide information about technological evolution, as well as to contribute to the conservation of Proto-historic gold artefacts.

The elemental analysis of eight plain gold rings from LBA showed that all were made in a gold alloy with 10-17 wt.% Ag and <2 wt.% Cu. Through the analysis by pXRF (using Kα and Lα Ag lines) and SEM-EDS (and comparison with previous results obtained by OES and EDXRF), it was possible to reveal the presence of depth compositional differences. It was found that Ag had a tendency to be present at higher contents at greater depths (i.e. an increase from 5-7.5 wt.% to 12.5-15 wt.% was found from more superficial analyses to deeper ones), thus referring to the dissolution of the anodic constituents at the surface of the objects. It was also possible to verify that in some cases, this depth compositional deference was not very significant, probably due to previous conservation and restoration treatments, where abrasive treatments removed the most superficial Ag-depleted layer. These results show that the presence of such a surface layer can be altered by conservation and restoration treatments, with implications for the analytical results obtained. The observation by OM allowed the identification of simple decorative motifs, often not perceptible to the naked eye. The observations at higher magnifications also revealed a surface with a lot of irregularities, probably associated with the manufacturing process and the conditions to which the pieces were subjected when buried.

Concerning the earrings with complex goldwork from IA, the elemental analysis identified a larger dispersion of Ag and Cu contents if compared to the LBA rings. The artefacts present Ag contents among 8 and 17 wt.%. The artefact Au 16 showed the highest Cu content (Cu 4 wt.%), while in the pXRF analyses of the Au 494 and Au 561 artefacts no Cu was detected (exception made to one element/piece in Au 494). The absence of Cu can be considered an uncommon aspect for objects attributed to IA, being that the present analysis shows that such alloys were also in use during IA. The analysis of object PART01 showed that a gilding process was used to cover an interior Ag-rich. The coating was determined as an Au-Cu-rich alloy. The gilding of a silver piece was probably

done to provide a greater value to the object. With the detailed OM observations of these five objects, it was possible to determine the use of different torsion techniques such as strip and block-twist, in different directions and with different cross-sections, as well as the use of gold sheets and granules for the generation of volume and for decoration. It was found that within the present pieces the goldsmiths were able to produce gold wires and granules with <1 mm in diameter and gold sheets with a thickness inferior to 0.2 mm.

By comparing the weight of the objects with their volume (calculating the density), it was found that the plain gold rings, attributed to the LBA/IA, present a much higher density than the IA objects (9-13g/cm^3 and 3-6g/cm^3, respectively), revealing that in the IA the economization of the raw material used was a common practice, probably compensated by the use of fine workmanship in their decoration.

It was also demonstrated that through the use of non-destructive techniques it is possible to determine several characteristics of the artefacts (both compositional and typological), which help their detailed study and a better understanding of the technologies used in Proto-historic metalworks. This information is very relevant for future conservation approaches, since artefacts of distinct compositions can be more or less susceptible to surface corrosion, and the surface composition of an artefact can also be influenced by conservation and restoration treatments.

Bibliography

[1] M. L. Vitobello and T. Rehren. *A Quest for Authenticity: Authentication methodologies for metal artefacts based on material composition and manufacturing techniques.* Institute for Archaeo-Metallurgical Studies (IAMS) UCL Institute of Archaeology, 2009 (cit. on pp. xvii–xix, 29, 30).

[2] R. Parreira and C. V. Pinto. *Tesouros da Arqueologia Portuguesa no Museu Nacional de Arqueologia e Etnologia.* Museu Nacional de Arqueologia e Etnologia, 1980 (cit. on pp. xvii–xix, 5–7).

[3] M. J. C. de Carvalho e Sousa. "O Património Arqueológico na longa duração: Ourivesarias Antiga e Tradicional Actual no Norte de Portugal". MA thesis. Guimarães: Universidade do Minho - Instituto de Ciências Sociais, 2004 (cit. on pp. xvii, xix).

[4] J. Falke. "Filigree". In: *The Workshop* 7.11 (1874), p. 161. DOI: 10.2307/25586785 (cit. on p. xvii).

[5] J. Ogden. "Classical gold wire: Some aspects of its manufacture and use". In: *Jewellery Studies* 5 (Jan. 1991), pp. 95–105 (cit. on pp. xvii, 30).

[6] D. A. Scott. "The deterioration of gold alloys and some aspects of their conservation". In: *Studies in Conservation* 28.4 (1983), pp. 194–203. DOI: 10.2307/1505967 (cit. on pp. xviii, 4, 5).

[7] J. A. García Castro. *El Oro en la España Prerromana: Arqueologia del Oro.* Caja de Madrid, 1989 (cit. on pp. xviii, 19, 30).

[8] X.-L. Armada and Ó. García-Vuelta. "Plano-convex ingots and precious metalwork in northwestern Iberia during the late Iron Age and early roman period: An analytical approach". In: *Archaeological and Anthropological Sciences* 13.5 (2021). DOI: 10.1007/s12520-021-01323-2 (cit. on pp. xviii, 3, 18).

[9] M. F. Guerra and I. Tissot. "Bronze age and iron age gold torcs and earrings from the Iberian Atlantic façade: A non-invasive multi-analytical approach to the characterisation of the alloys and the corrosion". In: *X-Ray Spectrometry* 45.1 (2015), pp. 5–13. DOI: 10.1002/xrs.2628 (cit. on pp. xviii, 2, 3, 6, 7, 17, 18).

[10]   I. Montero and S. Rovira. "El Oro y sus aleaciones en la Orfebrería Prerromana". In: *Archivo Español de Arqueología* 64.163-164 (2018), p. 7. DOI: 10.3989/aespa.1991.v64.496 (cit. on p. xviii).

[11]   M. Murillo-Barroso et al. "A reappraisal of Iberian Copper Age Goldwork: Craftmanship, symbolism and art in a non-funerary gold sheet from Valencina de la Concepción". In: *Cambridge Archaeological Journal* 25.3 (2015), pp. 565–596. DOI: 10.1017/s0959774314001127 (cit. on pp. xviii, 13).

[12]   E. Mello, P. Parrini, and E. Formigli. "Etruscan filigree: Welding techniques of two gold bracelets from Vetulonia". In: *American Journal of Archaeology* 87.4 (1983), pp. 548–551. DOI: 10.2307/504114 (cit. on pp. xix, 2, 3).

[13]   M. Cardozo. *Das origens e técnica do trabalho do ouro e sua relação com a joalharia arcaica portuguesa*. Guimarães, 1957 (cit. on pp. 1, 2).

[14]   A. Hauptmann. *Archaeometallurgy – Materials Science Aspects*. Springer, Germany, 2020. ISBN: 978-3-030-50367-3 (cit. on pp. 1, 2).

[15]   A. Perea. *Orfebrebría Prerromana: Arqueologia del Oro*. Casa de Madrid, Spain, 1991 (cit. on pp. 1, 2).

[16]   Ó. García-Vuelta et al. "Iron Age goldwork as Cultural Heritage: Building strategies for its research". In: *Science and Technology for the Conservation of Cultural Heritage - Proceedings of the International Congress on Science and Technology for the Conservation of Cultural Heritage*. CRC Press/Balkema, 2013, pp. 401–405 (cit. on p. 1).

[17]   H. C. Virgílio, R. Parreira, and A. C. F. da Silva. *Ourivesaria Arcaica em Portugal: O Brilho do Poder*. CTT, 2013 (cit. on pp. 1, 2).

[18]   X.-L. Armada and Ó. García-Vuelta. "Iron Age Gold in Northwestern Iberia: Technology, Chronology and Social Meaning". In: *Early Iron Age Gold in Celtic Europe: Society, Technology and Archaeometry*. 2018, pp. 321–338 (cit. on pp. 1, 2).

[19]   X.-L. Armada and Ó. García-Vuelta. "Plano-convex ingots and precious metalwork in northwestern Iberia during the late Iron Age and early roman period: An analytical approach". In: *Archaeological and Anthropological Sciences* 13.5 (2021). DOI: 10.1007/s12520-021-01323-2 (cit. on p. 1).

[20]   B. Armbruster and R. Parreira. *Inventário do Museu Nacional de Arqueologia: Coleção de Ourivesaria - do Calcolítico à Idade do Bronze*. Vol. 1º. Secretaria de Estado da Cultura, 1993 (cit. on p. 1).

[21]   M. F. Guerra and I. Tissot. "Analytical Study of Bronze Age goldwork from Northwest Iberia". In: *Journal of Archaeological Science: Reports* 39 (2021), pp. 103–117. DOI: 10.1016/j.jasrep.2021.103117 (cit. on pp. 2, 3).

[22] M. F. Guerra and I. Tissot. "The role of Nuclear Microprobes in the study of Technology, provenance and corrosion of cultural heritage: The case of gold and silver items". In: *Nuclear Instruments and Methods in Physics Research Section B: Beam Interactions with Materials and Atoms* 306 (2013), pp. 227–231. DOI: `10.1016/j.nimb.2012.11.053` (cit. on p. 2).

[23] M. F. Guerra and T. Calligaro. "Gold Cultural Heritage Objects: A review of studies of provenance and Manufacturing Technologies". In: *Measurement Science and Technology* 14.9 (2003), pp. 1527–1537. DOI: `10.1088/0957-0233/14/9/305` (cit. on p. 2).

[24] B. Armbruster and A. Perea. "Macizo/Hueco, Soldado/Fundido, Morfología/ Tecnología. El ámbito Tecnológico Castreño a través de los torques con remates en doble escocia". In: *Trabajos de Prehistoria* 57.1 (2000), pp. 97–114. DOI: `10.3989/tp.2000.v57.i1.262` (cit. on p. 2).

[25] A. Perea and O. García-Vuelta. "Gold usage: wear marks and/or deterioration in site conditions". In: *"Historical Technology, Materials and Conservation: SEM and Microanalysis"*. Nov. 2020 (cit. on pp. 2, 4, 5).

[26] M. Martinón-Torres and L. Ladra. "A Ourivería prehistórica no Museo Provincial de Lugo: unha aproximación desde a química". In: *A colección de ourivería antiga do Museo Provincial de Lugo*. 1st ed. Servizo de Publicacións da Deputación de Lugo, 2018, pp. 46–59 (cit. on p. 3).

[27] A. Monge Soares, M. Araújo, and L. Alves. "Análise química não-destrutiva de artefactos em ouro pré e proto-históricos: Alguns exemplos". In: *Revista portuguesa de arqueologia, ISSN 0874-2782, Vol. 7, Nº. 2, 2004, pags. 125-138* 7 (Jan. 2004) (cit. on p. 3).

[28] A. M. Monge Soares et al. "Early iron age gold buttons from south-western Iberian Peninsula. identification of a Gold Metallurgical Workshop". In: *Trabajos de Prehistoria* 67.2 (2010), pp. 501–510. DOI: `10.3989/tp.2010.10053` (cit. on p. 3).

[29] Ó. García-Vuelta, I. Montero Ruiz, and Á. Villa Valdés. "Orfebrería Castreña en el Museo Arqueológico de Asturias (Oviedo): Aproximación a su caracterización arqueométrica y problemas de estudio". In: *Trabajos de Prehistoria* 77.1 (2020), p. 163. DOI: `10.3989/tp.2020.12252` (cit. on p. 3).

[30] X.-L. Armada and Ó. García-Vuelta. "Dating iron age goldwork: First direct AMS 14C results from Northwestern Iberia". In: *Trabajos de Prehistoria* 72.2 (2015), pp. 372–382. DOI: `10.3989/tp.2015.12160` (cit. on p. 3).

[31] X.-L. Armada et al. "Characterization of cores and organic remains in Iron Age Gold Objects: The recouso treasure". In: *Materials and Manufacturing Processes* 32.7-8 (2016), pp. 740–748. DOI: `10.1080/10426914.2016.1232818` (cit. on p. 3).

[32] E. Günter. *Noble Metal Systems: Selected systems from Ag-Al-Zn to Rh-Ru-Sc.* Springer, 2006 (cit. on pp. 3, 57).

[33] H. Arslan and H. Arslan. "Surface Tension and Surface Tension Assessment of Ag-Au-Cu Ternary and Sub-Binary Alloy Systems". In: Dec. 2019, pp. 1–25. ISBN: 978-1-78984-619-5. DOI: 10.5772/intechopen.84701 (cit. on pp. 3, 47, 56).

[34] A. J. Forty. "Corrosion micromorphology of noble metal alloys and depletion gilding". In: *Nature* 282.5739 (1979), pp. 597–598. DOI: 10.1038/282597a0 (cit. on p. 4).

[35] URL: http://www.museunacionalarqueologia.gov.pt/ (cit. on p. 5).

[36] URL: http://www.matriznet.dgpc.pt/MatrizNet/Objectos/ObjectosListar.aspx?TipoPesq=4&NumPag=1&RegPag=50&Modo=1&BaseDados=12&Cat=81&IdAutor= (cit. on pp. 6, 7).

[37] P. Valério et al. "Micro-EDXRF investigation of Chalcolithic gold ornaments from Portuguese Estremadura". In: *X-Ray Spectrometry* 46.4 (2017), pp. 252–258. DOI: 10.1002/xrs.2764 (cit. on p. 11).

[38] M. F. Guerra and I. Tissot. *A ourivesaria pré-histórica do ocidente peninsular atlântico: Compreender Para Preservar.* PROJETO AuCORRE, 2013 (cit. on pp. 11, 12).

[39] J. Loureiro et al. "Metal alloys, matrix inclusions and manufacturing techniques of Moinhos de Golas Collection (North Portugal): A study by micro-EDXRF, SEM–EDS, optical microscopy and X-ray radiography". In: *Applied Physics A* 122.9 (2016). DOI: 10.1007/s00339-016-0354-7 (cit. on p. 11).

[40] I. Tissot et al. "The earrings of Pancas Treasure: Analytical study by X-ray based techniques – a first approach". In: *Nuclear Instruments and Methods in Physics Research Section B: Beam Interactions with Materials and Atoms* 306 (2013), pp. 236–240. DOI: 10.1016/j.nimb.2012.11.054 (cit. on pp. 13, 19).

[41] A. Hartmann. *Prähistorische goldfunde aus Europa; Spektralanalytische Untersuchungen und Deren Auswertung.* Gebr. Mann, 1982 (cit. on pp. 18, 24, 25).

[42] R. B. Warner and M. Cahill. "Analysing ancient Irish gold: an assessment of the Hartmann database". In: *The Journal of Irish Archaeology* XX (2011), pp. 45–52 (cit. on p. 18).

[43] Ó. García-Vuelta. *Orfebrería Castreña del Museo Arqueológico Nacional.* Ministerio de Cultura, Subdirección Generalde Publicaciones, Información y Documentación, 2002 (cit. on p. 19).

[44] "Nomenclature, symbols, units and their usage in spectrochemical analysis - II. data interpretation". In: *IUPAC Standards Online* (2016). DOI: 10.1515/iupac.45.0021 (cit. on p. 55).

[45] L. A. Currie. "Limits for qualitative detection and quantitative determination. application to radiochemistry". In: *Analytical Chemistry* 40.3 (1968), pp. 586–593. DOI: 10.1021/ac60259a007 (cit. on p. 55).

[46] T. B. Massalski et al. *Binary alloy phase diagrams*. American Society for Metals, 1986 (cit. on pp. 57, 58).

Annex

I.1 Quantification errors and detection and quantification limits

$$\mathbf{C_Q} = \frac{10\,C_L}{3} \quad \mathbf{C_L} = \frac{3\sqrt{background}}{S}$$

$$\mathbf{S} = \frac{pic\ area}{concentration\ chemical\ element}$$

$$\mathbf{E_Q} = \left|\frac{\%Certified\ Element - \%Quantified\ Element}{\%Certified\ Element}\right| \times 100$$

$\mathbf{C_L}$ — Detection Limit; $\mathbf{C_D}$ — Quantification Limit; $\mathbf{E_Q}$ — Quantification Error [44, 45].

Table I.1: Quantification errors for the pXRF analysis.

Reference Material	Element	Certified Conc. (wt.%)	Ag Kα lines used		Ag Lα lines used	
			Obtained Conc. (wt.%)	Error (wt.%)	Obtained Conc. (wt.%)	Error (wt.%)
ERM EB506	Au	58.56	59.10	0.92	59.40	1.43
	Ag	3.90	3.77	3.33	3.40	12.82
	Cu	35.65	35.20	1.26	35.30	12.82
	Zn	1.89	1.92	1.53	1.93	2.06
ERM EB507	Au	75.10	73.90	1.60	73.70	1.86
	Ag	3.02	3.17	4.97	3.43	13.58
	Cu	14.69	15.60	6.19	15.60	6.19
	Ni	4.99	5.16	3.41	5.15	3.21
	Zn	2.11	2.12	0.62	2.11	0.14
ERM EB508	Au	75.10	75.50	0.51	75.50	0.51
	Ag	24.90	24.50	1.61	24.50	0.51

Table I.2: Detection (C_L) and Quantification (C_D) limits for the pXRF analysis.

	Au (wt.%) (Lα lines)	Ag (wt.%) (Kα lines)	Ag (wt.%) (Lα lines)	Cu (wt.%) (Kα lines)
$\mathbf{C_L}$	0.02	0.03	0.03	0.01
$\mathbf{C_D}$	0.06	0.09	0.11	0.03

Table I.3: Quantification errors for the micro-XRF analysis.

Reference Material	Element	Certified Conc. (wt.%)	Ag Kα lines used		Ag Lα lines used	
			Obtained Conc. (wt.%)	Error (wt.%)	Obtained Conc. (wt.%)	Error (wt.%)
IAEA IV	Au	73.70	74.10	0.54	74.50	1.09
	Ag	23.87	23.70	0.71	23.20	2.81
	Cu	2.33	2.25	3.43	2.26	3.00

Table I.4: Detection (C_L) and Quantification (C_D) limits for the micro-XRF analysis .

	Au (wt.%) (Lα lines)	Ag (wt.%) (Kα lines)	Ag (wt.%) (Lα lines)	Cu (wt.%) (Kα lines)
C_L	0.01	0.39	0.40	0.04
C_D	0.03	1.30	1.34	0.15

I.2 Phase diagrams
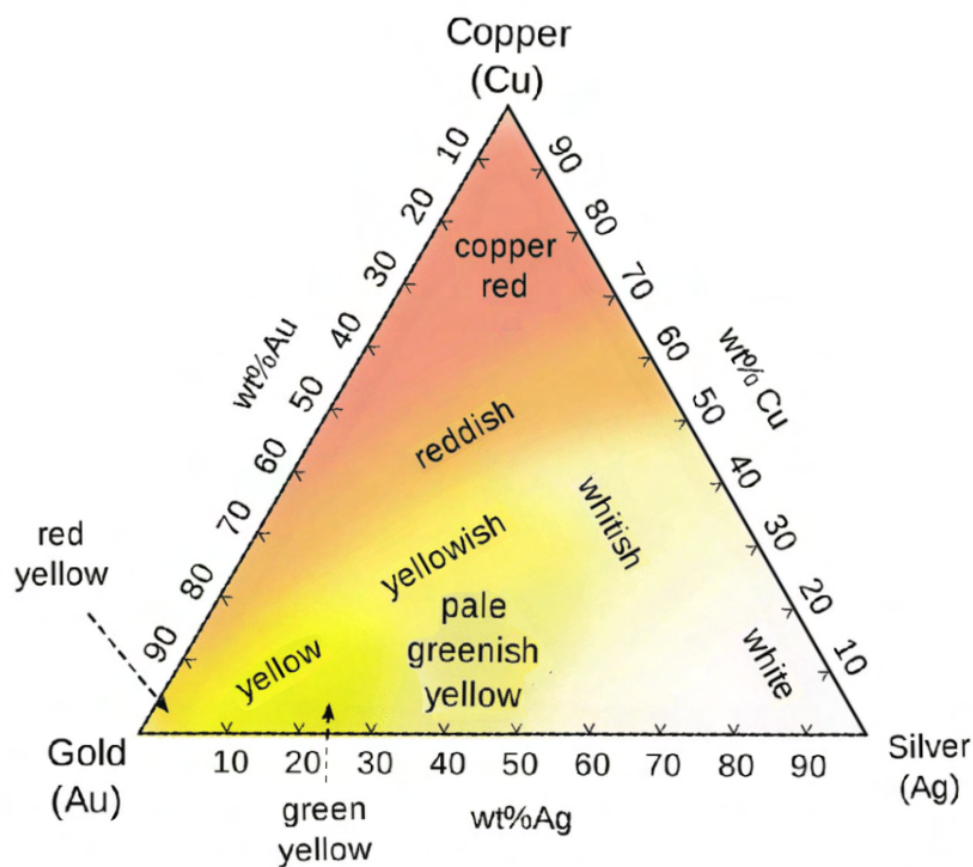
Figure I.1: Ternary diagram of the Au-Ag-Cu alloy: different colors obtained with different alloy compositions [33].
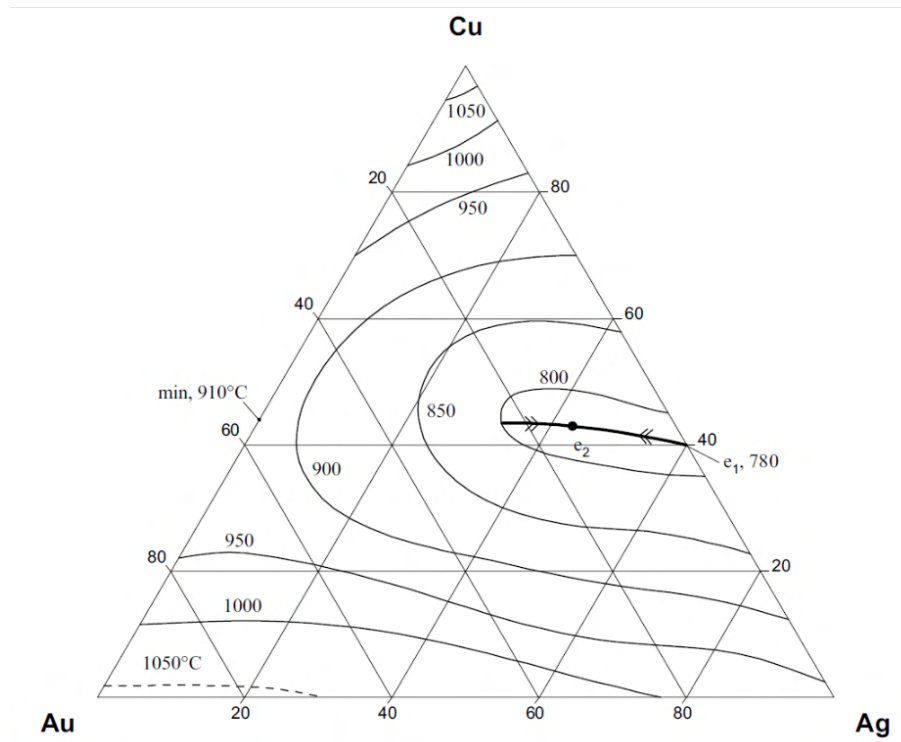
Figure I.2: Ternary phase diagram of the Au-Ag-Cu alloy [32].
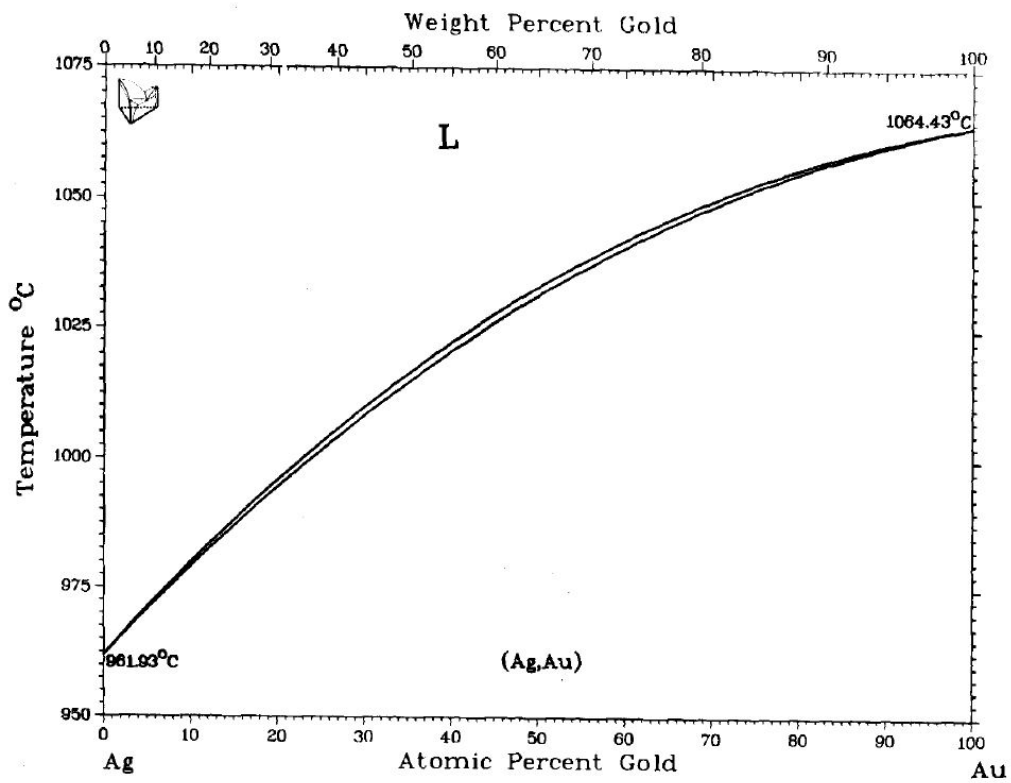
Figure I.3: Binary phase diagram of the Ag-Au alloy [46].

57
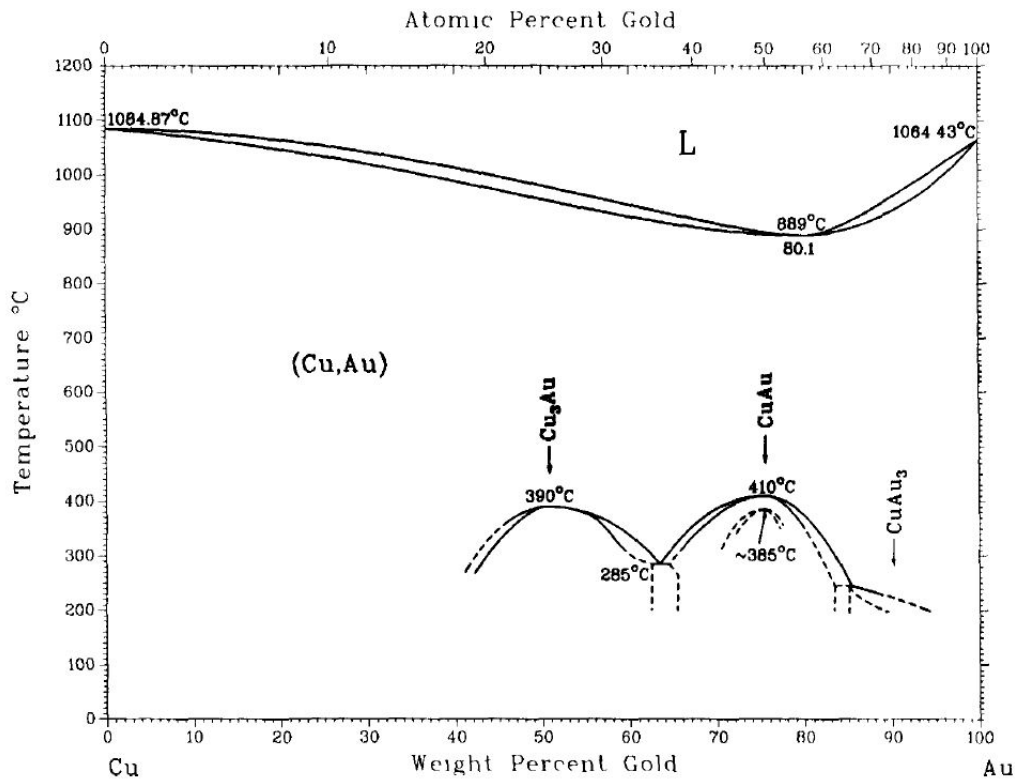
Figure I.4: Binary phase diagram of the Au-Cu alloy [46].
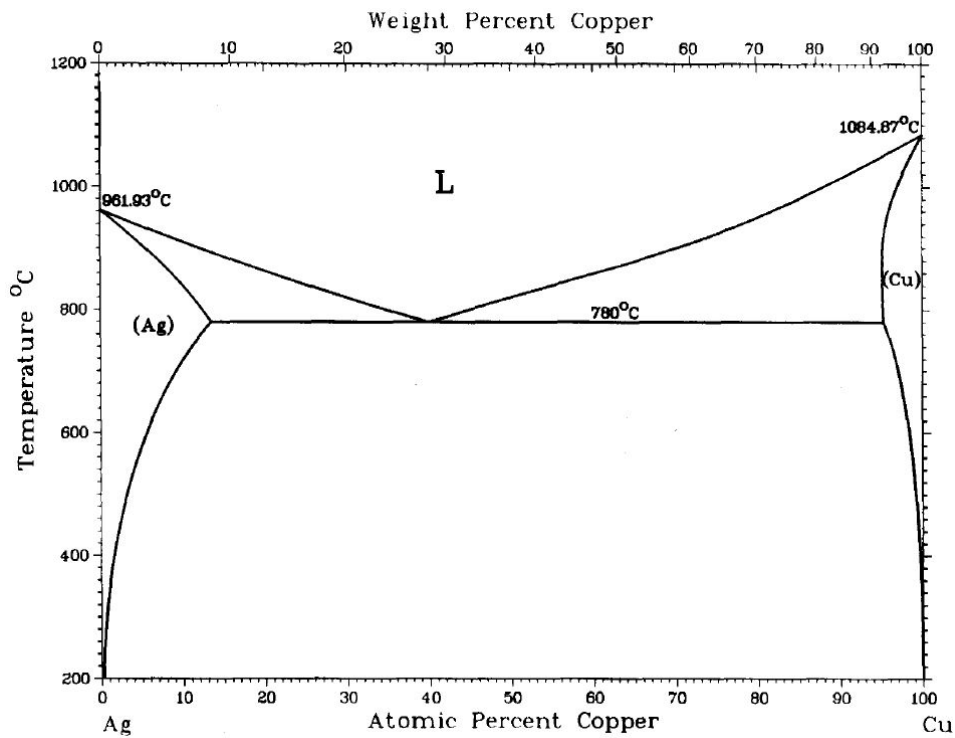
Figure I.5: Binary phase diagram of the Ag-Cu alloy [46].

I.3 2017.5135

Table I.5: pXRF qualitative and quantitative analyses of the artefact 2017.5135 (image of the obverse (left) and reverse (right) of the artefact).

2017.5135

No. analysis	Ag Kα lines (wt.%)			Ag Lα lines (wt.%)			Other elements*
	Au	Ag	Cu	Au	Ag	Cu	
01	85.30	13.30	1.42	91.90	6.60	1.51	Ni, Sn (Ti, Mn, Fe)
02	83.80	14.70	1.52	91.40	6.92	1.63	Ni, Sn (Ti, Mn, Fe)

*The presence of the elements between brackets may be due to deposits from the conditions were the object was found or due to previous conservation and restoration treatments.

Table I.6: SEM-EDS qualitative and quantitative analyses of the artefact 2017.5135.

2017.5135				
Analysis area	Au (wt.%)	Ag (wt.%)	Cu (wt.%)	Other elements (traces)
Bottom surface, thickest area	93.18	5.99	0.89	Sn
Bottom surface, thickest area	93.33	5.58	1.09	Sn
Area near the edge – relief	95.17	4.31	0.52	Sn
Area near the edge	90.50	8.36	1.15	–
Area near the edge – relief	90.45	8.82	0.73	Sn
Area near the edge – relief	90.95	8.12	0.94	–

I.4 2017.5136

Table I.7: pXRF qualitative and quantitative analyses of the artefact 2017.5136 (image of the obverse (left) and reverse (right) of the artefact).

2017.5136

No. analysis	Ag Kα lines (wt.%)			Ag Lα lines (wt.%)			Other elements*
	Au	Ag	Cu	Au	Ag	Cu	
03	86.60	12.70	0.69	94.10	5.18	0.74	Ni, Sn (Ti, Mn, Fe)
04	85.80	13.40	0.74	96.00	3.19	0.81	Ni, Sn (Ti, Mn, Fe)

*The presence of the elements between brackets may be due to deposits from the conditions were the object was found or due to previous conservation and restoration treatments.

Table I.8: SEM-EDS qualitative and quantitative analyses of the artefact 2017.5136.

2017.5136				
Analysis area	Au (wt.%)	Ag (wt.%)	Cu (wt.%)	Other elements (traces)
Bottom surface, thickest area	97.25	2.45	0.3	–
Bottom surface, thickest area – in the centre of the points marking the triangle	96.61	3.17	0.22	–
Bottom surface, thickest area – in the centre of the points marking the triangle	97.05	2.57	0.37	–
Area near the edge – relief	93.67	5.74	0.59	–
Area near the edge – relief	92.25	6.69	1.06	–
Area near the edge – relief	93.15	6.23	0.61	–
Area near the edge	86.73	11.17	2.09	–
Area near the other end – relief	89.08	9.84	1.08	–
Area near the other end	95.77	3.69	0.54	–

I.5 Au 11

Table I.9: pXRF qualitative and quantitative analyses of the artefact Au 11 (image of the obverse (left) and reverse (right) of the artefact).

Au 11

No. analysis	Ag Kα lines (wt.%)			Ag Lα lines (wt.%)			Other elements*
	Au	Ag	Cu	Au	Ag	Cu	
05	86.90	12.60	0.49	92.20	7.27	0.52	Ni, Sn (Ca, Ti, Mn, Fe)
06	87.10	12.40	0.51	92.70	6.73	0.53	Ni, Sn (Ca, Ti, Mn, Fe)
07	87.70	12.20	0.18	91.80	8.00	0.18	Ni, Sn (Ca, Ti, Mn, Fe)
08	87.10	12.50	0.42	92.40	7.12	0.45	Ni, Sn (Ca, Ti, Mn, Fe)
09	86.80	12.20	1.05	90.50	8.43	1.08	Ni, Sn (Ca, Ti, Mn, Fe)
10	85.50	13.60	0.96	92.30	6.65	1.01	Ni, Sn (Ca, Ti, Mn, Fe)

*The presence of the elements between brackets may be due to deposits from the conditions were the object was found or due to previous conservation and restoration treatments.

Previous analyses:

- **EDXRF** (M. F. Guerra and I. Tissot. "Bronze age and iron age gold torcs and earrings from the Iberian Atlantic façade: A non-invasive multi-analytical approach to the characterisation of the alloys and the corrosion". In: *X-Ray Spectrometry* 45.1 (2015), pp. 5–13. doi: 10.1002/xrs.2628): **Cu = 0.9 wt.%; Ag = 12.5 wt.%; Au = 86.6 wt.%.**

- **OES** (A. Hartmann. *Prähistorische goldfunde aus Europa; Spektralanalytische Untersuchungen und Deren Auswertung*. Gebr. Mann, 1982):

Au 11 (Au 2840)	Au	Ag*	Cu	Sn	Other elements
A. Hartmann (1982) (wt.%)	–	19	1.9	0.25	Bi ca. 0.01
Normalized Values (100 wt.%)	78.9	19	1.9	0.24	–

*Relative uncertainty (1 s.d.) of 25% (R. B. Warner and M. Cahill (2001))

I.6 Au 12

Table I.10: pXRF qualitative and quantitative analyses of the artefact Au 12 (image of the obverse (left) and reverse (right) of the artefact).

Au 12

No. analysis	Ag Kα lines (wt.%)			Ag Lα lines (wt.%)			Other elements*
	Au	Ag	Cu	Au	Ag	Cu	
11	87.80	10.90	1.28	92.50	6.15	1.34	Ni, Sn (Ca, Ti, Mn, Fe)
12	88.00	10.50	1.50	92.40	6.09	1.56	Ni, Sn (Ca, Ti, Mn, Fe)
13	88.50	10.30	1.24	92.20	6.56	1.28	Ni, Sn (Ca, Ti, Mn, Fe)
14	87.20	11.20	1.60	92.80	5.52	1.68	Ni, Sn (Ca, Ti, Mn, Fe)
15	88.00	10.90	1.15	92.70	6.15	1.20	Ni, Sn (Ca, Ti, Mn, Fe)
16	87.80	10.80	1.39	93.10	5.42	1.45	Ni, Sn (Ca, Ti, Mn, Fe)

*The presence of the elements between brackets may be due to deposits from the conditions were the object was found or due to previous conservation and restoration treatments.

Previous analyses:

- **EDXRF** (M. F. Guerra and I. Tissot. "Bronze age and iron age gold torcs and earrings from the Iberian Atlantic façade: A non-invasive multi-analytical approach to the characterisation of the alloys and the corrosion". In: *X-Ray Spectrometry* 45.1 (2015), pp. 5–13. doi: 10.1002/xrs.2628): **Cu = 1.6 wt.%; Ag = 10.4 wt.%; Au = 88.0 wt.%.**

- **OES** (A. Hartmann. *Prähistorische goldfunde aus Europa; Spektralanalytische Untersuchungen und Deren Auswertung*. Gebr. Mann, 1982):

Au 12 (Au 2841)	Au	Ag*	Cu	Sn	Other elements
A. Hartmann (1982) (wt.%)	–	15	4.2	0.37	–
Normalized Values (100 wt.%)	80.6	15	4.0	0.35	–

*Relative uncertainty (1 s.d.) of 25% (R. B. Warner and M. Cahill (2001))

I.7 Au 195

Table I.11: pXRF qualitative and quantitative analyses of the artefact Au 195 (image of the obverse (left) and reverse (right) of the artefact).

Au 195

No. analysis	Ag Kα lines (wt.%)			Ag Lα lines (wt.%)			Other elements*
	Au	Ag	Cu	Au	Ag	Cu	
17	89.80	10.10	0.11	90.80	9.12	0.11	Ni, Sn (Ca, Ti, Mn, Fe)
18	89.50	10.20	0.36	91.60	8.08	0.36	Ni, Sn (Ca, Ti, Mn, Fe)
19	89.40	10.30	0.27	94.10	5.58	0.28	Ni, Sn (Ca, Ti, Mn, Fe)

*The presence of the elements between brackets may be due to deposits from the conditions were the object was found or due to previous conservation and restoration treatments.
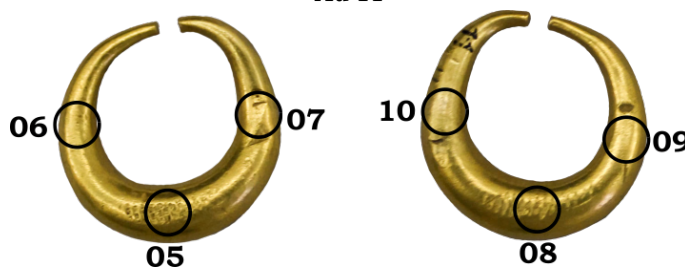
Previous analyses:

- **EDXRF** (M. F. Guerra and I. Tissot. "Bronze age and iron age gold torcs and earrings from the Iberian Atlantic façade: A non-invasive multi-analytical approach to the characterisation of the alloys and the corrosion". In: *X-Ray Spectrometry* 45.1 (2015), pp. 5–13. doi: 10.1002/xrs.2628): **Cu = 0.5 wt.%; Ag = 8.9 wt.%; Au = 90.5 wt.%.**

- **OES** (A. Hartmann. *Prähistorische goldfunde aus Europa; Spektralanalytische Untersuchungen und Deren Auswertung*. Gebr. Mann, 1982):

Au 195 (Au 2757)	Au	Ag*	Cu	Sn	Other elements
A. Hartmann (1982) (wt.%)	–	8	0.86	0.066	–
Normalized Values (100 wt.%)	91.1	8	0.85	0.065	–

*Relative uncertainty (1 s.d.) of 25% (R. B. Warner and M. Cahill (2001))

I.8   Au 196

Table I.12: pXRF qualitative and quantitative analyses of the artefact Au 196 (image of the obverse (left) and reverse (right) of the artefact).

Au 196

No. analysis	Ag Kα lines (wt.%)			Ag Lα lines (wt.%)			Other elements*
	Au	Ag	Cu	Au	Ag	Cu	
20	85.70	12.70	1.54	90.30	8.06	1.61	Ni, Sn (Ca, Ti, Mn)
21	85.00	12.50	2.56	88.50	8.83	2.64	Ni, Sn (Ca, Ti, Mn, Fe)
22	84.60	12.90	2.49	89.10	8.33	2.59	Ni, Sn (Ca, Ti, Mn, Fe)

*The presence of the elements between brackets may be due to deposits from the conditions were the object was found or due to previous conservation and restoration treatments.

Previous analyses:

- **EDXRF** (M. F. Guerra and I. Tissot. "Bronze age and iron age gold torcs and earrings from the Iberian Atlantic façade: A non-invasive multi-analytical approach to the characterisation of the alloys and the corrosion". In: *X-Ray Spectrometry* 45.1 (2015), pp. 5–13. doi: 10.1002/xrs.2628): **Cu = 1.9 wt.%; Ag = 12.1 wt.%; Au = 86 wt.%.**

- **OES** (A. Hartmann. *Prähistorische goldfunde aus Europa; Spektralanalytische Untersuchungen und Deren Auswertung*. Gebr. Mann, 1982):

Au 196 (Au 2756)	Au	Ag*	Cu	Sn	Other elements
A. Hartmann (1982) (wt.%)	–	12	3.5	0.21	–
Normalized Values (100 wt.%)	84.4	12	3.4	0.20	–

*Relative uncertainty (1 s.d.) of 25% (R. B. Warner and M. Cahill (2001))

I.9 Au 571

Table I.13: pXRF qualitative and quantitative analyses of the artefact Au 571 (image of the obverse (left) and reverse (right) of the artefact).

Au 571

No. analysis	Ag Kα lines (wt.%)			Ag Lα lines (wt.%)			Other elements*
	Au	Ag	Cu	Au	Ag	Cu	
23	86.60	11.80	1.64	88.70	9.62	1.67	Ni, Sn (Ca, Ti, Mn, Fe)
24	86.50	12.00	1.55	89.60	8.85	1.60	Ni, Sn (Ca, Ti, Mn, Fe)
25	86.70	12.00	1.32	88.70	10.00	1.34	Ni, Sn (Ca, Ti, Mn, Fe)

*The presence of the elements between brackets may be due to deposits from the conditions were the object was found or due to previous conservation and restoration treatments.

Previous analyses:

- **EDXRF** (M. F. Guerra and I. Tissot. "Bronze age and iron age gold torcs and earrings from the Iberian Atlantic façade: A non-invasive multi-analytical approach to the characterisation of the alloys and the corrosion". In: *X-Ray Spectrometry* 45.1 (2015), pp. 5–13. doi: 10.1002/xrs.2628): **Cu = 1.5 wt.%; Ag = 11.2 wt.%; Au = 87.3 wt.%.**

I.10 Au 592

Table I.14: pXRF qualitative and quantitative analyses of the artefact Au 592 (image of the obverse (left) and reverse (right) of the artefact).

Au 592

No. analysis	Ag Kα lines (wt.%)			Ag Lα lines (wt.%)			Other elements*
	Au	Ag	Cu	Au	Ag	Cu	
26	82.40	17.30	0.30	90.70	8.99	0.32	Ni, Sn (Ca, Ti, Mn, Fe)
27	82.80	16.70	0.54	91.80	7.64	0.59	Ni, Sn (Ca, Ti, Mn, Fe)
28	82.30	17.10	0.58	91.20	8.22	0.62	Ni, Sn (Ca, Ti, Mn, Fe)

*The presence of the elements between brackets may be due to deposits from the conditions were the object was found or due to previous conservation and restoration treatments.

Previous analyses:

- **EDXRF** (M. F. Guerra and I. Tissot. "Bronze age and iron age gold torcs and earrings from the Iberian Atlantic façade: A non-invasive multi-analytical approach to the characterisation of the alloys and the corrosion". In: *X-Ray Spectrometry* 45.1 (2015), pp. 5–13. doi: 10.1002/xrs.2628): **Cu = 0.9 wt.%; Ag = 12.8 wt.%; Au = 86.3 wt.%.**

I.11 Au 16

Table I.15: pXRF qualitative and quantitative analyses of the artefact Au 16 (image of the obverse (left) and reverse (right) of the artefact).

Au 16

No.	Ag Kα lines (wt.%)			Ag Lα lines (wt.%)			Other elements*
analysis	Au	Ag	Cu	Au	Ag	Cu	
29	88.60	7.67	3.75	86.50	9.82	3.68	Ni (Ca, Ti, Mn)
30	87.70	8.25	4.03	89.50	6.38	4.09	Ni, Sn (Ca, Ti, Mn, Fe)
31	85.80	8.37	5.87	87.10	6.94	5.95	Ni, Sn (Ca, Ti, Mn, Fe)

*The presence of the elements between brackets may be due to deposits from the conditions were the object was found or due to previous conservation and restoration treatments.

Previous analyses:

- **OES** (A. Hartmann. *Prähistorische goldfunde aus Europa; Spektralanalytische Untersuchungen und Deren Auswertung.* Gebr. Mann, 1982):

Au 16 (Au 2853)	Au	Ag*	Cu	Sn	Other elements
A. Hartmann (1982) (wt.%)	–	ca. 8	9.9	0.013	Sb
Normalized Values (100 wt.%)	83.0	ca. 8	9.0	0.012	–

*Relative uncertainty (1 s.d.) of 25% (R. B. Warner and M. Cahill (2001))

I.12 Au 180

Table I.16: pXRF qualitative and quantitative analyses of the artefact Au 180 (image of the obverse (left) and reverse (right) of the artefact).

No. analysis	Ag Kα lines (wt.%)			Ag Lα lines (wt.%)			Other elements*
	Au	Ag	Cu	Au	Ag	Cu	
32	85.10	12.70	2.17	89.00	8.80	2.25	Ni, Sn (Ca, Ti, V, Mn)
33	86.40	11.80	1.83	90.70	7.43	1.90	Ni, Sn (Ca, Ti, V, Mn, Fe)
34	86.10	12.10	1.81	88.70	9.41	1.86	Ni, Sn (Ca, Ti, V, Mn, Fe)
35	87.90	11.10	1.09	89.40	9.50	1.11	Ni, Sn (Ca, Ti, V, Mn, Fe)

*The presence of the elements between brackets may be due to deposits from the conditions were the object was found or due to previous conservation and restoration treatments.

Previous analyses:

- **OES** (A. Hartmann. *Prähistorische goldfunde aus Europa; Spektralanalytische Untersuchungen und Deren Auswertung*. Gebr. Mann, 1982):

Au 180 (Au 2845)	Au	Ag*	Cu	Sn	Other elements
A. Hartmann (1982) (wt.%)	–	ca. 12	5.4	*n.d.*	Bi ca. 0.01
Normalized Values (100 wt.%)	82.9	ca. 12	5.1	–	–

*Relative uncertainty (1 s.d.) of 25% (R. B. Warner and M. Cahill (2001))

I.13 Au 494

Table I.17: pXRF qualitative and quantitative analyses of the artefact Au 494 (image of the obverse (left) and reverse (right) of the artefact).

Au 494
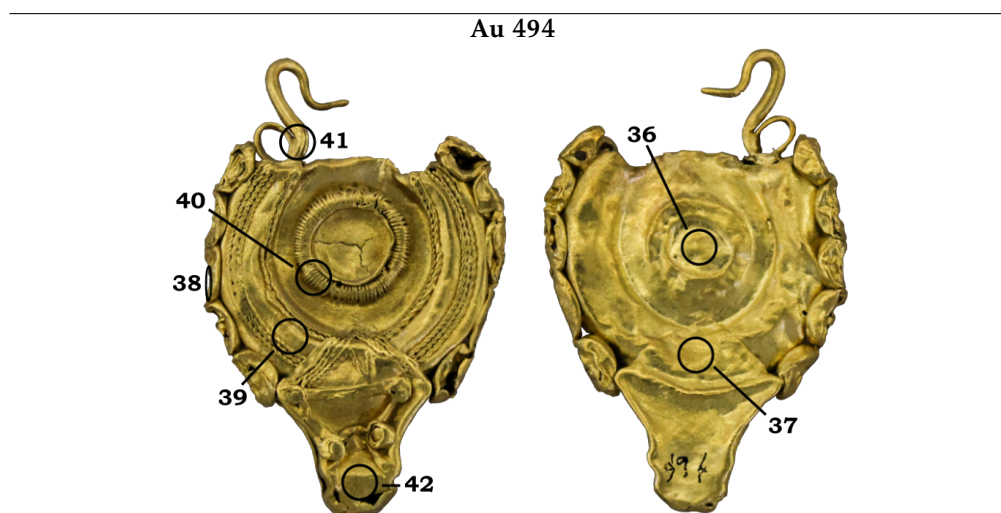
No.	Ag Kα lines (wt.%)			Ag Lα lines (wt.%)			Other elements*
analysis	Au	Ag	Cu	Au	Ag	Cu	
36	87.60	12.40	*n.d.*	87.00	13.00	*n.d.*	Ni, Sn (Ca, Ti, Mn, Fe)
37	87.10	12.90	*n.d.*	86.50	13.50	*n.d.*	Ni, Sn (Ti, Mn, Fe)
38	87.50	12.50	*n.d.*	88.60	11.40	*n.d.*	Ni, Sn (Ca, Ti, Mn, Fe)
39	87.20	12.80	*n.d.*	87.10	12.90	*n.d.*	Ni, Sn (Ca, Ti, V, Mn, Fe)
40	87.80	12.20	*n.d.*	87.50	12.50	*n.d.*	Ni, Sn (Ca, Ti, V, Mn, Fe)
41	83.00	14.80	2.19	84.50	13.30	2.22	Ni, Sn (Ca, Ti, V, Mn, Fe)
42	87.70	12.30	*n.d.*	87.10	12.90	*n.d.*	Ni, Sn (Ca, Ti, V, Mn)

*The presence of the elements between brackets may be due to deposits from the conditions were the object was found or due to previous conservation and restoration treatments.

Previous analyses:

- **OES** (A. Hartmann. *Prähistorische goldfunde aus Europa; Spektralanalytische Untersuchungen und Deren Auswertung*. Gebr. Mann, 1982):

Au 494 (Au 2804)	Au	Ag*	Cu	Sn	Other elements
A. Hartmann (1982) (wt.%)	–	ca. 10	0.9	0.37	–
Normalized Values (100 wt.%)	88.7	ca. 10	0.9	0.37	–

*Relative uncertainty (1 s.d.) of 25% (R. B. Warner and M. Cahill (2001))

I.14   Au 561

Table I.18: pXRF qualitative and quantitative analyses of the artefact Au 561 (image of the obverse (left) and reverse (right) of the artefact).

Au 561

No. analysis	Ag Kα lines (wt.%)			Ag Lα lines (wt.%)			Other elements*
	Au	Ag	Cu	Au	Ag	Cu	
43	83.70	16.30	*n.d.*	86.70	13.30	*n.d.*	Ni, Sn (Ca, Ti, V, Mn, Fe)
44	83.70	16.30	*n.d.*	86.50	13.50	*n.d.*	Ni, Sn (Ca, Ti, Mn, Fe)
45	83.70	16.30	*n.d.*	86.10	13.90	*n.d.*	Ni, Sn (Ca, Ti, V, Mn, Fe)

*The presence of the elements between brackets may be due to deposits from the conditions were the object was found or due to previous conservation and restoration treatments.

Previous analyses:

- **OES** (A. Hartmann. *Prähistorische goldfunde aus Europa; Spektralanalytische Untersuchungen und Deren Auswertung*. Gebr. Mann, 1982):
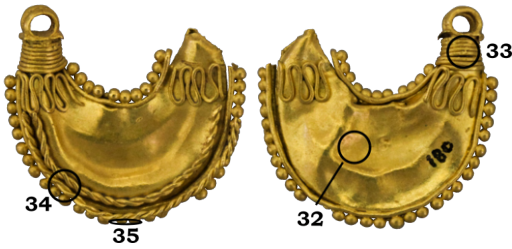
Au 561 (Au 2807)	Au	Ag*	Cu	Sn	Other elements
A. Hartmann (1982) (wt.%)	–	15-20	0.19	0.13	Bi <0.01
Normalized Values (100 wt.%)	79.7-84.7	15-20	0.19	0.13	–

*Relative uncertainty (1 s.d.) of 25% (R. B. Warner and M. Cahill (2001))

I.15 PART01

Table I.19: pXRF qualitative and quantitative analyses of the artefact PART01 (image of the obverse (left) and reverse (right) of the artefact).

PART01

No. analysis	Ag Kα lines (wt.%) Au	Ag	Cu	Ag Lα lines (wt.%) Au	Ag	Cu	Other elements*
46	60.40	32.50	7.15	66.20	26.10	7.70	Ni (Si, K, Ca, Ti, V, Cr, Mn, Fe)
47	62.80	28.80	8.37	66.70	24.50	8.78	Ni, Sn (Si, K, Ca, Ti, V, Mn, Fe)
48	61.20	30.40	8.42	67.10	23.80	9.06	Ni (Al, Si, K, Ca, Ti, V, Cr, Mn, Fe)

*The presence of the elements between brackets may be due to deposits from the conditions were the object was found or due to previous conservation and restoration treatments.

Table I.20: Micro-XRF qualitative and quantitative analyses of the artefact PART01

Analysis spot	micro-XRF (normalised values 100 wt.%) Ag Kα lines			Ag Lα lines			Other elements
	Au	Ag	Cu	Au	Ag	Cu	
Wire-6-01	49.70	45.00	5.33	49.90	44.70	5.35	Fe
Wire-6-02	53.40	41.00	5.61	54.50	39.80	5.71	Fe
Wire-6-03	52.70	41.60	5.66	57.40	36.60	6.07	Fe
Wire-6-04	58.50	34.00	7.52	58.70	33.80	7.55	Fe
Wire-5-01	38.10	57.20	4.77	45.40	49.10	5.54	Fe
Wire-5-02	50.90	41.50	7.52	57.10	34.60	8.26	–
Wire-5-03	47.90	46.60	5.44	50.10	44.30	5.65	Fe
Wire-5-04	57.50	35.10	7.49	62.20	29.80	7.98	Fe
Wire-5-05	55.10	38.40	6.51	56.90	36.50	6.69	Fe
Wire-4-01	38.00	57.40	4.64	46.40	48.00	5.51	–
Wire-4-02	49.40	45.00	5.64	56.30	37.40	6.29	Fe
Wire-4-03	61.90	30.80	7.34	63.50	29.00	7.49	Fe
Wire-4-04	55.20	37.90	6.87	45.40	48.70	5.84	Ti, Mn, Fe
Wire-4-05	66.50	24.70	8.82	64.50	26.90	8.61	Fe
Wire-3-01	47.00	44.90	8.06	46.40	45.60	7.97	Fe
Wire-3-02	55.30	39.60	5.08	64.40	29.80	5.76	Fe
Wire-3-03	45.00	48.60	6.40	49.10	44.00	6.88	Fe
Wire-3-04	61.80	31.20	6.99	63.20	29.60	7.12	Fe
Wire-2-01	56.60	37.40	6.01	62.20	31.30	6.49	Fe

Wire-2-02	64.80	28.50	6.73	68.40	24.50	7.03	Fe
Wire-2-03	62.00	30.60	7.44	65.70	26.50	7.79	Fe
Wire-2-04	62.30	30.80	6.88	65.70	27.20	7.18	Fe
Wire-1-01	37.50	58.40	4.16	42.80	52.60	4.66	Fe
Wire-1-02	59.60	34.30	6.10	66.00	27.40	6.63	Fe
Wire-1-03	60.90	32.00	7.09	62.20	30.60	7.21	Fe
Wire-1-04	49.70	44.90	5.37	51.60	42.90	5.54	Fe
Betw_Wires-5-01	51.00	41.00	7.97	50.60	41.50	7.92	Fe
Betw_Wires-4-01	60.10	30.60	9.31	60.90	29.70	9.41	Fe
Betw_Wires-3-01	56.50	37.70	5.83	87.30	4.50	8.25	Si, K, Ca, Ti, Mn, Fe
Betw_Wires-3-02	49.00	47.30	3.69	87.20	6.91	5.91	Si, K, Ti, Mn, Fe
Betw_Wires-3-03	66.50	24.70	8.82	64.50	26.90	8.61	Fe
Betw_Wires-2-01	65.90	25.50	8.65	67.40	23.80	8.81	Fe
Betw_Wires-1-01	63.20	28.40	8.43	64.70	26.70	8.59	Fe
Betw_Wires-1-02	61.70	28.70	9.58	62.30	28.00	9.66	Fe
Betw_Wires-1-03	62.10	28.10	9.72	62.00	28.30	9.71	Fe
Betw_Wires-1-04	61.80	28.80	9.36	62.40	28.20	9.43	Fe
Betw_Wires-1-05	62.10	28.70	9.21	61.90	28.90	9.18	Fe
Betw_Wires-1-06	62.70	29.00	8.33	62.30	29.40	8.29	Fe
Betw_Wires-1-07	61.80	29.30	8.89	62.20	28.80	8.94	Fe
Betw_Wires-1-08	61.90	28.70	9.35	62.40	28.20	9.40	Fe
Betw_Wires-1-09	61.50	29.00	9.47	62.40	28.10	9.57	Fe
Betw_Wires-1-10	62.20	28.60	9.15	62.50	28.40	9.17	Fe
Betw_Wires-1-11	62.40	28.60	8.95	63.40	27.50	9.07	Fe
Betw_Wires-1-12	62.60	28.60	8.83	63.80	27.20	8.97	Fe
Betw_Wires-1-13	63.80	26.80	9.38	63.70	26.90	9.37	Fe

Betw_Wires-1-14	62.50	28.50	9.00	63.90	26.90	9.16	Fe
Int_Grn-1-01	8.32	91.30	0.35	10.60	88.90	0.45	Cl, Ti, Fe
Int_Grn-1-02	9.59	90.10	0.35	12.20	87.40	0.44	Cl, Ti, Fe
Int_Grn-2-01	7.28	92.10	0.58	8.30	91.00	0.66	Cl, Ti, Fe
Int_Grn-3-01	9.68	89.70	0.66	13.20	85.90	0.89	Cl, Ti, Fe
Int_Grn-3-02	14.10	85.40	0.49	17.90	81.50	0.62	Cl, Ti, Fe
Int_Grn-3-03	6.68	92.60	0.76	8.64	90.40	0.97	Cl, Ti, Fe
Ext_Grn-1-01	48.40	47.50	4.05	56.30	39.10	4.60	Fe
Ext_Grn-1-02	32.40	64.20	3.32	40.00	56.00	3.99	Ti, Fe
Ext_Grn-2-01	62.00	31.20	6.86	65.70	27.10	7.19	Fe
Ext_Grn-3-01	18.70	79.10	2.18	27.10	69.80	3.05	Cl, Fe
Ext_Grn-3-02	60.90	31.10	8.07	57.30	35.00	7.69	Fe
Ext_Grn-3-03	61.00	30.10	8.90	61.30	29.80	8.94	Fe
Ext_Grn-3-04	60.80	31.60	7.64	62.80	29.30	7.84	Fe
Gaps-1-01	26.10	71.60	2.29	40.10	56.50	3.35	Ti, Fe
Gaps-1-02	32.50	64.30	3.16	40.50	55.70	3.83	Fe
Gaps-2-01	16.40	81.80	1.78	21.40	76.30	2.28	Ti, Fe
Gaps-2-02	17.20	80.10	2.77	21.30	75.30	3.38	Ti, Fe
Gaps-2-03	12.90	85.60	1.42	19.00	78.90	2.04	Cl, Ti, Fe
Gaps-3-01	59.20	34.00	6.86	73.80	18.00	8.19	Si, K, Ca, Ti, Mn, Fe
Gaps-3-02	51.50	42.00	6.51	63.00	29.30	7.67	Si, K, Ti, Fe
Grn-7-01	55.80	36.50	7.78	57.80	34.20	8.00	Ti, Fe
Grn-7-02	55.50	37.30	7.22	57.70	34.80	7.46	Ti, Fe
Grn-7-03	55.20	38.40	6.37	60.70	32.40	6.89	Fe
Grn-7-04	58.70	34.10	7.25	58.20	34.60	7.20	Fe
Wire-6-V-01	63.50	27.10	9.45	66.30	24.00	9.78	Ti, Fe
Wire-3-V-01	50.60	42.70	6.73	59.00	33.30	7.64	Si, Cl, K, Ca, Ti, Mn, Fe
Hole-01	34.60	62.70	2.68	40.40	56.50	3.07	K, Ti, Fe
Polished-01	32.10	64.80	3.04	36.23	60.40	3.37	–
Polished-02	20.98	76.43	2.59	23.30	73.85	2.85	–
Polished-03	24.17	72.93	2.89	26.30	70.58	3.12	–
Polished-04	30.77	65.75	3.48	32.64	63.69	3.67	–
Polished-05	22.77	74.68	2.55	26.86	70.18	2.96	–
Polished-06	22.38	74.77	2.84	25.78	70.99	3.23	–
Polished-07	31.23	65.42	3.35	34.32	62.03	3.64	–
Polished-08	26.82	70.44	2.74	33.53	66.39	3.07	–
Polished-09	31.25	65.63	3.11	35.12	61.43	3.45	–
Polished-10	18.41	78.70	2.89	20.40	76.43	3.17	–
Polished-11	18.91	78.75	2.34	22.53	74.72	2.75	–
Polished-12	44.46	51.88	3.67	40.35	56.28	3.38	–
Polished-13	42.56	53.88	3.56	48.63	47.38	3.99	–
Polished-14	24.95	72.28	2.77	29.40	67.39	3.20	–
Polished-15	22.74	74.61	2.65	25.46	71.60	2.94	–

Polished-16	22.55	74.55	2.90	24.75	72.10	3.15	–
Polished-17	30.63	66.34	3.03	34.73	61.89	3.39	–
Polished-18	29.20	68.00	2.80	34.64	62.11	3.25	–
Polished-19	40.61	55.75	3.64	45.29	50.72	3.99	–
Polished-20	30.65	66.30	3.05	36.22	60.24	3.53	–
Polished-21	53.62	40.00	6.37	52.65	41.08	6.28	–
Polished-22	56.21	36.31	7.48	54.05	38.70	7.24	–
Polished-23	54.01	40.06	5.92	52.62	41.58	5.80	–
Unpolished-01	40.08	56.37	3.56	47.52	48.37	4.12	–
Unpolished-02	50.62	44.57	4.81	53.71	41.24	5.05	–
Unpolished-03	56.09	36.93	6.97	55.79	37.26	6.94	–

NOVA
SCHOOL OF SCIENCE
& TECHNOLOGY

STUDY OF GOLD ALLOY PRODUCTIONS FROM LATE BRONZE AGE AND IRON AGE

Sofia Serrano

2022